Hood Canal Bridge
Ecosystem Impact Assessment:
Phase 1 Report

September 28, 2020

Prepared by:

Hood Canal Bridge Assessment Team and contributing experts (see reverse)

Cite document as: Hood Canal Bridge Assessment Team. 2020. Hood Canal Bridge Ecosystem Impact Assessment: Phase 1 Report. Long Live the Kings, Seattle, WA.

Bridge Assessment Team

Barry Berejikian, NOAA Northwest Fisheries Science Center
Megan Moore, NOAA Northwest Fisheries Science Center*
Tarang Khangaonkar, Pacific Northwest National Laboratory*
Hans Daubenberger, Port Gamble S'Klallam Tribe*
Emily Bishop, Westward Ecology
Paul McCollum, Port Gamble S'Klallam Tribe
Scott Pearson, Washington Department of Fish and Wildlife*
Carl Ward, Washington Department of Transportation
Dave Molenaar, Washington Department of Transportation
Scott Brewer, Hood Canal Coordinating Council
Dale Norton, Washington Department of Ecology

Contributors
Heather Gordon, Immrama Ecology
Adi Nugraha, Pacific Northwest National Laboratory
Daniel Deng, Pacific Northwest National Laboratory
Chris Jones, Port Gamble S'Klallam Tribe
Julianna Sullivan, Port Gamble S'Klallam Tribe
Kevin Redman, RPS Evans Hamilton
Julie Keister, University of Washington
Theodore Castro-Santos, U.S. Geological Survey
Jessica Stocking, Washington Department of Fish and Wildlife
Monique Lance, Washington Department of Fish and Wildlife
Steve Jeffries, Washington Department of Fish and Wildlife
Kelly Beach, Washington Department of Fish and Wildlife
Caanan Cowles, Washington Department of Fish and Wildlife
Chad Norris, Washington Department of Fish and Wildlife
D. Schwitters, Washington Department of Fish and Wildlife
William Simper, Washington Department of Fish and Wildlife
E. Weiss, Washington Department of Fish and Wildlife

Coordinators
Iris Kemp, Long Live the Kings+
Lucas Hall, Long Live the Kings
Michael Schmidt, Long Live the Kings

***Principal Investigators**
+Senior Project Manager. For more information, contact ikemp@lltk.org.

Contents

Executive Summary

Hood Canal is a long, narrow fjord that forms the western lobe of Puget Sound. Coined "the wild side of Washington", many tourists and locals visit or move to the Hood Canal region to experience nature. While Hood Canal's natural ecosystem is more intact than many other regions of Puget Sound, vital elements are at risk. Abundances of wild Chinook salmon, chum salmon and steelhead native to Hood Canal are low and all three species are listed as threatened under the Endangered Species Act (ESA). Also, fish kills from low dissolved oxygen events occur periodically and ocean acidification threatens commercially important shellfish beds in Hood Canal more so than the rest of Puget Sound.

The Hood Canal Bridge carries traffic across the northern outlet of Hood Canal, connecting the Olympic and Kitsap peninsulas and supporting tourism and other economic activities. As a 1.5-mile long floating bridge, its pontoons span over 80% the width of Hood Canal and extend 15 feet underwater. Because of its location, all salmon and steelhead must navigate around or underneath the Hood Canal Bridge on their migration to and from the Pacific Ocean. In 2015, federal, state, tribal, and nonprofit partners convened to develop the Hood Canal Bridge Ecosystem Impact Assessment Plan. The plan was designed to pinpoint how the bridge affects ESA-listed juvenile steelhead survival; determine whether other salmon may also be affected; and determine whether, and if so, to what extent the bridge impacts the health of the Hood Canal ecosystem. Phase 1 of the Assessment Plan consisted of two years of intensive data collection, analysis, and modeling to characterize physical and biological dynamics near the bridge and identify impacts to juvenile steelhead and salmon, predator assemblages, and water quality parameters.

This document describes the research conducted during the first phase of the assessment and the resulting outcomes and recommendations. Phase 1 research addressed these primary questions:

I. **How is the bridge acting as a barrier to juvenile steelhead migration and leading to increased mortality? How does the bridge influence other fish, including salmon?**

   Researchers studied juvenile steelhead migration behavior and mortality, surveyed predator abundances and collected observational data on predator behavior, and investigated light, shade, and noise impacts from the bridge. These datasets were used to determine what species are most likely predating upon steelhead and how the bridge functionally leads to increased predation.

II. **Is the bridge impacting the entire Hood Canal ecosystem?**

   Because species throughout Hood Canal respond to changes in water quality, any effects of the bridge on ecosystem processes may ripple throughout the food web in unknown ways. Phase 1 research included collecting field data and refining circulation models to characterize the extent of bridge impacts on water quality.

During this first phase of the assessment, the project's Assessment Team performed these activities:

- **Track steelhead migration and mortality** – Juvenile steelhead were acoustically tagged and their migration pattern tracked past the bridge to determine where mortality is occurring and most likely causes of mortality.
- **Map fish densities** – The distribution and density of epipelagic biomass in the area were assessed near the bridge to characterize density patterns along the bridge.

- **Identify predators and map their densities** – Potential steelhead and salmon predators were identified and their distribution and abundance mapped along the bridge to identify hotspots of predation risk.
- **Assess light/shade and noise near the bridge** – Pilot studies of light and noise levels at and near the bridge were carried out to determine whether further investigation on potential impacts is warranted.
- **Evaluate the impact of pools and eddies caused by pools at the center of the bridge** – Open pools into which the bridge's center drawspan retracts to let ships pass form open-bottom enclosures. Pools were investigated to determine whether this infrastructure aggregates plankton, thus attracting planktivorous salmon and steelhead (or other prey fish species like herring) and increasing their susceptibility to predation**.**
- **Collect and model oceanographic data near the bridge** – Devices were placed in proximity to the bridge to precisely measure impacts to water circulation. These data were used to refine models simulating the extent of this impact to the overall circulation and flushing of Hood Canal, and to what extent dissolved oxygen, temperature, acidity, and nutrient dynamics are affected.

Research efforts were conducted throughout steelhead outmigration periods (April-June) of 2017 and 2018 and spanned a range of conditions that could affect the extent of bridge impacts: tidal cycles, day versus night, and periods of time during which the center drawspan of the bridge (used to allow large ships to pass) was both open and closed.

Results from Phase 1 of the Hood Canal Bridge Ecosystem Impact Assessment include:

1. The Hood Canal Bridge significantly contributes to early marine mortality of juvenile Hood Canal steelhead by impeding fish passage and facilitating predation.
2. The bridge impacts other fish species such as juvenile Chinook and chum.
3. The bridge significantly impacts water quality parameters (temperature, salinity, currents) in its vicinity. Although bridge effects on water quality dissipate with increasing distance from the bridge and do not appear to propagate throughout Hood Canal, these near-bridge changes in circulation and flow may be linked to impacts on juvenile salmon and steelhead behavior and mortality.
4. Avian and mammalian predators were documented near the bridge. Harbor seal predation on juvenile steelhead was the most frequent source of mortality based on tagged juvenile steelhead mortality patterns.

With this information, the Hood Canal Bridge Assessment Team, Engineer Team, and Management Committee members participated in workshops and exercises to develop solutions to test during Phase 2, and to identify the research needed beyond the scope of Phase 1 to address bridge impacts on other juvenile salmon species, potential bridge impacts on returning adult salmon, and predator deterrence options. With the guidance of the Assessment Team, engineers at R2 Resource Consultants completed initial scoping and design recommendations for Phase 2 solutions. Solutions were prioritized into three categories: 1) management actions recommended for early implementation, 2) management actions that were high-ranking but need additional research, and 3) management actions ranked lower. Solutions in category 1 are being proposed for installation, effectiveness testing, and further investigation in Phase 2. This category includes installing fillet and eddy reduction structures to reduce or restrict fish access to existing pontoon corners of the infrastructure, as well as pilot testing longer-duration bridge drawspan openings timed on strong ebb tides to encourage fish passage and investigating modifications to luminaries to reduce overwater light spillover. Phase 2 may also provide an opportunity to conduct the research necessary to move towards implementing solutions in category 2: bridge re-design and replacement/modifications and pinniped deterrence activities such as restricting haul-out and bridge access.

Figure 1. Hood Canal Bridge is located at the north end of Hood Canal near its entrance to Puget Sound. Image from Google Maps.

Background and Overview

The Hood Canal Bridge is the longest floating bridge in a saltwater tidal basin in the world, and the third-longest floating bridge overall. It is an important regional transportation asset in western Washington, providing a vital connection between the Olympic and Kitsap peninsulas with over 18,000 trips per day[1] by local commuters and commercial vehicles. During the tourist season, the bridge helps drive the economy by bringing visitors to the Olympic Peninsula to recreate on land and water. Locals and visitors alike expect Hood Canal to be a healthy, vibrant ecosystem, teeming with life including salmon and steelhead that define their home and the purpose of their visit.

All salmon originating from Hood Canal rivers must pass the Hood Canal Bridge as juveniles on their way out to the Strait of Juan de Fuca and the Pacific Ocean (Figure 1). They must pass through the bridge again as adults on their return trip to spawn in their natal streams. Three species of Hood Canal salmon and steelhead are listed as *Threatened* under the Endangered Species Act (ESA): Puget Sound Chinook, Hood Canal Summer Chum, and Puget Sound steelhead. Millions of dollars have been spent on efforts to restore and protect these fish and their habitat throughout Hood Canal. The Hood Canal Bridge carries State Route 104 across the northern outlet of Hood Canal in Puget Sound. As a 1.5-mile long floating bridge, its pontoons span over 80% of the width of Hood Canal and extend 15 feet underwater (Figure). Slower migration times, higher mortality rates in the vicinity of the bridge relative to other areas on their migration route, and unique behavior and mortality patterns at the bridge

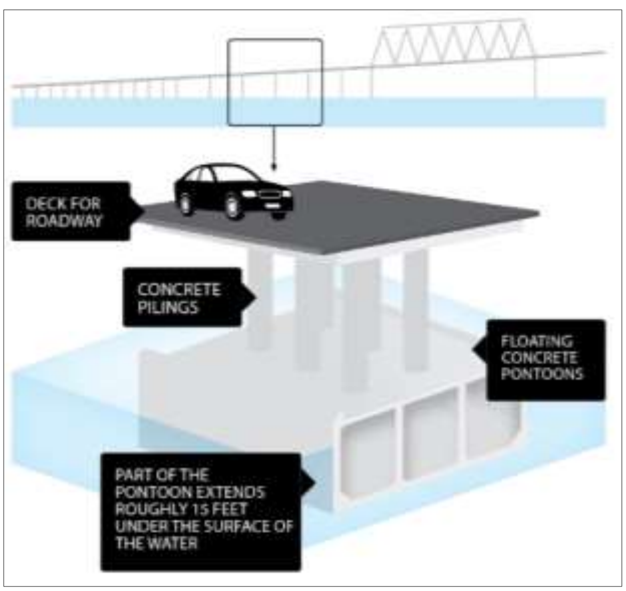

Figure 2. The Hood Canal Bridge floats on pontoons that span much of the width of Hood Canal and extend roughly 15 feet underwater. Image property of Long Live the Kings.

[1] https://www.wsdot.gov/Traffic/API/PermanentTrafficRecorder/?siteId=R085, data from April-June 2017-2018

suggest the bridge impedes steelhead migration and facilitates predation[2]. The bridge may also disrupt Hood Canal circulation and water quality[3].

In 2015, federal, state, tribal, and nonprofit partners convened to develop the Hood Canal Bridge Ecosystem Impact Assessment Plan, designed to pinpoint how the bridge is negatively affecting ESA-listed juvenile steelhead survival; determine whether other salmon may also be affected; and determine whether, and if so, to what extent the bridge is impacting the health of the Hood Canal ecosystem. This effort was driven by increasing recognition of the evidence and need for understanding and mitigating bridge impacts in the context of salmon and steelhead recovery.

Puget Sound steelhead populations (including Hood Canal) have declined to under 10% of historic run sizes over the past three decades and many wild populations now face possible extinction[4]. Juvenile mortality in the marine environment is a major cause of population declines, and the Phase 1 research conducted during the Hood Canal Bridge Ecosystem Impact Assessment shows that the Hood Canal Bridge significantly contributes to early marine mortality of steelhead populations native to Hood Canal: approximately half of the juvenile steelhead that arrive at the bridge die there. The bridge serves as a physical barrier to steelhead fish passage, slowing migration by 1-2 days on average, and facilitates predation (Figure 3. The bridge pontoons are a physical barrier for surface-oriented juvenile steelhead, slowing migration and increasing vulnerability to predation.). Of the predator species observed at the bridge, harbor seals are a likely candidate for a majority of observed juvenile steelhead mortality.

Figure 2. The bridge pontoons are a physical barrier for surface-oriented juvenile steelhead, slowing migration and increasing vulnerability to predation. Image property of LLTK.

The bridge also affects other fish, including ESA-listed Chinook and Hood Canal chum. All juvenile salmon must pass the Hood Canal Bridge while outmigrating, and Phase 1 research findings indicate that large numbers of juvenile chum and chinook aggregate around bridge infrastructure during the spring outmigration season, spanning across the full width of the bridge. Some evidence supports the "reef effect" hypothesis, which posits that the bridge's unique infrastructure has created low-complexity artificial habitat for plankton, fish, and predator species: zooplankton sampling suggests community differences near the bridge vs. away from the bridge in Hood Canal waters, smaller species of salmon appear to school along the length of the bridge infrastructure and exhibit milling and feeding behaviors in certain areas, and predator species interact with the bridge structure as artificial shoreline. Specific features of the bridge appear to elicit different behavior than others, such as corners made from pontoons oriented perpendicular to the road deck and partially enclosed pools that allow retraction of

[2] Moore et al. 2013. A floating bridge disrupts seaward migration and increases mortality of steelhead smolts in Hood Canal, Washington State. https://doi.org/10.1371/journal.pone.0073427
[3] Khangaonkar & Wang 2013. Potential alteration of fjordal circulation due to a large floating structure – numerical investigation with application to Hood Canal basin in Puget Sound. https://doi.org/10.1016/j.apor.2012.11.003
[4] Federal Registry Notice: 72 FR 26722

the bridge draw span during bridge openings (Figure 4). Observations on the bridge suggest that certain species of predators, like harbor seals, exploit these features to capture prey in areas where fish are aggregated with little refuge. It is noteworthy that most steelhead mortalities occurred in close proximity to the bridge structure, and in several cases where tagged steelhead were consumed by predators and the tag data began reflecting predator movement, that those predators remained in proximity to the bridge.

Figure 3. On left, the east bridge pool area, looking towards the closed center drawspan. On right, one of the corner areas created by cross-pontoons that jut out from the bridge structure. Photos courtesy of LLTK.

Light and noise/sound levels are increased at the bridge relative to surrounding waters. Observed noise levels during the steelhead outmigration period did not rise to a level of immediate concern based on previous studies of noise and pressure sensitivity in salmonids. However, observed nighttime light levels from artificial lights installed on the bridge deck spilling over to surface waters were within a range that previous studies have reported to affect salmon behavior. Increased nighttime light levels may either attract or deter juvenile salmon from lit areas, may alter feeding behavior of fish and predators, and may affect a fish's vulnerability to predation. However, no relationships between tagged steelhead behavior and noise levels varying between daytime and nighttime periods were apparent in the telemetry data.

The natural ecosystem in Hood Canal is controlled by deep narrow estuarine circulation with classic fjord-like features where mean circulation and mixing is dominated by the influence of freshwater runoff. This balance of surface outflow of buoyant freshwater and the corresponding inward-bound deep saltwater compensation current is essential to sustaining the water quality and overall health of fjord-like waterbodies such as Hood Canal. Unimpeded outflow of brackish water from typical fjords through the shallow surface layers is responsible for setting up stratification, salinity gradients, and resulting exchange flow and flushing of the basin needed for maintenance of water quality.

Preliminary modeling studies which formed the basis of development for Phase 1 research suggested localized and wide-ranging impacts of the bridge on water quality. During Phase 1, models were validated and refined with oceanographic data collected at the

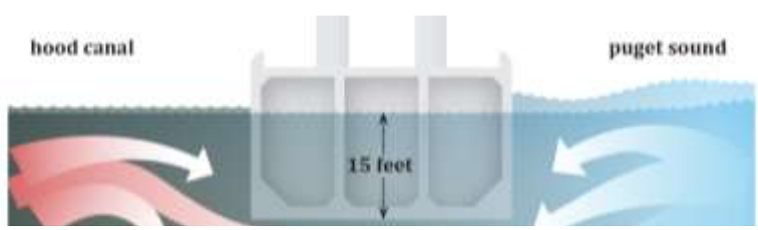

Figure 4. The bridge pontoons extend into the surface layer of the water column, impacting temperature, salinity, and currents and causing increased mixing near the bridge. Image property of Long Live the Kings.

bridge, near the bridge, and away from the bridge during the juvenile steelhead outmigration season. Results from these improved modeling studies confirmed that the floating bridge has localized impacts on water quality, obstructing the brackish outflow surface layer, and thereby causing increased mixing near the bridge, pooling of up-current water, and shadow/sheltering of down-current water across the tidal cycle (Figure 5).

Impacts on currents, salinity, and temperature are highest at the bridge and extend about 20 m below the water's surface and up to 5 km away from the bridge before dissipating to within a 10% deviation from ambient conditions. Model results did not predict significant bridge impacts to Hood Canal-wide circulation/flushing or water quality.

Individual Assessment Components: Brief Methods and Outcomes

The Hood Canal Bridge Ecosystem Impact Assessment was structured following an adaptive management approach: an iterative process where work occurred in phases, building from the information described in the Hood Canal Bridge Ecosystem Impact Assessment Plan[5]. Studies conducted during Phase 1 of the assessment were under the purview of the Assessment Team members listed at the beginning of this document. The Assessment Team worked with a Management Committee to evaluate Phase 1 progress and develop recommendations for Phase 2 actions and effectiveness testing. External reviewers and contributors were engaged as needed along the way to ensure Phase 1 results and recommendations are broadly accepted.

Phase 1 of the assessment was structured around a multi-question framework described in full in the Hood Canal Bridge Ecosystem Impact Assessment Plan. Briefly, Phase 1 consisted of investigating two main questions: 1) how does the bridge impact juvenile steelhead migration and mortality and potentially other fish species (including salmon) and 2) what are the bridge's effects on water quality and do those effects impact the entire Hood Canal ecosystem? These questions and associated sub-questions served to define assessment components that were addressed in a stepwise process through multiple Phase 1 studies and subsequent synthesis across studies.

The following provides a brief summary of the methods and outcomes of each assessment component included in Phase 1 research. Extended methods and results for each assessment component, as well as technical reports and peer-reviewed publications associated with select assessment components, are provided in full in Appendices A-F. Assessment components are ordered and numbered consistently with the framework developed in the Hood Canal Bridge Impact Assessment Plan for cross-reference across sections and documents. **Due to the complex interconnected nature of this assessment, the component numbers do not reflect order or priority**. The key questions, sub-questions, associated hypotheses and affiliated assessment components, along with Principal Investigators, are all mapped in Appendix G. Hood Canal Bridge Impact Assessment Matrix.

[5] Hood Canal Bridge Assessment Team. 2016. Hood Canal Bridge Ecosystem Impact Assessment Plan: Framework and Phase 1 Details. Long Live the Kings, Seattle, WA.

I. How is the bridge acting as a barrier to juvenile steelhead migration and leading to increased mortality? How does the bridge influence other fish, including salmon?

A. What are fish migration behavior and fish distribution patterns at versus away[6] from the bridge? For steelhead, what defines a successful migration past the bridge versus one that results in mortality?

Juvenile steelhead acoustic telemetry provided the core data of the Phase 1 investigation of bridge impacts on fish migration and mortality. Prior telemetry research (Moore et al. 2013) indicated the Hood Canal Bridge might delay migration of steelhead smolts and contribute to disproportionately high mortality at this location compared to the rest of the freshwater-to-ocean migration. During Phase 1, the telemetry receiver array at the bridge was expanded beyond previously established array designs to enable triangulation of tags and map individual migration paths and mortality locations of tagged fish. Hydroacoustic surveys in North Hood Canal provided context on broader fish distribution patterns during the outmigration season.

1. Track steelhead migration behavior at bridge and steelhead mortality before, at, and after bridge

Megan Moore and Barry Berejikian, NOAA Northwest Fisheries Science Center

For detailed methods and results, see Appendix A.

Wild steelhead smolts were collected from the South Fork Skokomish River and Big Beef Creek during April-May 2017 and 2018. Each smolt was surgically implanted with an acoustic transmitter. Different types of transmitters were used throughout the study period: some tag groups were implanted with basic transmitters, some were implanted with transmitters that contained pressure sensors, and some were implanted with transmitters that contained temperature sensors. One additional group was implanted with transmitters programed to be silent for a portion of the migration to test the “dinner bell” hypothesis, which suggests that pinnipeds may hear and target actively-pinging transmitters; no evidence was found for differential mortality between steelhead implanted with silent transmitters versus actively-pinging transmitters.

Acoustic receivers were deployed at various locations along the steelhead outmigration route from Hood Canal rivers to the Pacific Ocean, including a network of receivers at the bridge placed closely together such that individual transmitter positions could be calculated as tagged steelhead moved through the receiver array (Figure 5). After the outmigration season, a boat-based receiver was deployed to compare locations of stationary transmitters (mortalities) at fixed stations situated both near and far from the bridge.

[6] Within this document, the terms “at the bridge”, “near the bridge”, and “within the bridge zone of influence” refer to the yet established geographic area around the bridge that is impacted by the various causal agents being investigated, whereas “away from the bridge” refers to the area beyond impact zone of the bridge.

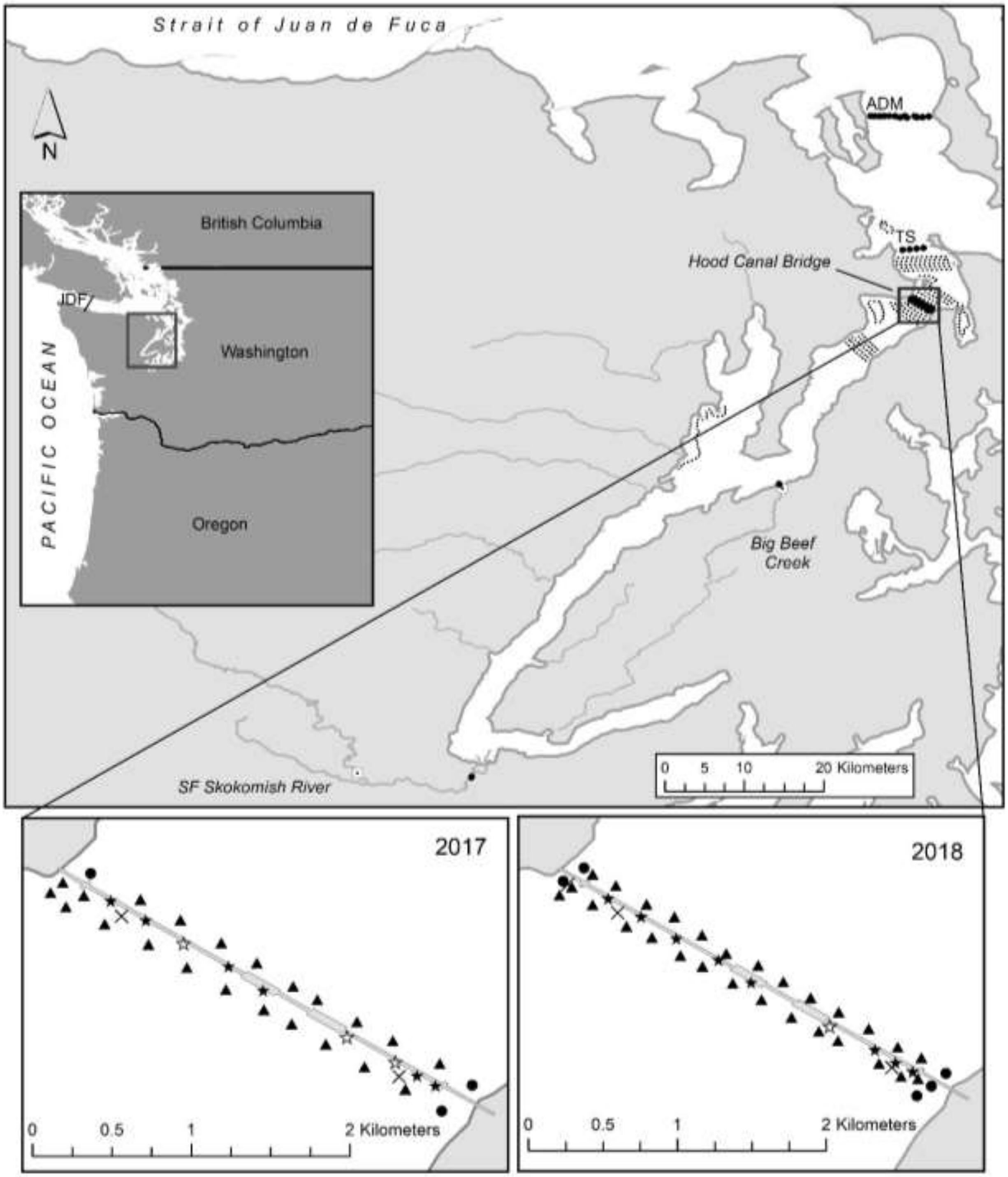

Figure 5. Receiver locations (black dots) at the mouths of Big Beef Creek and the Skokomish River downstream of in-river release locations for tagged steelhead (white dots), the Hood Canal Bridge, Twin Spits (TS), Admiralty Inlet (ADM), and the Strait of Juan de Fuca (JDF, black line). Boat-based survey locations are shown as tiny black dots. Lower insets show the receiver array installed at the bridge in 2017 and 2018 (various shapes denote types of receiver deployments; see Appendix A).

On average, the bridge delayed surviving tagged steelhead by 1-2 days, which means fish spent roughly 6-10% of their total migration time on a distance representing 0.5% of their total journey. About half of the tagged steelhead that encountered the Hood Canal Bridge died there; survival probabilities for the 7 km migration segment including the bridge were 49-57% across the two years of study. Survival probability was not related to smolt size, the location at which smolts first approached the bridge, tidal stage, current velocity at time of first approach, or time (day vs. night) of first approach. However, survival probabilities did vary by week during the outmigration period, with later-arriving fish having higher probability of survival (Figure 6).

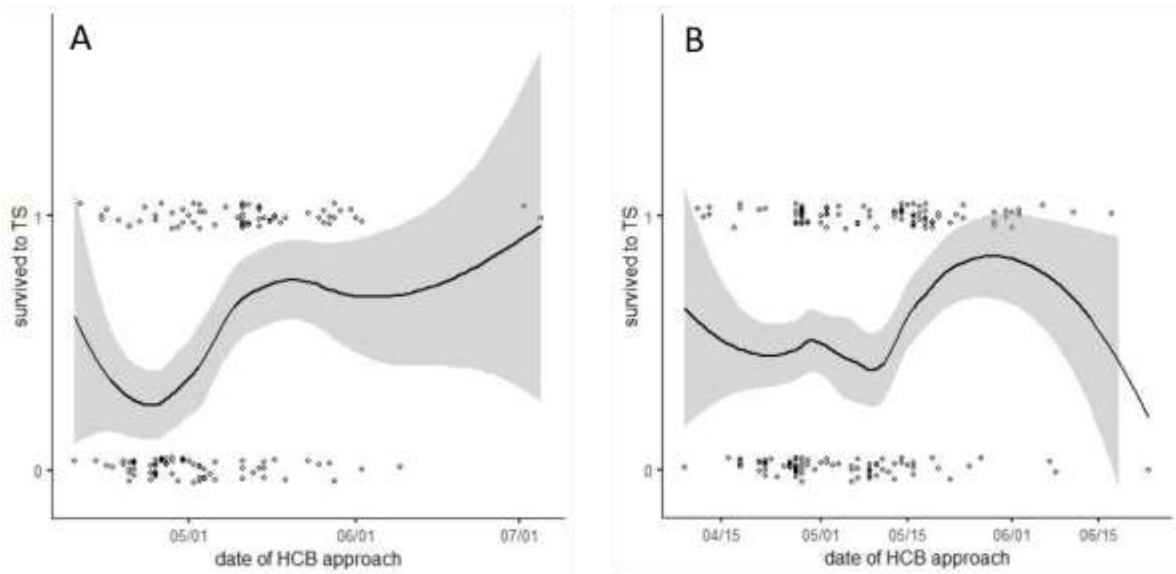

Figure 6. Logistic regression showing the relationship (black line = moving average of odds of survival) between survival probability (1 = survived, 0 – did not survive) past the Hood Canal Bridge (HCB) to the Twin Spits (TS) receiver array and the date of first approach at the HCB in 2017 (panel A) and 2018 (panel B).

Density patterns of surviving steelhead smolts were consistent across years, with high densities observed in corner locations formed by pontoons that extend perpendicularly out into the water from the bridge's deck (Figure 7 A, B). Density patterns of non-surviving tagged fish (presumed mortalities) were also consistent across years. Similar to survivors, mortalities were concentrated along the south side of the bridge and in corner locations (Figure 7 C, D). However, survivors were more frequently located near the center drawspan and on the east side of the bridge than mortalities. Stationary tags (see Appendix A, Figure A6) were less likely to be found further away from the bridge structure, although a few were identified in nearby Port Gamble Bay and along the route from the Hood Canal Bridge to Port Gamble Bay.

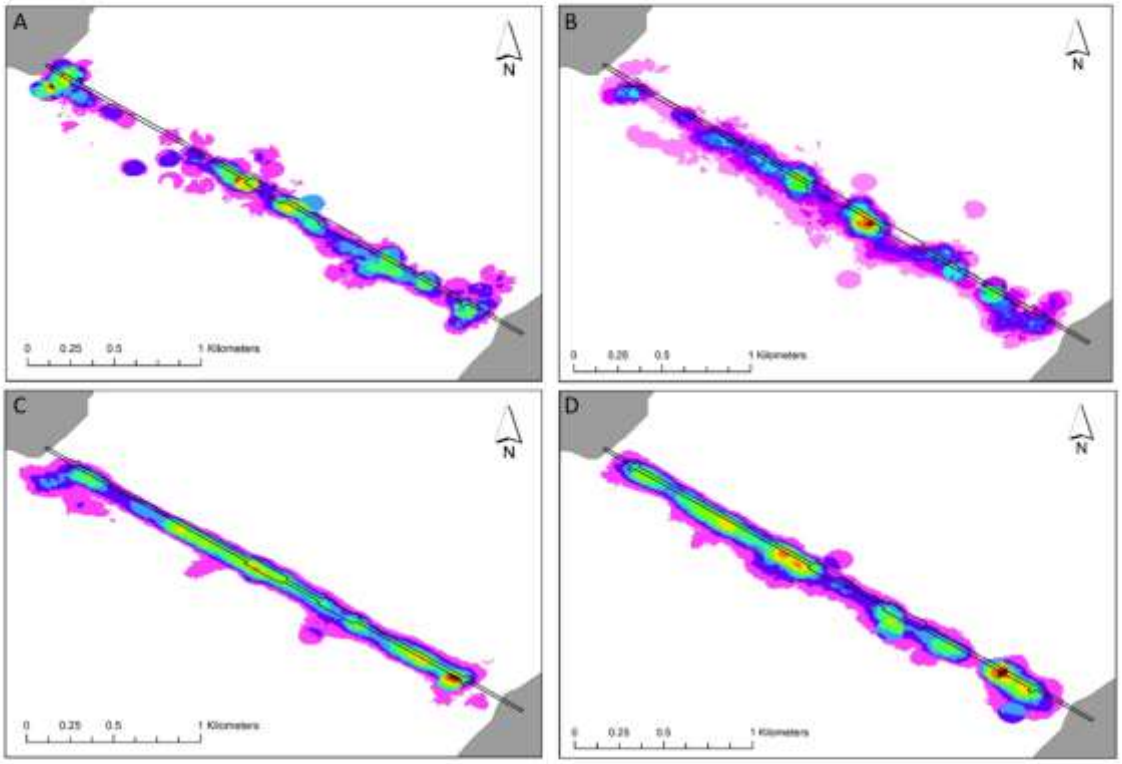

Figure 7. Density of tagged steelhead encountering the HCB that survived past the bridge in 2017 (A) and 2018 (B) compared to density of tagged steelhead that did not survive past the bridge in 2017 (C) and 2018 (D). Dark red indicates highest densities, blue/green represent intermediate densities, and pink/purple represent lowest densities. Density values differ between figures and scale with sample size.

Steelhead that successfully crossed the bridge did so by crossing through open east and west spans (2017: 49%, 2018: 23%) that are not obstructed by bridge pontoons or by diving underneath the bridge pontoons (2017: 51%, 2018: 77%). Crossing locations were distributed fairly evenly along the length of the bridge (Figure 8). Most (84%) crossings took place during daylight hours, and crossing was much more likely to occur during ebb tides. Except for the brief dive period of those fish that crossed underneath bridge pontoons, tagged steelhead were strongly surface-oriented and traveled in the upper 1 meter of the water column.

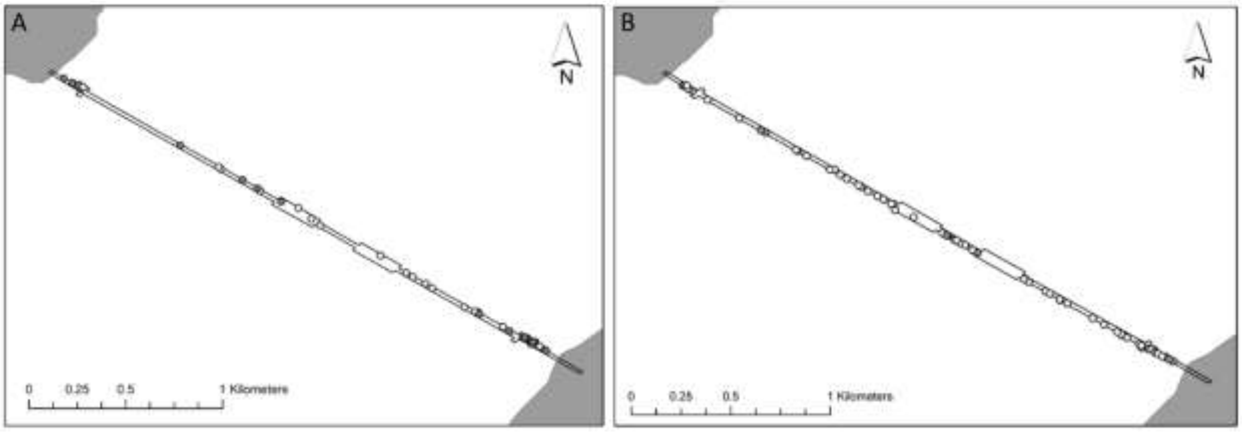

Figure 8. Locations where tagged steelhead crossed the HCB in 2017 (A) and 2018 (B). Open circles represent day crossings; filled circles represent night crossings.

2. Map fish densities and distribution at vs. away from bridge
   Hans Daubenberger, Port Gamble S'Klallam Tribe and Emily Bishop, Westward Ecology

For detailed methods and results, see Appendix B.

Fish abundance and distribution in the upper 10 meters of the water column near the bridge were mapped weekly using a split-beam hydroacoustic transducer deployed from a boat running along predetermined transect lines both perpendicular (2017) and parallel (2018) to the bridge infrastructure (Figure 10). Data were filtered to exclude bridge infrastructure and isolate acoustic returns corresponding to juvenile salmonid-sized fish. Visual observations from the bridge deck (further described in Assessment Component 14) suggest that fish aggregate at some portions of bridge infrastructure; those patterns are not apparent in this particular dataset as the methods used were insufficient to characterize the 15m adjacent to bridge infrastructure.

Figure 9. Transect lines surveyed in 2017 (red) and 2018 (yellow). The long center transect perpendicular to the bridge was sampled across both years.

No significant trend in fish density was observed with distance from the bridge (excluding the 15 m directly adjacent to the structure), and the probability of high/low fish density did not differ among areas 15-200 meters away from the bridge and areas 200 meters to 2 km from the bridge. Fish density along the length of the bridge was similarly stochastic. Areas of both high and low densities appeared across both survey seasons, but no consistent spatial or temporal patterns in densities were observed. When averaged across all weeks, the center transect perpendicular to the bridge structure showed a slight increase in density with increasing proximity to the south side of the bridge, but this correlation was not consistent across individual weeks.

An initial alignment of fish detection data with the zooplankton data described in Assessment Component 14 suggests a positive relationship between plankton density and fish density, which may be indicative of fish response to plankton patterns near the bridge.

B. Are steelhead and other fish at the bridge more susceptible to predation (vs away from the bridge)? If so, who are the primary culprits?

Migration delays described in Assessment Component 1 increase the density of migrating smolts on the south side of the bridge and channel migrating smolts through more densely concentrated routes, potentially attracting predators and facilitating predation. Additionally, pontoons extending from the bridge deck create corner areas which aggregate fish and may reduce their ability to evade predators.

3. Map predator (marine mammal and seabird) densities

Jessica Stocking and Scott Pearson, Washington Department of Fish and Wildlife

Hans Daubenberger, Port Gamble S'Klallam Tribe and Emily Bishop, Westward Ecology

For detailed methods and results on boat-based predator surveys, see Appendix C and bridge-based surveys, see Appendix B.

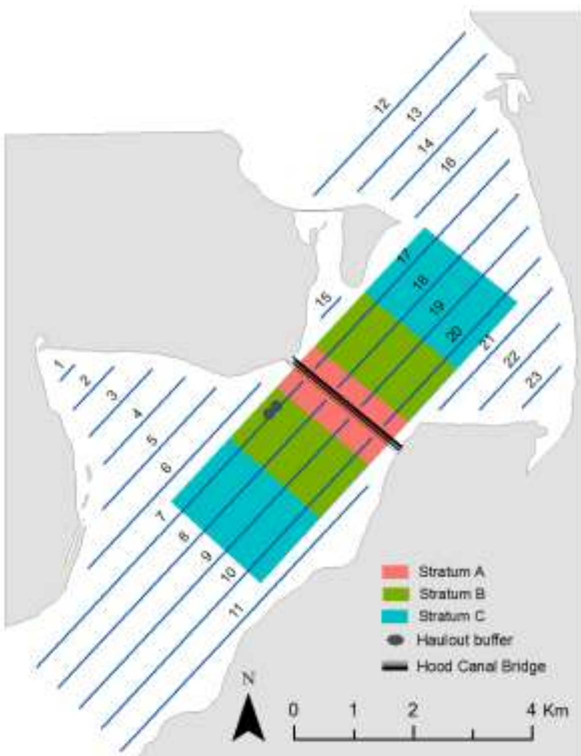

Figure 10. Predator survey transects used to survey potential steelhead predators near vs. far from the bridge (bold blue lines) and within three distance strata from the bridge (A = 0-300 m, B = 301-1500 m, C = 1501-3000 m).

Boat-based visual predator surveys were conducted weekly along transects running perpendicular to the bridge (Figure 11). Only in-water/on-water predators were counted; flying birds were not included in the count unless they were observed landing or foraging within the survey area or unless they were an aerial hunting species (bald eagles, osprey, terns). All harbor seals and cormorants within 100 m of the Sisters Rock seal haulout site southwest of the bridge were removed from analysis since they were not actively foraging.

The density of predators in pool areas of the bridge infrastructure (further described in Assessment Component 14) was quantified using a survey method intended to produce comparable density estimates to boat-based surveys. Observers recorded predator presence within the pools for 40 seconds, based on the estimated time it would take to observe the same area during a boat-based survey.

Boat-based surveys recorded over 13,000 individual observations of predators, including 22 piscivorous avian species and three marine mammal species. We note only a few species here; all are detailed in Appendix C. Pigeon guillemots were the most numerous predator species observed throughout the study, with highest distributions along shorelines and at the bridge. Pigeon guillemots are unlikely to be a major source of juvenile steelhead mortality as there is little overlap in the prey sizes guillemots consume and the size distribution of outmigrating juvenile steelhead. However, juvenile Chinook, coho, and chum all fall within the preferred prey length of pigeon guillemots and observers on the bridge deck noted guillemots feeding on chum and Chinook.

Figure 11. Harbor seal in the water next to one of the bridge pontoons. Photo courtesy of Port Gamble S'Klallam Tribe.

Harbor seals and harbor porpoises were observed in generally low densities throughout the study area, although boat-based surveys may not have fully captured the area directly alongside the bridge due to restrictions on vessel distance from the bridge infrastructure. Seals and porpoises were typically observed as single animals rather than foraging in groups (Figure 12). Both species were observed at higher densities near the bridge than away from the bridge in 2017; that pattern was not apparent in 2018, when densities were similar across the entire survey region. In-pool densities of harbor seals were slightly lower but not significantly different than out-of-pool densities (see Appendix C, Figure C17). Harbor seals are a known predator of juvenile steelhead in other regions of Puget Sound, although no diet information for harbor seals at the bridge was collected through this study.

While not considered to be potential major predators on juvenile steelhead, distribution patterns for two other avian species are of note: rhinoceros auklets were observed almost exclusively north of the bridge and marbled murrelets were more abundant to the south. These surprising distribution patterns raise questions about whether the bridge may influence the movement of bird populations into or out of Hood Canal.

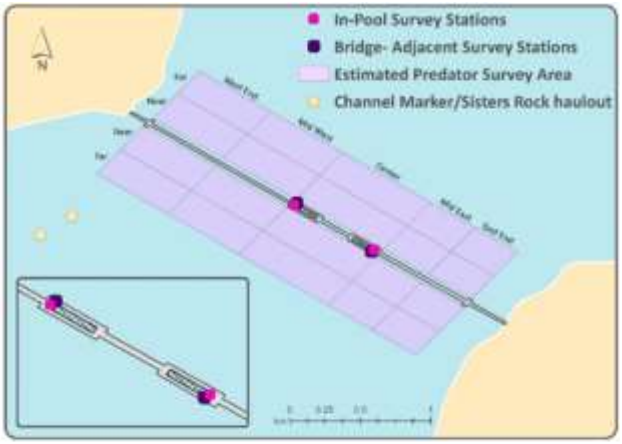

Figure 12. Observers stood on the upper bridge deck at locations marked with purple dots to survey the pale purple area. Pink dots represent observer locations on the lower bridge deck for pool surveys described in **Assessment Component 14**.

Bridge-adjacent predator surveys took place on the upper bridge deck. During these surveys, one observer visually swept surface waters with binoculars identifying and enumerating every predator observed in the gridded survey region (

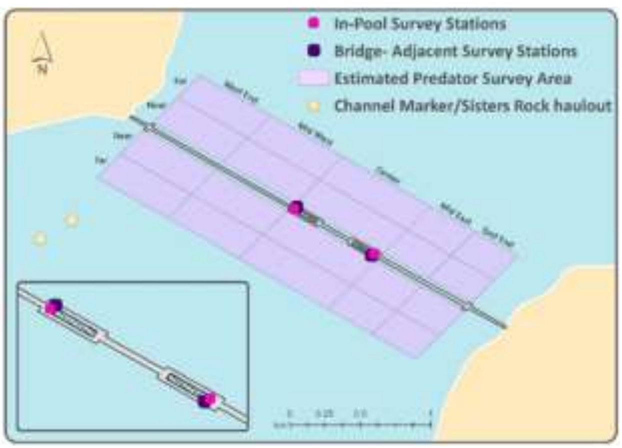

Figure 13), while another observer recorded data and assisted in identifying species as needed. Seabirds in flight were not counted, nor were birds perched on the bridge. Predators were only recorded at first detection to avoid recounting if an individual moved across survey regions.

Predators were observed in the vicinity of the bridge during every bridge-adjacent visual survey. Weather appeared to affect predator location: southerly winds were associated with higher abundances of avian predators on the north side of the bridge while northerly winds were associated with avian predator observations on the south side of the bridge. In light wind conditions, predators were always observed on both sides. Observers reported that predators did not appear deterred by bridge-associated noise and, while they avoided the center span during bridge openings, boat traffic did not cause them to leave the general area. For some predators, the bridge appeared to function as a shoreline. Pigeon guillemots were observed flying into open ledges on the bridge structure and seals were observed hauling out onto bridge floats at night. WSDOT workers reported pigeon guillemots breeding on the bridge. No nests were confirmed during predator surveys in April/May; however, during this time pigeon guillemots would be incubating eggs on the nests, so nesting activity may have gone unobserved.

Data collected from juvenile steelhead implanted with pressure-sensitive and temperature-sensitive transmitters (described in [Assessment Component 1]; detailed methods and results in [Appendix A]) allowed insight into which of the predator species described above was responsible for juvenile steelhead mortality. Of the steelhead smolts implanted with pressure-sensitive transmitters, all survivors exhibited strong surface orientation whereas 83-85% of mortalities approached the bridge near the surface then suddenly changed behavior and began exhibiting frequent deep dives, a subset of which eventually became stationary (Figure 14). Time between first detection at the bridge and the behavioral change indicating a predation event averaged 17 hours in 2017 and 1.6 hours in 2018; nearly all (90%) predation events occurred within two days of bridge encounter.

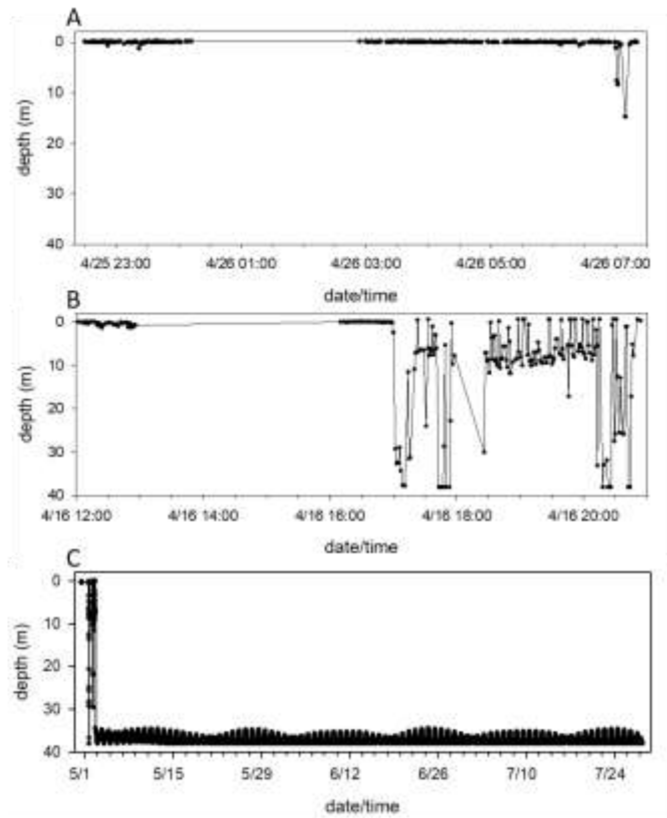

Figure 13. Depth profiles of tagged steelhead exhibiting behavior typical of a surviving smolt (A), a non-surviving smolt that was eaten by a deep and frequently-diving predator (B), and a non-surviving smolt that was eaten then excreted by the predator and became stationary on the seafloor, continually pinging until the transmitter battery expired. The maximum depth detectable by the tag sensors was 38 m.

Dive behavior of the predated tags was compared with literature values for dive behaviors of several different candidate predators (see [Appendix C2]). Of the candidate predators, avian species at the bridge are capable of diving to > 37 m deep but do not typically do so on a regular basis (pers comm Scott Pearson). The avian predators common at the bridge primarily forage in water shallower than 40 m. Less information was available on harbor porpoise behavior; observations at the bridge suggest they do not spend extended periods of time at the bridge but rather migrate through the area on a regular basis. Despite indications that porpoise behavior does not match with observed predation patterns at the bridge, they cannot be ruled out as a candidate predator. Harbor seals are likely to regularly dive to depths > 40 m, and are regarded as the most likely candidate predator that would cause the observed tag dive patterns.

Of the steelhead implanted with temperature-sensitive tags, 69% of mortalities exhibited elevated temperatures consistent with the internal body temperature of a marine mammal or bird, with temperature increases occurring an average of 18 hours after tagged steelhead arrived at the bridge. Nearly 40% of mortality sensors with elevated temperature were detected within range of Sisters Rock, a known harbor seal haulout 750 meters south of the bridge. As noted in Assessment Component 1, a few mortalities were associated with the nearby Port Gamble Bay site, where harbor seal haulouts have also been documented[7].

Locations of predation events as defined by behavioral change or temperature increase tended to be close to the bridge and dispersed along the length of the bridge, with a slightly western bias. Several (40%) of predation events occurred in close proximity to the corners formed by cross-pontoons extending from the main bridge infrastructure (Figure 14).

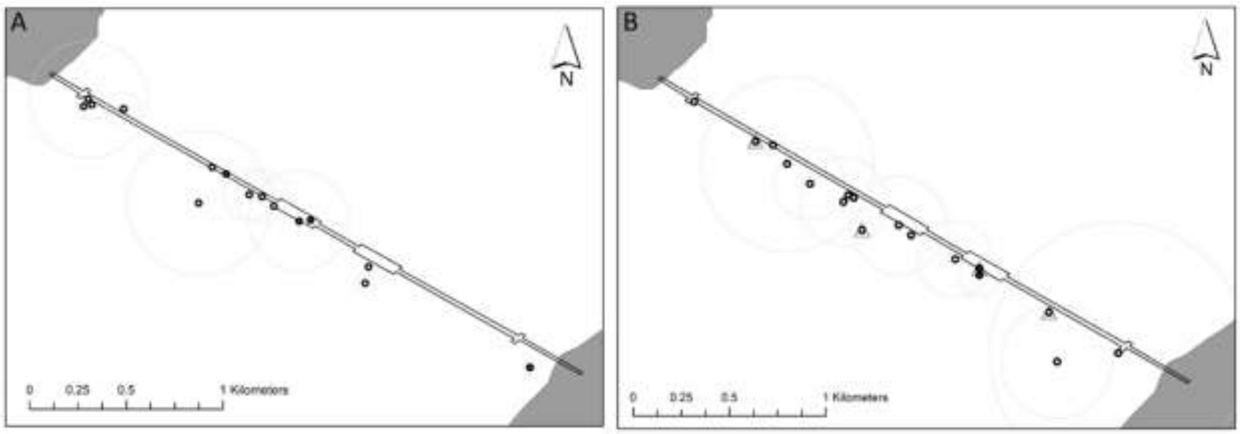

Figure 14. Locations of identified predation events in 2017 (A) and 2018 (B). Open circles represent predation events that occurred during daylight hours while filled circles represent events that occurred during nighttime hours. Gray circles represent the error radius in meters (some are so small they are obscured by the event symbol), with gray triangles marking locations where data were not available for error calculation.

4 & 5. [Potential] Assessing harbor seal-related steelhead (and other salmon) mortality

These components were not funded for Phase 1, and consequently, the Phase 1 remaining research needs and solutions prioritizations reflect this lack of data.

C. What is the influence of the bridge on the surrounding physical environment, at vs away from the bridge?

There are numerous pathways through which the bridge can lead to fish mortality. The data collected indicate that the most likely pathways include the bridge pontoons acting as a physical barrier for fish and/or altering water circulation and other water properties such that fish are deterred. This delay then increases fish densities in nearby areas, subsequently increasing susceptibility to predation. Other factors like noise or light may intensify or exacerbate these impacts. Vehicle traffic across the bridge generates sound and vibrations into the surrounding waters. The bridge's design includes light posts along the length of the southern side of the upper bridge deck, additional lighting around the east and west control towers, and a navigation light on the center drawspan. Light spillover from the bridge lighting into surface water at night (Figure 16) may impact juvenile salmon, steelhead, and their predators.

[7] Jeffries et al. 2003. Trends and status of harbor seals in Washington state: 1978-1999. Journal of Wildlife Management 67(1): 207-218.

6. Measure light and shade impacts to fish and predator behavior

Hans Daubenberger, Port Gamble S'Klallam Tribe and Emily Bishop, Westward Ecology

For detailed methods and results, see Appendix B.

A LiCor sensor attached to an extendable pole was held over the lower deck's railing, about one meter horizontally away from the bridge and three meters vertically over the water's surface, and walked around the perimeter of the lower bridge deck during a full moon with partial to no cloud cover and a new moon under heavy cloud cover. Lux values (illuminance) were highest on the south side of the bridge and the pool areas described in Assessment Component 14, exceeding the typical value for a full moon at mid-latitudes.

Figure 15. The Hood Canal Bridge viewed from the water at night. Photo courtesy of Port Gamble S'Klallam Tribe.

All but one of the nighttime mortality locations were near the well-lit pool areas. Turning bridge lights off at night was not possible during Phase 1 and we therefore cannot speculate whether tagged steelhead behavior would have changed if bridge lighting was not present. Light levels observed along the bridge at night are within a range that may affect juvenile chum and Chinook salmon behavior. Preliminary data from within the well-lit pool and at a section of the bridge with less artificial light indicate harbor seals foraged in both areas across day and night hours, but in the less well-lit area seal activity was lower at nighttime than daytime whereas in the well-lit pool seal activity was relatively consistent across day/night hours. Additional work would be necessary to understand and quantify light effects across bridge infrastructure on smaller salmonids and on predator behavior; the growing body of literature regarding artificial light impacts on salmon passage and predation dynamics and precedent from other bridges in the region raise the importance of continued consideration of potential light impacts at the Hood Canal Bridge.

7. Measure noise impacts to fish behavior

Daniel Deng, Xiaoqin Zang, Jayson Martinez, Jun Lu, Scott Titzler, Pacific Northwest National Laboratory

For detailed methods and results, see Appendix D.

A pilot study was conducted to characterize noise propagation from the bridge and determine whether sound (pressure and particle motion) was in a range that could negatively impact juvenile salmon and steelhead behavior. Three sets of sound and vibration monitoring systems which included hydrophones and accelerometers were installed along the bridge near the metal section of the roadway which produces loud sounds when vehicles cross. Traffic volume data were provided by the Washington State Department of Transportation. Wind speed could affect measurements of sound pressure levels and particle speed accelerations; wind data were collected from a nearby buoy to evaluate the relationship between wind and noise. Background noise levels were measured with a hydrophone deployed while drifting a boat with the motor off about 70 m away from the bridge. To evaluate sound attenuation with distance from the bridge, a sound broadcasting test was conducted by deploying an underwater speaker from the bridge and measuring sound levels with the boat positioned 60, 80, and 120 m away from the bridge.

Vehicle crossing noise was easily identified in audio files collected by the sound and vibration monitoring systems. There was strong diurnal variation in sound pressure levels and particle speed accelerations – quiet and low acceleration during the night versus loud and high acceleration during the day – which was not unexpected given typical traffic patterns. Observed measurements correlated closely with observed traffic volumes, especially when accounting for type of vehicle (motorcycles/cars, single-unit trucks, double-unit trucks, triple-unit trucks). Wind speed was also weakly correlated with sound pressure levels and particle speed accelerations.

NOAA Fisheries and US Fish and Wildlife Service have suggested 150 dB re 1 µPa rms as the threshold for behavioral effects to fish species that are listed as being threatened or endangered, although the specific threshold for salmon response to sound levels in saltwater has not been well-defined. Salmon are believed to be more sensitive to particle motion than sound pressure, and based on a literature synthesis of juvenile salmon avoidance responses to sound, the threshold for adverse impacts to juvenile salmon and steelhead was set at 0.01 m/s^2 in the 5-10 Hz band. Observed sound pressure levels and particle speed acceleration at the bridge were mostly below these thresholds of adverse effects, and sound pressure levels 70+ m away from the bridge were always below the adverse effects threshold.

There were no differences observed in tagged steelhead migration behavior or mortality over day (high traffic volumes, high sound pressure and particle acceleration) versus night (low traffic volumes, low sound pressure and particle acceleration), and observers on the bridge reported no obvious changes in either fish or predator behavior associated with noise.

D. What are the impacts of pools and eddies created by bridge pontoons adjacent the center drawspan?

The bridge infrastructure design includes cross-pontoons that jut out perpendicularly from the bridge deck into the surrounding waters, forming 90˚ corners in several spots along the bridge. Additionally, large open sections are cut into the sub-deck of the bridge. When the bridge opens to allow vessel traffic the drawspan retracts into these sections; when the bridge is closed, these sections create large pools of water that can aggregate debris and plankton. These corner areas and bridge pools affect water flow and fine-scale circulation, potentially impacting plankton, fish, and predator behavior.

Zooplankton abundance and species composition were important considerations as indicators of bridge effects. Altered circulation caused by water moving past the bridge could clump plankton into dense patches or force plankton away from their typical positions within the water column.

14. Comparative assessment of fish, predator, zooplankton densities in pools and eddies vs away from them

Hans Daubenberger, Port Gamble S'Klallam Tribe and Emily Bishop, Westward Ecology

For detailed methods and results, see Appendix B.

Zooplankton and water quality parameters (including temperature, salinity, pH, dissolved oxygen, chlorophyll, and blue-green algae) were sampled at locations spanning areas both north and south of the bridge as well as within bridge pools (Figure 17). Water quality was measured over the top 50 meters of the water column. Zooplankton samples followed protocols developed through the Salish Sea Marine Survival Project[8], except that sampling was restricted to the surface 0-5 meters of the water column.

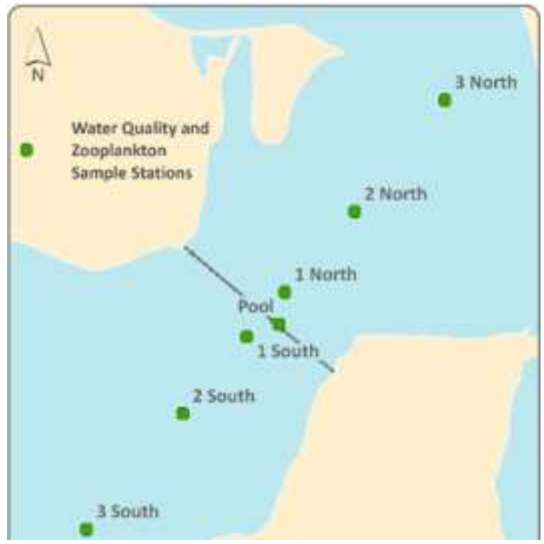

Figure 16. Stations sampled April-May 2017; stations labeled "2 North" and "2 South" were also sampled weekly April-May 2018.

Within three of the seven weeks sampled, differences in surface water temperature and dissolved oxygen at the surface between north and south sampling stations were measurable and significant based on Washington State water quality standards[9]. These results align with the model output and conclusions described in Assessment Component 9.

Figure 17. Juvenile chum salmon swimming in a cloud of larval crab within one of the bridge pools. Photo courtesy of Port Gamble S'Klallam Tribe.

Although limited by small sample sizes, zooplankton density appeared slightly higher within bridge pools than at stations north/south of the bridge infrastructure, and slightly higher south of the bridge than north of the bridge. The vertical tow sampling method and small net mesh size used in this sampling design likely did not accurately reflect the abundance of fast-moving, larger plankton taxa. Visual observations showed dense aggregations of these large plankton taxa (euphausiids/krill, larval crab) within bridge pools which were not well-captured in zooplankton samples (Figure 18).

[8] Keister and Winans 2015. SSMSP Zooplankton Sampling Protocol. Full protocol linked here.
[9] WAC 173-201A-320, Ecology. Full legislative text linked here.

Tagged steelhead were rarely observed in pools, however they were disproportionately observed in corner areas of the bridge. To determine steelhead associations with bridge corners, unique steelhead transmitters were quantified within a 150 m along-bridge x 100 m perpendicular-to-bridge area adjacent to all corners formed by bridge pontoons. Only surviving fish were included in this analysis, because it was not possible to determine whether a non-surviving transmitter was in a steelhead or a predator at the time of position triangulation within the corner. Therefore, this analysis represents a minimum estimate of the number of fish affected by corner structures and does not take into account steelhead that may have died as a result of being eaten in a corner area. In 2017, approximately 60% of surviving fish encountered a corner area on the bridge; in 2018, 73% of survivors were detected in corner areas.

Surface predator surveys within bridge pools were designed to complement the boat surveys described in Assessment Component 3 to compare in-pool/out-of-pool predator presence. Surveyors observed the 90mx20m body of water and recorded the number of each predator species present. Predators were observed in 45% of the bridge pool surveys. Pigeon guillemots were the most frequently seen predator species within the pools, with as many as three individuals recorded during a 40-second survey period. No predators other than pigeon guillemots were recorded in the east pool, despite frequent observations of seals made by surveyors before and after the official survey period. Seals were observed twice in the west pool; three on 5/9/17 and two on 5/31/18. No other predator species were observed in bridge pools during surveys.

As described in Assessment Components 1 and 3, corner areas created by cross-pontoons were associated with higher densities of tagged steelhead (Figure 7) and with predation events on tagged steelhead (Figure 14). A BlueView imaging sonar unit was deployed in three locations to capture underwater predator presence: 1) within the bridge pool, 2) outside of the pool facing away from the bridge structure, and 3) in one of the corner areas created by a cross-pontoon (Figure 19).

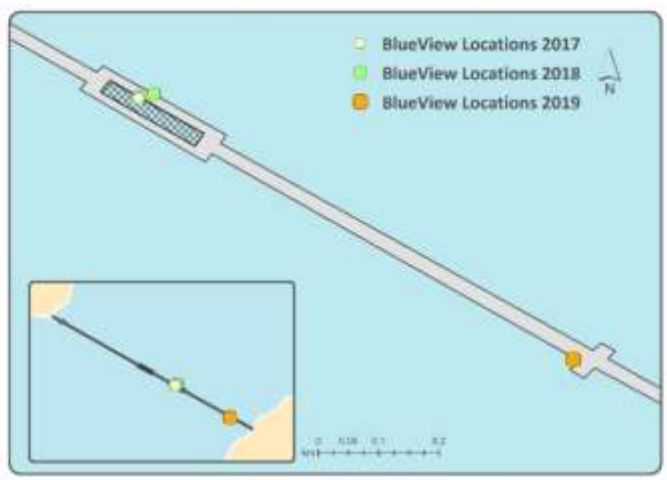

Figure 18. BlueView imaging sonar deployments in 2017 (deployed in east pool April 12-June 2, recording intermittently), 2018 (deployed in eastpool for 2 days, deployed on bridge structure facing away from bridge for 2 days), and 2019 (deployed in southeast corner for 20 days).

Seals were observed in the pool area at all hours of the day and night, spending an average of 39 seconds every hour within 30 m of the BlueView device in 2017 (Figure 19) and a maximum time of 9 minutes 17 seconds in a single hour. Seal presence was slightly higher during daylight hours versus nighttime hours. Comparison of in-pool and out-of-pool data in 2018 did not show large differences in seal presence or behavior in these two areas (Figure 20).

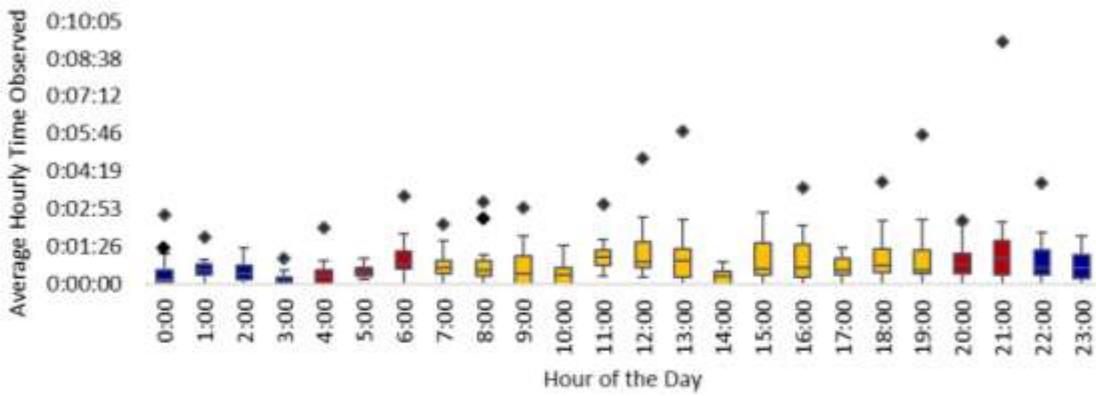

Figure 19. Hourly time observed (a summation of time seals were observed within 30 m of the BlueView unit over the course of one hour) averaged for each hour of the day across 20 days of BlueView placement within the east bridge pool in 2017. Blue bars represent nighttime hours, red represent dawn and dusk, and yellow represent daylight hours.

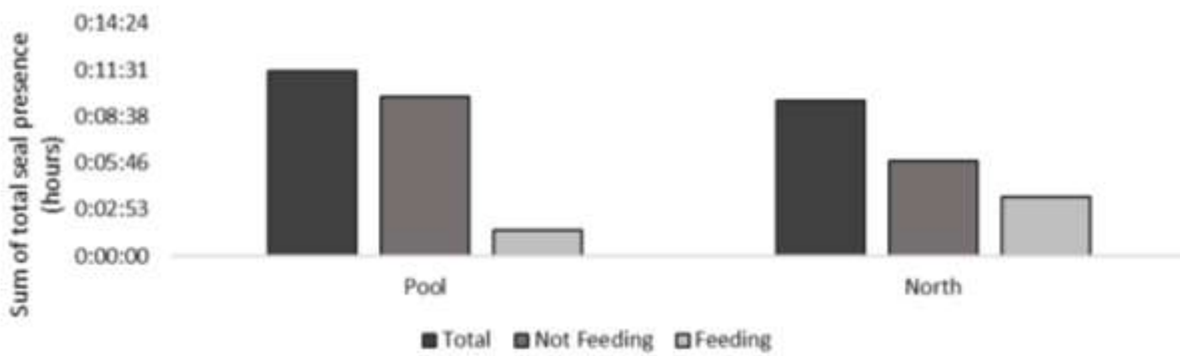

Figure 20. Sum of seal presence over 24 hours within 30 m of the BlueView unit deployed inside the east bridge pool (June 5, 2018) and on the north side of the bridge outside the east pool (June 7, 2018) looking away from the structure. The light gray and intermediate gray bars reflect time spent feeding and not feeding, respectively, and the dark gray bar represents the sum of the two behavior categories.

Seal presence was higher in a southeast corner area created by a cross-pontoon; seals spent an average of 111 seconds every hour within 30 m of the BlueView device (Figure 21) with a maximum time of 18 minutes 28 seconds in a single hour. Seal presence in the corner was significantly higher during daylight hours (155 seconds/hour) than during nighttime hours (51 seconds/hour).

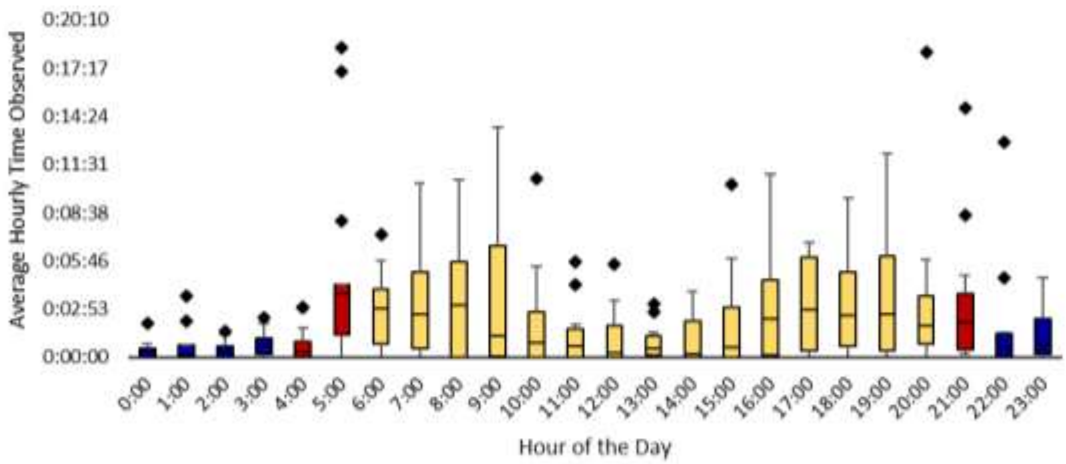

Figure 21. Hourly time observed (a summation of time seals were observed within 30 m of the BlueView unit over the course of one hour) averaged for each hour of the day across 20 days of BlueView placement within a southeast corner area in 2019. Blue bars represent nighttime hours, red represent dawn and dusk, and yellow represent daylight hours.

E. What influences steelhead migration/mortality and fish distribution patterns near the bridge? What are the spatial-temporal relationships between steelhead migration and mortality patterns, fish densities, predator densities and how the bridge is impacting the surrounding physical environment?

13. Synthesize patterns of steelhead migration behavior and mortality and fish distribution with predation densities and distribution, and the physical impacts of the bridge (physical barrier, water circulation, water quality, light and noise)

The Assessment Team spent a considerable amount of time reviewing data and results of each assessment component and synthesizing across components both qualitatively and quantitatively. Tagged steelhead migration behavior and mortality data were considered in combination with predator survey data, hatchery salmon release data, rainfall data, day/night, bridge opening data, near-bridge fish biomass, and water characteristics (e.g., tide, turbidity). Maps of fish biomass and predator density were compared visually to assess patterns. Some of these comparisons (e.g., noise/light effects on tagged steelhead behavior and mortality) are described in preceding individual assessment components; this section focuses on data comparisons and analyses that exceeded the scope of other individual components.

Increasing survival probabilities across the outmigration season associated with hatchery releases and higher turbidity

Survival of tagged steelhead smolts was related to the date the fish approached the bridge, with higher probabilities of survival after early-to-mid May each year. Two factors co-varied with steelhead mortality probability across the outmigration season: turbidity and hatchery salmon releases. Higher turbidity was correlated with higher survival probabilities, although the mechanism underlying this relationship is not yet understood. Three hatcheries (Quilcene, Cushman, and George Adams) release several million salmon into Hood Canal each spring. Releases include coho, chinook, and steelhead, and typically are performed over April and May. A preliminary pairing of known release timing, estimated travel time of hatchery fish from release to bridge, and observed fish species at the bridge suggests that the arrival of hatchery releases at the bridge roughly aligns with an increase in survival probability for tagged steelhead (Figure 23). This may be due to a buffering effect where the large number of hatchery fish present at the bridge temporarily alleviates the predation pressure experienced by the relatively few steelhead at the bridge.

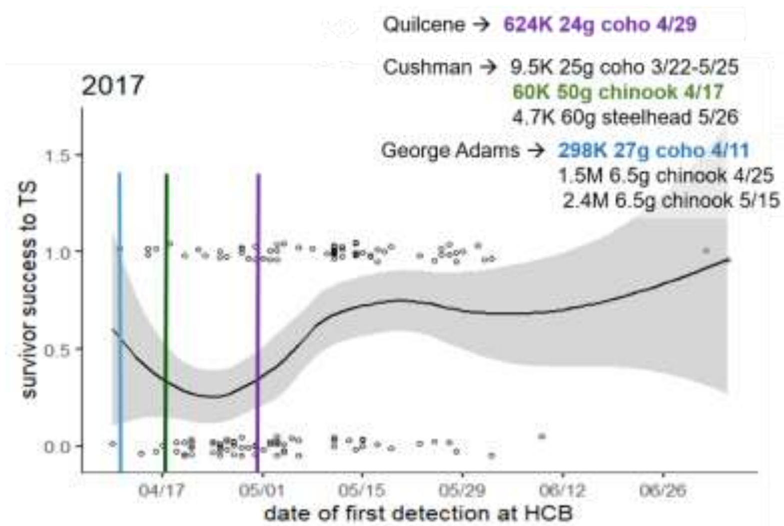

Figure 22. Survival probability over the outmigration season, overlaid with timing of Quilcene coho (purple line), Cushman Chinook (green line), and George Adams coho (blue line) hatchery releases.

Time to event analysis

To understand whether the length of delay in migration caused by the bridge influenced the rate of predation we compared passage rate and predation rate. We were able to determine the time of predation for smolts tagged with depth sensors, and the time of passage for fish that were detected on both sides of the bridge, so we developed Kaplan-Meier curves for a subset of 32 steelhead smolts in 2017 (Figure 24). Smolts pass the bridge (blue line) at the same rate they are being eaten (red line) during the first two days of encounter (after

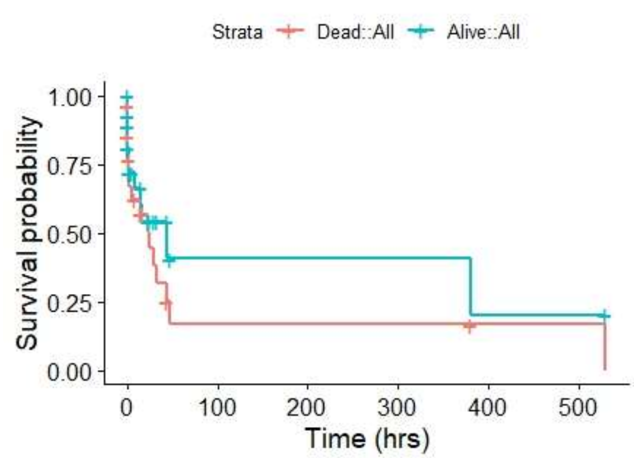

Figure 23. Time to passage versus time to predation upon tagged steelhead first encountering the bridge.

that sample sizes are too low to make a reliable comparison). This analysis shows that smolts spending more time at the bridge are not necessarily more susceptible to predation than those taking less time to pass. Rather, both passage events and predation events are occurring fairly quickly upon arrival at the bridge. Therefore, resolving issues of predation and delay are equally important.

Predator versus fish abundance and density patterns

Pigeon guillemots were the only predator species detected commonly enough to generate a weekly abundance estimate; no relationship was apparent between steelhead mortalities and pigeon guillemot presence/abundance over time. In four weeks of the assessment, data were sufficient to map harbor seal counts (Assessment Component 3) alongside fish biomass densities (Assessment Component 2); however, there appeared to be little consistency and no detectable correlation between the two, likely due to the stochastic nature of both fish density patterns and observed harbor seal in-water locations (Figure 24).

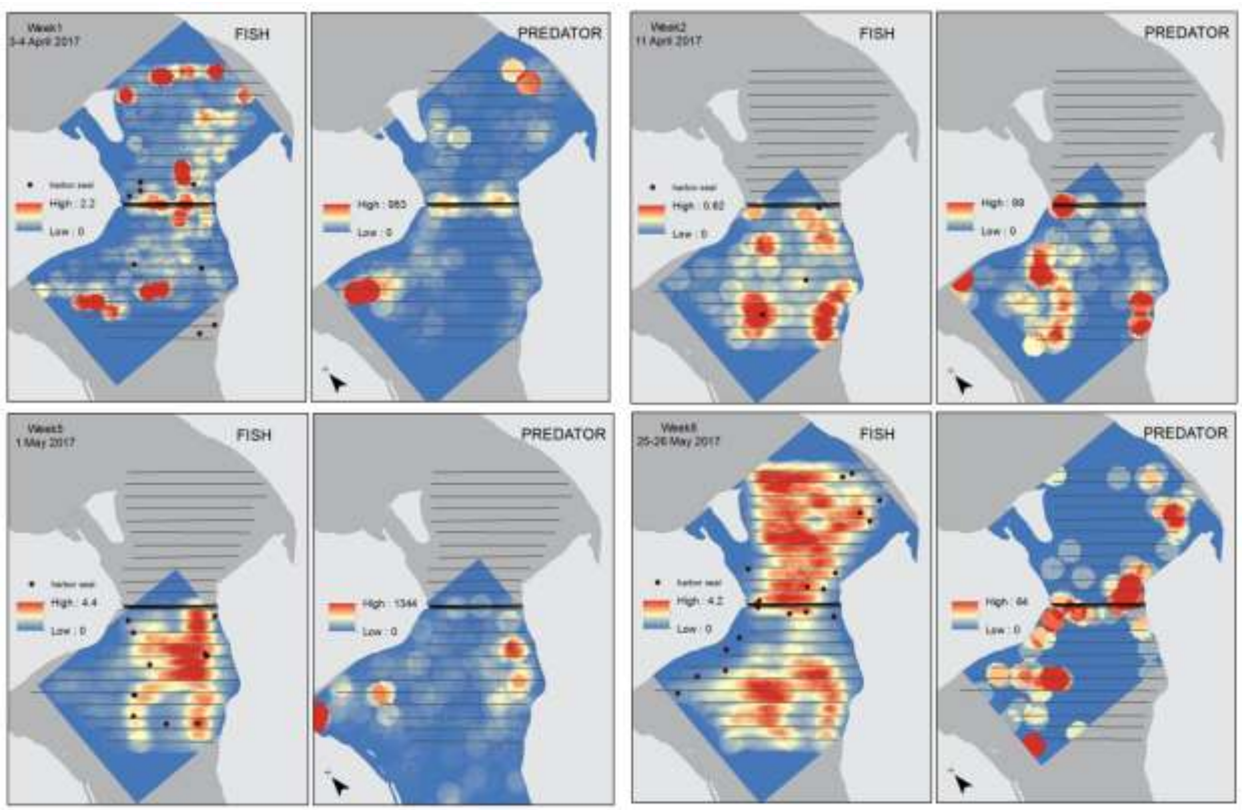

Figure 24. Side-by-side density maps of fish biomass (left panel in each week) overlaid with single harbor seal observations and harbor seal densities (right panel in each week) over four weeks of the 2017 outmigration season. Red colors indicate higher densities. Density values differ among panels.

Successful steelhead passage at the bridge associated with ebbing tidal currents

Tidal currents at the bridge had a strong effect on tagged steelhead passage. Almost all tagged steelhead migrated past the bridge on an ebbing current as water drains from Hood Canal towards the ocean. Steelhead that migrated through the open spans at the side of the bridge were less dependent on the tidal cycle; most steelhead that dove underneath the bridge only did so during high velocity ebb currents (Figure 25).

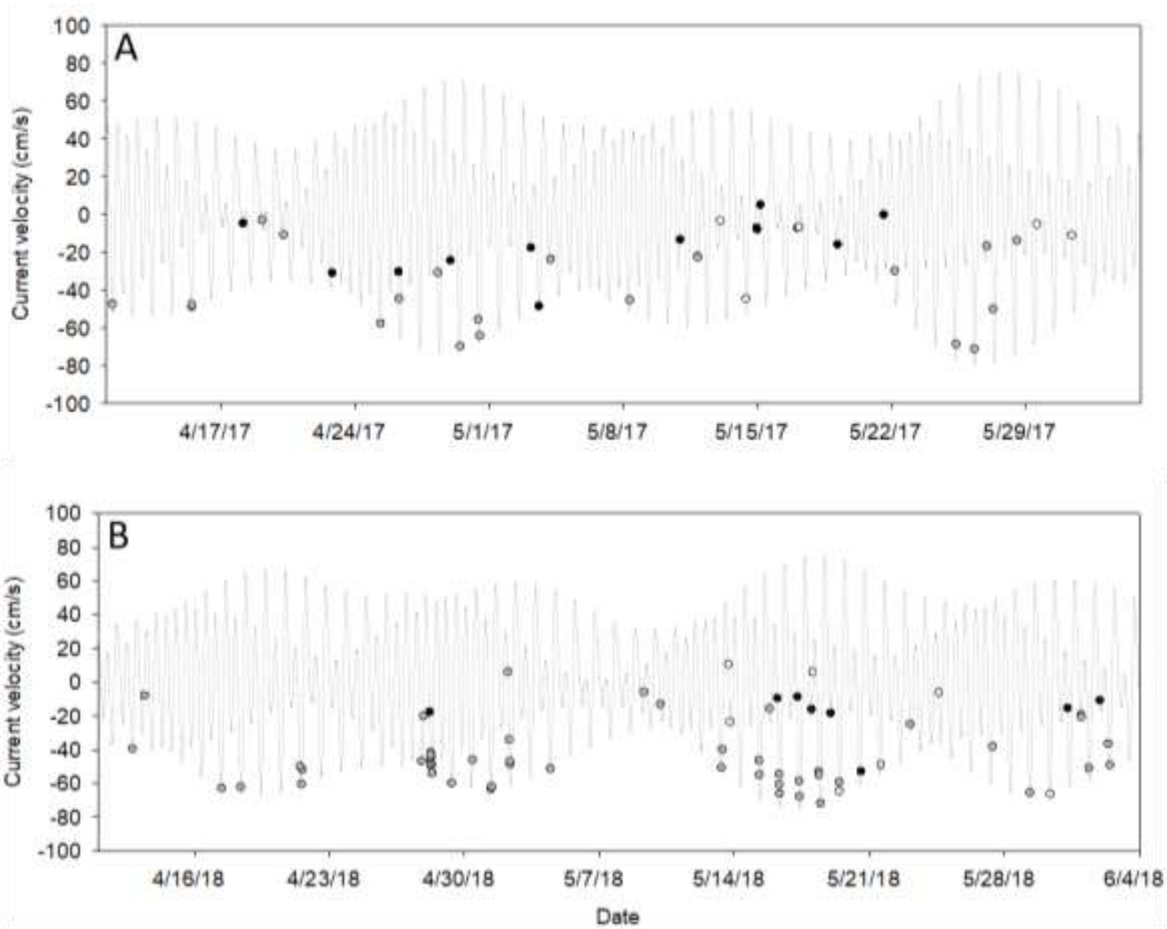

Figure 25. Crossing location times of smolts that crossed under (light gray circles), around through the east drawspan (black circles), or around through the west drawspan (open circles) in 2017 (A) and 2018 (B) in relation to current velocity (predictions at NOAA current station PUG1603, https://tidesandcurrents.noaa.gov/noaacurrents/Predictions?id=PUG1603_20).

Drawspan openings and tagged steelhead passage

The bridge's center drawspan is retractable to allow for vessel traffic and maintenance operations. Data on timing and duration of bridge openings were paired with tagged steelhead behavior to determine whether steelhead crossed through the open center when the option was available. Over the 2017 and 2018 outmigration periods, the center drawspan was opened partially or fully a total of 55 times in 2017 and 101 times in 2018, generally remaining open for approximately 15-20 minutes. Only two tagged steelhead each year were within 200 m of the center span during the time periods when the bridge was open. Distance from center span was calculated between the location of the tagged fish and the closest point of the drawspan. One 2017 crossing occurred during a full bridge opening; the other three crossings occurred during partial openings. In 2017, one of the two tagged steelhead was detected within 100 m of the center for the first seven minutes of bridge opening but subsequently moved away from the center span despite a strong ebb tide; the other steelhead moved within 25 m of the center span and remained there for five minutes but did not pass through. In 2018, one of the two tagged steelhead within 200 meters during a drawspan opening moved through on a strong ebb tide, while the other steelhead moved back and forth parallel to and 30-60 m from the drawspan before moving away without crossing during a moderate ebb tide.

Since more frequent and longer duration center span openings were one proposed solution to facilitate steelhead passage, an additional analysis was conducted to determine how many tagged fish were in proximity (within 100 m) of the center span at any point during the steelhead outmigration season and, of the fish that entered that area, how long they remained there. Of the surviving tagged steelhead smolts, about 30% were detected near the center span at some point during their migration. On average, fish spent 29 ± 9 (2017) and 12 ±3 (2018) continuous minutes within 100 m of the center span. Of the fish that were detected within 100 m of the center span, nearly all were detected in this area during ebbing currents. Upon further investigation, surviving tagged steelhead smolts were located much closer to the bridge infrastructure during ebb currents and moved further away from the structure (but still within a detectable range) during slack and flood currents (Figure 27).

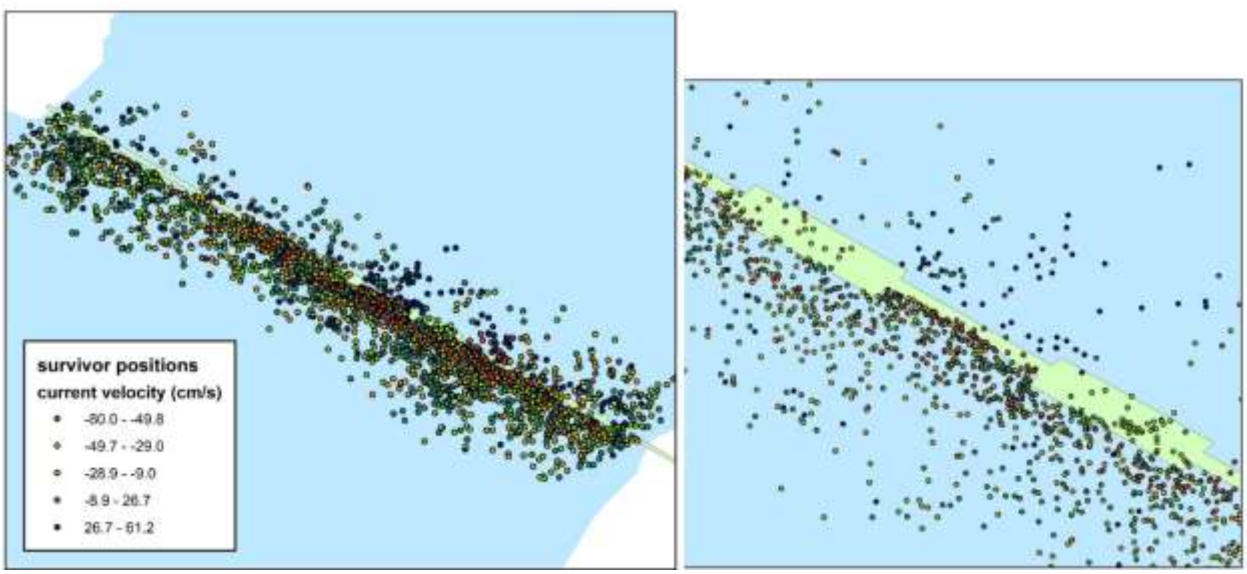

Figure 26. Positions of tagged steelhead in 2017 along the entire bridge (left) and within 100 m of the center span (right). Position dots are colored to reflect current velocity at the time of position, where redder dots indicate stronger ebb currents.

Stormwater impacts at the bridge

Rainfall patterns were investigated using data from nearby NOAA stations and stations monitored by citizen scientists to determine whether there was any signal of stormwater impacts on tagged steelhead mortality. Timing and level of precipitation did not appear related to steelhead mortality patterns across the migration season.

II. Is the bridge impacting the entire Hood Canal ecosystem?

A. Does the bridge obstruct ebb - flood currents & impact flushing of brackish outflow water?

Previous circulation models suggested the bridge had the potential to impede flushing of Hood Canal. However, at the time no field data in the vicinity of the bridge was available to validate model results. During Phase 1, researchers collected *in situ* oceanographic data near the bridge structure, increased model resolution and accuracy, and used the improved model to investigate circulation and water quality parameters near the bridge and throughout Hood Canal. These studies defined the bridge's zone of influence: the distance from the bridge where relative difference induced by bridge infrastructure on water quality parameters reduces to < 10% of the maximum deviation.

8. Collect oceanographic data at Bridge (current, salinity, and temperature profiles)

Tarang Khangoankar, Adi Nugraha, Taiping Wang, Pacific Northwest National Laboratory

For detailed methods and results, see Appendix E.

Three *in situ* current and conductivity, temperature, and depth sensors were deployed at the bridge, 500 m upstream of the bridge, and 500 m downstream of the bridge. A water level station placed just north of the bridge measured water surface elevation. These instruments collected data throughout the 2017 steelhead outmigration period. Additional conductivity, temperature, and depth data were collected from vessels during sensor deployment and retrieval. These observed data were then compared with model-predicted water surface elevations, currents, salinities, and temperatures to validate the model described in Assessment Component 9.

9. Characterize the bridge zone of influence – Hydrodynamic Modeling

Tarang Khangoankar, Adi Nugraha, Taiping Wang, Pacific Northwest National Laboratory

For detailed methods and results, see Appendix E.

To quantify the spatial extent of the bridge's effect on hydrodynamic parameters, the Salish Sea model – an externally coupled three-dimensional hydrodynamic and biogeochemical model – was validated and refined to embed the Hood Canal floating bridge in high resolution. Several techniques were explored:

1. Implementation of a velocity block, wherein the bridge was embedded as an impermeable surface block,
2. Implementation of momentum sink at the bridge using form drag, wherein the bridge was represented in the model as densely-packed hypothetical cylinders which resulted in blockage of nearly ~95% of surface currents. This scenario represents a leaking bridge but allows effects on continuity and momentum.

3. Free surface pressure modification with a bottom drag, wherein the pressure boundary condition is manipulated to cause a model response of surface depression down to the extent that the bridge sits in the water. This method also employs drag formulation for the water layer immediately under the modified pressure boundary, inducing reduction in flow velocity.

Results using each of these modeling techniques were tested against the observed data collected in Assessment Component 8, and all methods performed similarly in terms of near-field impacts of the bridge. Model predictions compared favorably to observed water surface elevations, currents, salinities, and temperatures, and implementation of the bridge module in the Salish Sea model was successful in reproducing the observed reduction in velocity near the bridge. Sensitivity tests were performed by running additional model scenarios with the bridge module removed from the model, representing Hood Canal conditions without the bridge, and with the bridge module altered to leave the center span open, representing bridge openings due to, e.g., vessel traffic. Predictions across all model scenarios were compared to define the bridge's zone of influence.

The model results confirm that the Hood Canal Bridge obstructs the brackish outflow surface layer of water, inducing increased local mixing near the bridge and causing pooling of up-current water and shadow/sheltering of down-current water (Figure 28). In addition, surface layers of water are forced underneath the bridge, creating warmer, fresher waters at depth. The effect on currents, salinity, and temperature is highest at the bridge and reduces with increasing distance from the bridge. The bridge's zone of influence extends ~20 m below the surface and varies from 2-3 km for currents, from 2-4 km for salinity, and from 2-5 km for temperature before effects diminish to <10% relative to simulated conditions without the bridge.

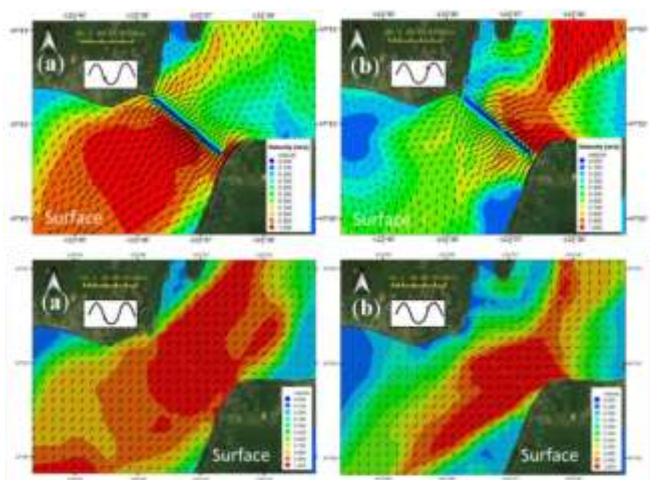

Figure 27. Upper panels: model-predicted horizontal velocity contour and vector plots with the HCB present for (a) ebb and (b) flood currents in the surface layer. Lower panels: model-predicted horizontal velocity contour and vector plots with no HCB for (a) ebb and (b) flood currents in the surface layer. Both upper and lower panel scenarios represent a typical spring tide (April 27, 2017).

B. What is the impact of Hood Canal Bridge on basin wide circulation and water quality?

Previous modeling studies suggested the Hood Canal Bridge may have a subtle but persistent and cumulative effect on the residence and flushing of the Hood Canal basin. While low DO levels, nutrients, pollutants and pH in Hood Canal have received much attention, potential effects of the Hood Canal Bridge on these issues had not been examined prior to Phase 1 of the Hood Canal Bridge Ecosystem Impact Assessment. Phase 1 work included a coarse analysis using the refined model developed through assessment component 9 to determine whether proceeding with a more extensive investigation of potential bridge impacts to the Hood Canal ecosystem was warranted.

10. Model the bridge's effect on flushing, biogeochemistry, dissolved oxygen, and pH of Hood Canal

Tarang Khangoankar and Adi Nugraha, Pacific Northwest National Laboratory

For detailed methods and results, see Appendix F.

This modeling effort investigated the bridge's effects on Hood Canal-wide circulation, determining whether the presence of the floating bridge significantly impacted basin circulation/flushing by blocking the surface brackish layer. The Hood Canal Bridge module was embedded within the Salish Sea model using the velocity block method as described in Assessment Component 9, and was then validated throughout Hood Canal using observational data collected by the Washington Department of Ecology. Model validations including tests of water quality parameters, nutrients, phytoplankton, and dissolved oxygen. The model was able to replicate a prior version of the Salish Sea model without a bridge block and also performed well in comparisons to observed data.

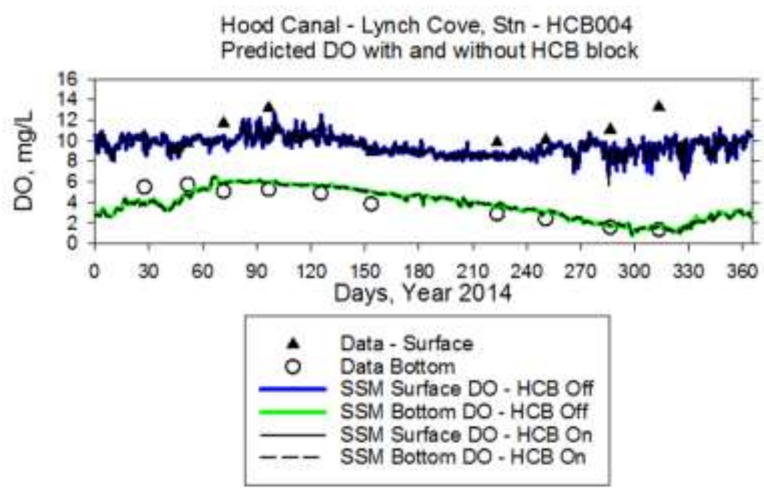

Figure 28. Model predictions for dissolved oxygen (DO) levels at Lynch Cove with and without the presence of the Hood Canal Bridge in the model.

The validated model was then used to simulate the entire Salish Sea domain for one year under three scenarios: 1) Hood Canal Bridge present, 2) no Hood Canal Bridge, and 3) Hood Canal bridge present but with center span always open. These scenarios were compared to determine the bridge's effect on circulation/flushing and exchange flows, and predict impacts on water quality parameters like temperature, salinity, dissolved oxygen, and pH. Results suggested that the bridge does not cause a large-scale impact on circulation: predicted parameters in simulations without the bridge were nearly identical to simulations with the bridge. Southern Hood Canal (Lynch Cove) was expected to show the strongest response since this region has the longest flushing time; however, comparisons of predicted parameters in simulations with and without the bridge as well as comparisons to observed data showed no differences large enough to be of practical significance (Figure 29Figure 29). Additional sensitivity tests (double precision, variations in bridge block formulation layering schemes, etc.) were conducted to ensure that these results were not simulation error.

A final set of flushing time tests were performed using a numerical dye tracer. To evaluate relative change in flushing time due to the bridge, focus was again placed on southern Hood Canal (Lynch Cove), a region with a flushing time that exceeds 200 days, although all Hood Canal regions were subjected to bridge/no-bridge simulation comparisons. Simulations were run without the Hood Canal Bridge and with the Hood Canal Bridge using two different approaches to represent the bridge's surface layer blockage. All three of these simulation tests resulted in flushing times of 229 days at Lynch Cove (Figure 30). These results suggest that, while the bridge does significantly affect currents, temperature, and salinity within its zone of influence as defined in Assessment Component 9, this effect is restricted to the zone of influence and is not strong enough to impact Hood Canal-wide circulation/flushing and water quality. These findings contrast with prior model research; in reviewing the prior model's methods and results, authors believe that the previous model produced a false positive based on inadequately specified ocean boundary conditions. Further investigation, while beyond the scope of this Phase 1 Assessment, should consider scenarios reflecting climate change and population growth in the Hood Canal region as these factors may exacerbate known Hood Canal water quality issues. Since fish and other biota can be sensitive to even small fluctuations in water quality parameters, additional investigation into potential impacts at specific locations within Hood Canal may be warranted.

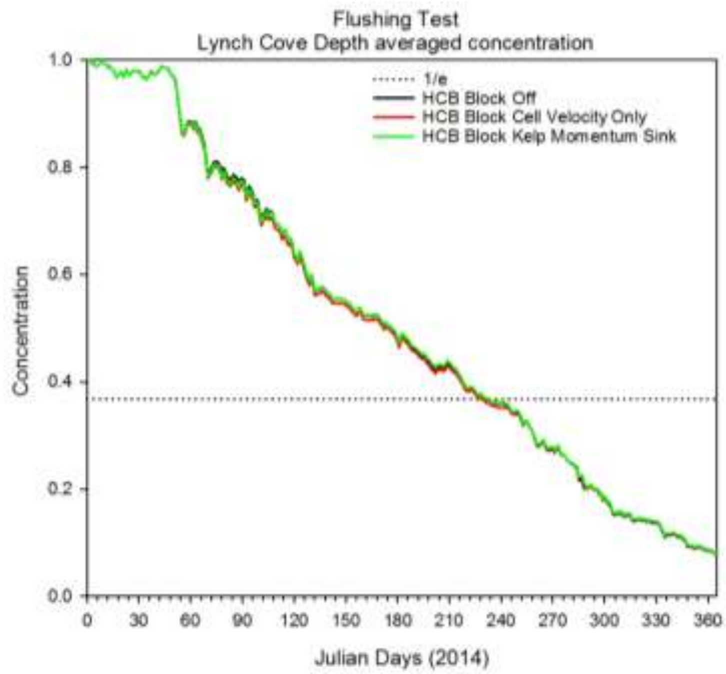

Figure 29. Time histories showing depth-averaged dye concentrations at Lynch Cove modeled without Hood Canal Bridge (black line), with HCB represented in the model with a velocity block (red line), and with HCB represented with a momentum sink (green line).

Conclusions

Results from Phase 1 of the Hood Canal Bridge Ecosystem Impact Assessment indicate that the Hood Canal Bridge significantly contributes to early marine mortality of juvenile Hood Canal steelhead by impeding fish passage and facilitating predation, resulting in mortality of about half the smolts that encounter the bridge. The structure also affects other fish species such as juvenile Chinook and chum, although the extent of bridge effects on smaller salmonids are not yet quantified, and significantly impacts water quality parameters (temperature, salinity, currents) in its vicinity. Specific portions of the bridge infrastructure cause problems beyond the initial deterrence of the bridge's pontoon structure (15 vertical feet of continuous underwater concrete): corner areas created by cross-pontoons that extend perpendicularly from the bridge structure are associated with high densities of fish, predator presence, and predation events. Although bridge effects on water quality dissipate with distance from the bridge and do not appear to propagate throughout Hood Canal, these near-bridge changes in circulation and flow may be linked to impacts on juvenile salmon and steelhead behavior and mortality. Tidal currents were closely linked to steelhead passage. No day/night effects or noise effects on tagged steelhead behavior and mortality were observed, but artificial light at night remains a concern in the vicinity of the bridge. Observational data supported the artificial reef effect hypothesis, where the bridge infrastructure aggregates plankton, fish, and predators; researchers observed higher zooplankton densities, large schools of juvenile salmon, and consistent predator presence at the bridge. However, quantifying the effects of this potential dynamic on salmon species was beyond the scope of the assessment Phase 1. A suite of avian and mammalian predators was associated with the bridge; based on tagged steelhead mortality patterns and predator behavior, harbor seals are the strongest candidate predator responsible for juvenile steelhead mortality at the bridge. Improving juvenile steelhead survival through this migration segment requires reducing the amount of time juvenile steelhead are delayed by the bridge's physical obstruction and minimizing the predation pressure that juvenile steelhead experience at the bridge.

Recommendations, Remaining Data Gaps, and Limitations

Based upon the findings reported above, the Hood Canal Bridge Assessment Team, Engineer Team, and Management Committee members participated in workshops and exercises to develop solutions to test during Phase 2, and to identify the research needed beyond the scope of Phase 1 to address bridge impacts on other juvenile salmon species, potential bridge impacts on returning adult salmon, and predator deterrence options. With the guidance of the Assessment Team, engineers at R2 Resource Consultants completed initial scoping and design recommendations for Phase 2 solutions. Solutions were prioritized into three categories: 1) management actions recommended for early implementation, 2) management actions that were high-ranking but need additional research, and 3) management actions ranked lower.

Solutions in category 1 are being proposed for installation and effectiveness testing in Phase 2. This category includes installing fillet and eddy reduction structures to reduce or restrict fish access to existing pontoon corners of the infrastructure, as well as pilot testing longer-duration bridge drawspan openings timed on strong ebb tides to encourage fish passage and investigating modifications to luminaries to reduce overwater light spillover. Phase 2 may also provide an opportunity to conduct the research necessary to move towards implementing solutions in category 2: bridge re-design and replacement/modifications and pinniped deterrence activities such as restricting haulout and bridge access and exploring targeted acoustic startle technology which has shown initial success at deterring pinnipeds in other areas of Puget Sound.

See appendices H, I, and J for details on the Assessment Team's process of identifying remaining research priorities and developing Phase 2 solutions as well as the full R2 Resource Consultants report on scoping and design of Phase 2 solutions. The Assessment Team recommends that Category 1 solutions undergo a more substantial feasibility and design process before they are installed and assessed during Phase 2 studies. To assess solution effectiveness while accounting for observed inter- and intra-annual survival variation across the steelhead outmigration period, Assessment Team members strongly recommend a series of replicated control (no solutions)/treatment (solutions installed) tests spanning two outmigration seasons.

Phase 1 studies addressed central questions of bridge effects, yet several research priorities remain. The most pressing priorities, and recommendations on addressing each, include:

- How do juvenile Chinook and chum interact with the bridge and do they experience increased mortality because of the bridge?

  During the Phase 1 assessment, on-bridge and near-bridge visual and acoustic surveys found schools of small Chinook and chum salmon aggregated within and around bridge infrastructure. These data also suggested a potential increase in milling behavior near corners in the bridge infrastructure. Quantifying juvenile Chinook and chum behavior and mortality at the bridge was beyond the scope of Phase 1, but the Assessment Team and Management Committee recommend this as needed research to support Hood Canal Chinook and chum population recovery efforts and to further inform or refine bridge solutions. Studies recommended for consideration in Phase 2 would quantify schooling/milling behavior along bridge infrastructure. Additional studies suggested but not recommended within the Phase 2 scope include tagging juvenile Chinook with small acoustic tags or a paired predator-fish PIT-tag study to directly measure consumption rates of juvenile Chinook by seals.

- How do returning adult salmon interact with the bridge and do they experience migration delays or increased mortality because of the bridge?

  No data were collected on adult salmon during the Phase 1 assessment. Anecdotal information from state and tribal representatives suggest potential bridge impacts to returning adult chum. The Assessment Team and Management Committee recommend a small, investigative tagging study on returning adult chum that takes advantage of the acoustic array that will be deployed at the Hood Canal Bridge during Phase 2. This research would determine whether the bridge impacts returning adult salmon and may further inform or refine bridge solutions.

- Is predation by harbor seals and other predators on juvenile Chinook and chum greater near to vs. away from the bridge?

  Juvenile Chinook and chum are susceptible to a wider array of potential predators than larger steelhead smolts. Understanding how predators near the bridge contribute to Chinook and chum mortality, and whether mortality at the bridge is disproportionately higher than in areas away from the bridge, is important information; however, it is not currently prioritized in Phase 2 given the lack of quantitative data on juvenile Chinook and chum behavior and mortality at the bridge.

- Which seals forage at the bridge, and what behavior patterns do seals employ while foraging at the bridge?

  Assessing the array of potential steelhead predators and predator density near to versus away from the bridge was an important component in the Phase 1 assessment. Studies of predator behavior and diet were not possible in Phase 1 but are recommended for consideration in Phase 2. The Assessment Team prioritizes research to identify which seals forage at the bridge – is bridge foraging a specialized behavior in which only a few repeat offenders engage? Or do all seals near the bridge engage in this behavior? – and what behaviors seals foraging at the bridge employ. Studies on seal behavior at and near the bridge may further inform and refine bridge solutions.

Recommended solution concepts for Phase 2, and what each concept will do:

Category 1 Management Actions, Recommended for Early Implementation	Bridge Corner Fillet Structures	Reduce or restrict access to the existing pontoon corners
	Eddy Reduction Structures at Corners	Eliminate or reduce the size of eddies formed at existing pontoon corners
	Open Bridge Span More Often for Fish Passage	Expedite fish passage through the bridge
	Lighting at Bridge	Modify luminaries to provide bridge deck lighting while reducing overwater light spill
Category 2 Management Actions, High Ranking but Need Research	Bridge Re-Design and Replacement/Modifications	Replace the bridge or bridge sections with a more fish-friendly design
	Pinniped Deterrence (excluding lethal removal)	Deter pinnipeds via haulout restriction and/or prevent pinniped access to the bridge
Category 3 Management Actions, Considered but Not Supported or Recommended	Behavioral Guidance System	Guide fish to existing passageways through bridge side spans
	Pumping Water to Signal Fish Passage	Guide fish to existing passageways through bridge side spans
	Guide Fish with Bubble Curtains	Guide fish to existing passageways through bridge side spans
	Noise Reduction	Reduce bridge noise in surrounding waters

	Marine Growth Removal/Control	Remove/control marine growth on the bridge structure
	Induced Turbidity	Increase turbidity to impede predator foraging efficacy near bridge

Additional detail on Category 1 Management Actions, Recommended for Early Implementation

Bridge Corner Fillet Structures

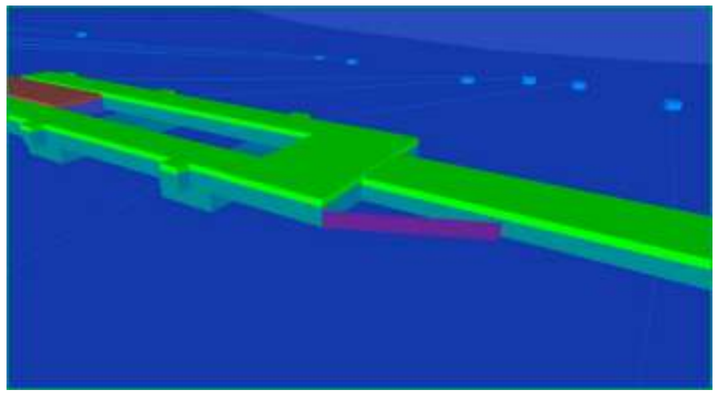

Figure 30. Conceptual full bridge depth corner fillet structure. Image courtesy of R2 Resource Consultants.

Existing corners created by bridge pontoons jutting perpendicularly out from the bridge deck are hypothesized to delay juvenile steelhead migration and aggregate smaller fish species by creating back-eddies or water velocity anomalies. Mammalian predators may corral fish in a corner as a foraging strategy. Telemetry data suggest elevated density in corner areas. To address this situation, flexible bridge corner fillet structures (Figure 31) will be placed at inside corners of east and west abutments, where they will reduce or restrict fish access and guide fish around these corner areas. Fillets will be either full bridge depth (15 ft) or half bridge depth (8 ft) and will be constructed of high density polyethylene (HDPE) pipe, synthetic netting, or fabric that is weighted with a continuous steel chain at the bottom. An HDPE plate will be welded to the top of the pipe to deter pinnipeds from hauling out onto the structure. The attachment to the bridge structure will include an elastic-type connection to absorb energy and limit forces on the fillet and the bridge during turbulent water conditions. The assembly is anticipated to be similar to fish guidance systems and debris booms that have been shown to be effective at several hydroelectric projects in the Pacific Northwest. The design of the fillet structures requires close coordination with WSDOT engineers to ensure suitable design load criteria, model fillet performance under varying conditions, and develop a system for fastening the structure to the bridge.

Eddy Reduction Structures at Corners

Eddy reduction structures at pontoon corners (Figure 32) will eliminate or reduce the size of the eddies described above to reduce predation in corners and expedite fish passage by creating more laminar flow around corners. A half-round or bull-nose eddy reduction structure will be constructed out of flexible HDPE pipe and plates attached to the corner of the bridge pontoon and extending 15 ft deep (full bridge depth). Eddy reduction structures will be designed for maximum benefit at peak flood and ebb tides. The assembly will be designed to be neutrally buoyant when deployed, and will require close coordination with WSDOT engineers throughout design, construction, and deployment of the structure.

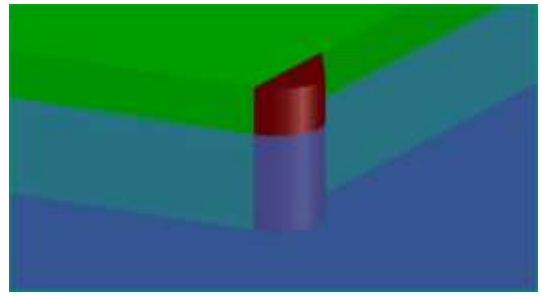

Figure 31. Conceptual full bridge depth eddy reduction structure. Image courtesy of R2 Resource Consultants.

Open Bridge Span More for Fish Passage

During the Phase 1 assessment, approximately a third of the tagged juvenile steelhead that survived bridge passage were detected in proximity to the bridge's center span during their outmigration, spending an average of 12 to 30 minutes in the vicinity. Tagged steelhead were consistently closest to the bridge infrastructure on ebb tides, and most steelhead passage occurred on ebb tides. Opening the bridge's center draw span during ebb tides is a relatively low-risk alternative to expedite fish passage and is a simple way to gain information on potential bridge design solutions currently ranked in Category 2: would additional fixed openings along the bridge structure increase fish passage? While existing Phase 1 data does not provide clarity on the optimum duration of bridge openings, the Assessment Team recommends testing openings of one hour during ebb tides, and prioritizing the strongest ebb tides. No further design work is needed to implement this solution, as the current bridge design readily allows openings (Figure 33). However, longer bridge opening durations would need approval from a number of relevant actors and an intensive public awareness and outreach campaign will be necessary to mitigate disruptions in traffic.

Figure 32. Vessels passing through the open Hood Canal Bridge drawspan. Image courtesy WSDOT.

Lighting at Bridge

Light levels at night around certain portions of the bridge structure are within the range expected to impact juvenile salmon behavior and migration. Additionally, anecdotal evidence suggests an association between the zooplankton aggregations and juvenile salmon behavior at certain areas of the bridge. The Hood Canal Bridge has more overhead lighting than other floating bridges because there is no separated bicycle path and interspersed bicycle and car/truck traffic requires more lighting for safety. Currently, luminaries are placed at 120 ft intervals along the bridge's lift deck and double luminaries light the pontoon and work decks of the bridge (Figure 34). Lights are high pressure 150-watt sodium bulbs producing 13,000-16,000 lumens. Luminaries could be modified to produce more lighting on the bridge deck while reducing the amount of light radiated into the water, or adapted to minimize blue-rich lighting and use "warm" color temperature or filtered light sources, while still maintaining the safety standards required of mixed-vehicle bridge decks. This solution has more uncertainties than the other Category 1 solutions; however, the growing body of literature regarding artificial light impacts on salmon passage and predation dynamics and precedent from other bridges in the region raise the importance of continued consideration of lighting options at the Hood Canal Bridge. Therefore, the Assessment Team recommended investigating the feasibility of lighting changes during phase 2, as this may be considered "best practice" to reduce impacts on salmonids.

Figure 33. Light luminaries on the east half of the Hood Canal Bridge. Image courtesy WSDOT.

List of Appendices

A. Moore & Berejikian 2019 Acoustic telemetry investigation of altered migration behavior and mortality of steelhead smolts at the Hood Canal Bridge, Puget Sound WA. Unpublished methods and results.
B. Daubenberger & Bishop 2019 Components of the Hood Canal Bridge Ecosystem Impact Assessment addressed by the Port Gamble S'Klallam Tribe: Split-beam acoustic surveys, water quality and zooplankton, predator surveys, visual acoustic surveys, and gopro and biota surveys. PGST technical briefs.
C. Stocking & Pearson 2019 Evaluating the potential influence of the Hood Canal Bridge on piscivorous bird and mammal density. WDFW technical report.
D. Deng et al. 2018 Hood Canal Bridge noise impact assessment: phase 1 findings. PNNL technical memorandum.
E. Khangaonkar et al. 2018 Hydrodynamic zone of influence due to a floating structure in a fjordal estuary—Hood Canal Bridge Impact Assessment. Journal of Marine Science and Engineering, 6:119. doi:10.3390/jmse6040119
F. Khangaonkar & Nugraha 2019 Hood Canal Bridge impact on basin-wide water quality – initial analysis. PNNL technical report.
G. Hood Canal Bridge Impact Assessment Matrix
H. Assessment Team and Management Committee Ranking Exercise: Phase 2 Solutions
I. R2 Resource Consultants: Phase 2 Scoping and Recommendations

Appendix A. Moore & Berejikian 2019

Acoustic telemetry investigation of altered migration behavior and mortality of steelhead smolts at the Hood Canal Bridge, Puget Sound WA

Megan E. Moore[1], Barry A. Berejikian[1]

[1]Environmental and Fisheries Sciences, Northwest Fisheries Science Center, National Oceanic and Atmospheric Administration, 7305 Beach Drive East, Port Orchard 98366, USA

Introduction

Threatened steelhead (*Oncorhynchus mykiss*), endangered summer chum salmon (*O. keta*), Chinook salmon (O*. tswaytscha*), and coho salmon (*O. kisutch*) originating in Hood Canal rivers must migrate past the Hood Canal Bridge (HCB) to complete their life cycle in the Pacific Ocean. However, the HCB floats on continuous concrete pontoons that extend 4.6 meters beneath the surface and occupy 90% of the width of Hood Canal. Despite openings (i.e., drawpans) that flank the east and west shoreline and comprise the remaining 10% of the canal width, migration delays at the bridge contribute to increased mortality of steelhead smolts attempting passage (Moore et al. 2013). The submerged structure also blocks brackish water outflow and disrupts natural currents, altering local salinity and temperature profiles (Khangaonkar and Wang 2013) that likely impact the movement of other salmonid species moving out of the basin. To understand the impact of the HCB on listed salmonid species' productivity, and to protect the significant investment made on salmonid habitat restoration in Hood Canal rivers, we used acoustic telemetry to conduct an intensive assessment of the HCB impact on juvenile salmon and steelhead outmigrants. Telemetry arrays set up during previous Hood Canal studies (2006-2010) were deployed to detect the presence of individual steelhead smolts at the Hood Canal Bridge, but lacked the precision to estimate exact locations of smolts encountering the bridge. The current study deployed an extensive acoustic telemetry array on either side of the HCB and along the steelhead migration route, providing the precise fish location data to (1) estimate the impact of the HCB on survival, (2) identify physical and biological factors contributing to migration delay and low survival, (3) map spatial patterns of movement and mortality, and (4) isolate potential predator species based on the behavior of transmitters retained at the HCB.

Methods

Fish Tagging

Wild steelhead smolts were collected from a rotary screw trap in the South Fork Skokomish River (river kilometer (rkm) 13.5) and a weir trap in Big Beef Creek (rkm 0.1) during April and May of 2017 and 2018 (Figure A1). Captured smolts were held in flow-through circular tanks for 1-48 (typically < 24) hours prior to tagging. Steelhead smolts were surgically implanted with one of five types of Vemco 69 kHz transmitters: (1) V8-4x (8 mm diameter x 20.5 mm length), (2) V9P-6L (9 mm x 31mm, 4.9 g, equipped with pressure sensor), (3) V7P-4H (7 mm x 24 mm, 2.0 g, equipped with pressure sensor), (4) V7T-4H (7 mm x 34 mm, 2.0 g, equipped with temperature sensor), or (5) 'delay' V8-4x (8 mm diameter x 20.5 mm length, 2.0 g in air), (https://www.vemco.com/products/v7-to-v16-69khz/, Table A1). All transmitters were programmed to ping continuously at random intervals between 30 and 60 seconds. Delay V8 tags were programmed to be off for the first 8 days (time it took 75% of smolts to travel to the Hood Canal Bridge in previous telemetry studies) after release before turning on again. Recent studies have demonstrated that pinnipeds are capable of hearing the sound emitted by a 69 kHz transmitter (Cunningham et al. 2014), so delay tags were deployed to test the null hypothesis that the survival rate of tagged steelhead emitting a signal at 69kHz did not differ from the survival rate of steelhead with silent transmitters. Vemco V7 and V9 pressure sensors recorded the depth (maximum depth = 38 m but sensor continued to record max depth if deeper), and temperature sensors record the ambient temperature (range = -5 – 35 °C) of the tagged animal when within range of a hydrophone. Tagged steelhead were held for 20-30 hours after surgery then released at the location of capture.

Receiver Deployment

A network of Vemco receivers was deployed at various locations along the steelhead outmigration route to record the unique signal of each tagged smolt as it migrated from river mouths (RM) to the Pacific Ocean (Figure 1). Receiver arrays were deployed to estimate survival and provide fine-scale behavior patterns within approximately 250 meters on either side of the Hood Canal Bridge (HCB). Two VR2W receivers were installed at the river mouths (RM) of the Skokomish River and Big Beef Creek to detect tagged smolts entering the marine waters of Hood Canal. A Vemco Positioning System (VPS) comprised of 24 VR2AR and 3 VR2W hydrophones (69 kHz acoustic receivers capable of decoding the signal from Vemco acoustic transmitters https://www.vemco.com/products/) in 2017 (March 5 – August 1), and 28 VR2AR and 14 VR2W hydrophones in (March 6 – September 13) 2018, was configured and deployed to provide fine-scale spatial information on tagged steelhead at the HCB (Figure 1). The VPS system uses an array of receivers equipped with co-located transmitters to communicate the instrument location to other system receivers. Receivers were deployed in close proximity to each other to facilitate detection of a single transmission by multiple receivers, which enabled triangulation of each transmitter as it moved through the array. Stationary reference transmitters (5 transmitters in 2017 and 4 transmitters in 2018) were deployed within the system to test the accuracy and precision of the VPS system each year. Four additional VR2AR receivers were deployed approximately 600 meters apart at Twin Spits (TS), 7 kilometers north of the HCB, to determine whether smolts migrated successfully past the HCB. Twelve Vemco VR3 receivers spanned Admiralty Inlet (ADM), and a final line of 29 Vemco VR3 and VR4 receivers (maintained by the Ocean Tracking Network, https://oceantrackingnetwork.org/) span the Strait of Juan de Fuca at Pillar Point (JDF; Figure 1).

Data Processing

All receiver files were downloaded from recovered receivers or via surface modem (VR3s and VR4s) and compiled into a database. Raw data from single node receivers were used for some analyses requiring only presence/absence information, while files from VPS array receivers were sent to Vemco to generate precise transmitter positions.

Vemco processed VPS receiver detection data using hyperbolic positioning techniques (Smith 2013). Briefly, hyperbolic positioning measures differences in transmission detection times between pairs of time-synchronized receivers, then converts the time differences to distance values using the signal propagation speed, allowing for triangulation of a transmitter position. VPS analysis returned the coordinates and date/time of each tagged animal as it moved through the array, coordinates and date/time of the reference transmitters throughout the length of each deployment, as well as an estimate of accuracy for each position that is unique to each VPS array. To calculate error, the VPS analysis software uses the known positions of the reference transmitters to measure the distance between the triangulated position and the true position (HPEm), then calculates a second error estimate (HPE) that incorporates variation based on receiver array geometry and effects of depth, temperature, and salinity on the speed of signal transmission. However, the true location is only known for reference transmitters and not for animal transmitters, so the relationship between HPEm and HPE can only be examined for reference transmitters then subsequently applied to animal positions. For both VPS arrays separately, we created bins for all HPE values and plotted them against median HPEm values. Where there was a steep increase in median HPEm we defined a threshold (same for both years), and deleted animal detections with HPE values larger than that threshold. After applying this filter, 96.2% (2017) and 87.6% (2018) of the animal positions were retained. Median HPEm values for identically filtered reference transmitter data were 4.4 m in 2017 and 5.0 m in 2018. These accuracy estimates can be applied to animal position data because HPE was calculated in the same way for both reference and animal transmitters. Processed data from all tagged animals were plotted for further analysis using ArcGIS 10.5.1.

Data Analysis

Survival estimation

Segment-specific survival of tagged steelhead smolts was estimated using separate Cormack-Jolly-Seber (CJS) mark-recapture models for 2017 and 2018 detection data (Cormack 1964, Jolly 1965, Seber 1965). The R (R Core Team 2019) package 'RMark' (Laake 2013) was used to construct and test models to jointly estimate both survival (ϕ) and detection probability (*p*) in concert with the program Mark (White and Burnham 1999). Presence or absence of all transmitters (except not V8 delay transmitters) at each receiver array were compiled to create encounter histories. Models were structured to estimate φ from release (REL) to river mouth (RM; $\phi_{REL\text{-}RM}$), RM to the Hood Canal Bridge (HCB; $\phi_{RM\text{-}HCB}$), HCB to Twin Spits (TS; $\phi_{HCB\text{-}TS}$), TS to Admiralty Inlet (ADM; $\phi_{TS\text{-}ADM}$), and ADM to the Strait of Juan de Fuca (JDF; $\phi_{ADM\text{-}JDF}$) in 2017. In 2018, our transmitters were not compatible with the ADM receiver code maps, so we combined $\phi_{TS\text{-}ADM}$ and $\phi_{ADM\text{-}JDF}$ to estimate $\phi_{TS\text{-}JDF}$ (Figure A1).

The survival probabilities from these models were compared between length-varying migration segments by distance-based Instantaneous mortality rates:

$$(-\ln\ \phi_s)/d_s$$

Where ϕ_s is the model-derived survival probability of migration segment s, and d is the distance in km between the initial and final detection at segment *s*.

We took a two-phase approach to modelling ϕ and *p*, using Akaike's Information Criteria for finite sample sizes (AICc) to identify the best models in each phase. Assuming separate parameters for all ϕ segments and all receiver array-specific *p*, the first phase compared a simple segment-varying model (ϕ (segment), *p*(array)) to models that incorporated additional effects of tag type (V8, V9P, V7P or V7T) on *p* and differences in $\phi_{REL\text{-}RM}$ and $\phi_{RM\text{-}HCB}$ by population since longer distances were covered by Skokomish smolts during these first two migration segments. Since we were primarily interested in the effect of the HCB on survival, the second round of model comparisons took the model with the lowest

AICc from the first phase and compared models with additional effects on $\phi_{HCB\text{-}TS}$. Covariates tested individually in the second phase models included smolt fork length, tag type, date of first detection at HCB (hereafter 'approach week' - binned by week and modeled as both factor and integer), HCB approach location (determined by the receiver location of the first detection, modeled as both 2-factor (side or middle) and 9-factor (250 m increments across the bridge span)), tidal stage (ebb or flow) at time of first HCB bridge detection, predicted current velocity https://tidesandcurrents.noaa.gov/noaacurrents/Predictions?id=PUG1603_20) at time of first HCB detection, and time of day of HCB first detection (day or night based on time of sunset and sunrise).

Goodness-of-fit-was assessed by computing Fletcher's c-hat (Fletcher 2012). Estimated C-hat was found to be 1.2 for the null 2017 mark-recapture model, so model comparison tables were adjusted accordingly. Models using 2018 data showed no evidence of overdispersion (c-hat ≈1.00), so no adjustments were made.

Survival of delay and continuous transmitters was compared by computing the proportion of each tag type found stationary (see 'Stationary Transmitters' below), as well as the proportions detected at the three final arrays along the migration route (TS, ADM, and JDF). Only detections of continuous transmitters recorded after 8 days from tagging were included in the analysis, which provided an identical and unbiased assessment of both tag types. Two-sample tests for equality of proportions, with a continuity correction, were used to determine the probability of equal proportions of delay and continuous tags detected at TS, ADM, and JDF arrays, as well as of those tags found to be stationary.

Travel/residence Times

Travel times were calculated by subtracting the date and time of a transmitter's last detection at the first receiver array along the migration route from the date and time of last detection at the subsequent receiver array. Travel distances were measured as the minimum straight line distance from the center of one receiver array to the next. Time spent at the HCB (HCB time) was calculated as the time between the first and last detection at any HCB array receiver. To calculate continuous HCB time, we subtracted all time greater than 24 hours during which a transmitter was not heard on any receivers. Travel time for the entire marine migration (RM-JDF) was calculated by summing average travel times for each migration segment (RM-HCB + HCB-HCB + HCB-TS + TS-ADM + ADM-JDF).

Stationary Transmitters

Mobile tracking at stations surrounding the HCB was performed using a Vemco VR100 and 69kHz omnidirectional hydrophone suspended approximately 3 m under the surface of the water. A set of 261 stations was designed to monitor: (1) the area immediately adjacent to the HCB, (2) areas on the migration route yet removed from the HCB, and (3) areas of predator aggregation (Figure A1). After the conclusion of the typical smolt migration period, we listened for 4 minutes at each station in both 2017 and 2018, recording any decoded transmitters during that time. Transmitters classified as stationary during mobile tracking had to be relocated on more than one occasion to ensure it had not moved, and never heard on any receivers further along the migratory route. A stationary tag was considered to be associated with the HCB if it was located at a tracking station within 3 km of the bridge structure.

To quantitatively identify stationary (or consumed) transmitters at the HCB, we fit a bivariate normal mixed model to (square-root transformed) continuous HCB time statistics for each tag detected at the

HCB to distinguish between transmitters in live steelhead and transmitters continually pinging within range of HCB receivers. The R package ‘mixtools’ (Benaglia et al, 2019) was used to fit the model and estimate the parameters of the two distributions (e.g., Romine et al 2013; Figure 2). Long HCB time (component 2) was indicative of a dead smolt, either consumed and detected while in a predator digestive tract or stationary. Short HCB time (component 1) indicated a live smolt, but may have included smolts (transmitters) consumed by a predator and subsequently deposited on land or at an unmonitored marine location. Using the distribution around longer continuous HCB time, we quantified the probability that each transmitter detected at the HCB behaved in a manner consistent with being consumed. Tags were classified as consumed or stationary if the probability of belonging to component 2 exceeded 0.95. Many of the transmitters identified as dead using these quantitative methods were also classified as stationary using mobile tracking methods. Data from the two independent methods both provided additional confirmation and compensated for imperfect detection ability of the alternate method.

Locations of stationary tags were resolved when more than 1000 detections were recorded repeatedly in the same place without subsequent detection elsewhere. We used the point of highest density of the spatial distribution to pinpoint the location of the stationary transmitter. When the transmitter was located using mobile tracking only, we used the location of the station with the loudest (highest dB) detections.

Density

Smolts were classified as survivors if they were detected at the Twin Spits receiver array (p_{2017} = 0.979, p_{2018} = 0.938), or at any other array further along the migration route, and were classified as non-survivors, or ‘mortalities’, if they were not detected after the HCB. Density plots for all survivors and all mortalities were executed with the Point Density tool in ArcMap using VPS positions (63 survivors and 68 mortalities in 2017, 86 survivors and 83 mortalities in 2018). The density tool divided the number of detections around each raster cell by the specified surrounding area (circle with radius = 50m) then plotted the values to create a density surface. To avoid pseudoreplication, position data were inversely weighted by number of detections per transmitter, so that the output density value reflected the number of fish (or predators), rather than the number of detections, per km^2. Stationary transmitter detections were removed from the datasets prior to density calculation.

HCB Crossing

The location and mode (around east drawspan, around west drawspan, or under pontoons) of HCB crossing was described for each surviving smolt if both a VPS location on the south side and on the north side of the HCB were observed within 20 minutes, though the time difference between locations was typically much shorter ($median_{2017}$ = 2.5 min, $median_{2018}$ = 3.3 min). The location of crossing was the point at which the line between south and north positions crossed the midline of the HCB. The approximate time of crossing was determined by dividing the difference between the time of south position and time of north position by two, then adding the quotient to the time of south detection. We then paired the time of crossing with NOAA current velocity data and light level (day or night based on sunrise and sunset) to investigate factors that may affect crossing success. If the crossing location was located within the open drawspan sections, we categorized the crossing strategy as ‘around’, and if the crossing location occurred along the length of the HCB pontoons, we assumed the smolt navigated 'under'. To identify any smolt preference for certain velocities, current velocity at each time of crossing was compared to mean daily current velocity using a paired t-test.

Sensor Transmitters

Recorded depths from 31 V9P (2017) and 31 V7P (2018) depth sensors, and temperature profiles from 34 V7T (2018) sensors detected at the HCB were used to quantify the behavior of migrating steelhead smolts and identify predation events. For smolts with depth transmitters, we created a depth profile for each pressure sensor, then quantified the number of dives per hour, dive depth range, and max dive depth. We only quantified behavior during time segments where sequential detections were less than 10 minutes apart. A dive was defined as an increase in depth from the surface (depth < 2) to 3 m or more with a return to the surface. We identified an abrupt changes in diving behavior that took place only in mortalities. Depth profiles of surviving transmitters exhibited nearly exclusive surface-oriented behavior, though sometimes with one or two short, shallow (<16 m) dives (that often corresponded with HCB crossing times), while mortality profiles featured short time periods of surface residence (while the transmitter was presumably still in a smolt) followed by frequent deep dives. For the first dive after which there were no periods of continuous surface residence (), the time of detection after a transmitter transitioned from continuous surface depth records (less than or equal to 2m) to depths greater than or equal to 3m was considered the time of a predation event. For temperature transmitters, we defined the time of predation as the first detection associated with a temperature increase that eventually rose to 35 °C (maximum sensor value), with the assumption that a temperature increase of this magnitude meant the smolt had been eaten by a warm-blooded predator. We defined the location of predation as the VPS position triangulated closest in time (21 min or less, median time = 4.7 min) to the time of predation. Spatial error around the predation location was calculated by multiplying the average speed of the tag movement within 1 hour after the putative predation event by the time between the behavioral shift or temperature increase and the closest VPS position.

Results

Survival

Steelhead smolts survival probabilities between the Hood Canal Bridge and Twin Spits were 49.4 ± 4.6% SE in 2017 and 56.5 ± 4.4% in 2018. Distance-based instantaneous mortality rates were markedly higher between the HCB and TS (2017 = 10.1%/km; 2018 = 8.2%/km) relative to migration segments before and after smolts encountered the HCB in 2017 ($RM\text{-}HCB_{BBC}$ = 1.3%/km, $RM\text{-}HCB_{Skokomish}$ = 0.4%/km, TS-ADM = 1.2%/km, ADM-JDF = 0.7%/km) and in 2018 ($RM\text{-}HCB_{BBC}$ = 0.6%/km, $RM\text{-}HCB_{Skokomish}$ = 0.9%/km%, TS-JDF = 1.0%/km; Figure 3). Survival probability in freshwater was high during both years (2017 = 93.4 ± 2.7%, 2018 = 98.1 ± 1.2% (BBC) and 92.3 ± 2.7% (Skokomish).

In 2017, mark-recapture model comparison suggested no differences in $\phi_{REL\text{-}RM}$ or $\phi_{RM\text{-}HCB}$ by population (Δ AICc = 0.56 and Δ AICc = 0.68, respectively). The best model from phase 1 included an effect of tag type and a difference in detection probability *p* at each river mouth (Table A2). The only models in phase 2 with AICc less than AICc values of the null model included approach week (Table A2). The best model estimated a linear effect of approach week on $\phi_{HCB\text{-}TS}$ (β = 0.35; Figure A4a), while the model with the second lowest AICc estimated separate ϕ_{HCB-TS} for each approach week (ΔAICc = 5.48). All ϕ and p values were derived from the best model.

In 2018, model comparison results indicated a difference in survival probabilies by population for both ϕ_{RM-HCB} and ϕ_{REL-RM}, and no differences in *p* by array or by tag (Table A3). Phase 2 model results supported an additional effect of approach week, with separate ϕ_{HCB-TS} for each approach week (Figure A4b). An effect of body length (β = -0.02) and a linear effect of approach week (β =0.21) were also supported by model comparison results (Table A3). All ϕ and p values were derived from the best model, except for ϕ_{HCB-TS} was derived from the second best model (Table A3) to obtain a single estimate rather than separate estimates by approach week.

Smolts tagged with delay transmitters and smolts tagged with continuous transmitters survived at similar rates from release to the TS array ($\chi2$ = 0.045, p = 0.832), to the ADM array ($\chi2$ = 0.236 p = 0.901), and to the JDF array ($\chi2$ = 0.00015, p = 0.990). The time between tagging and detection at the HCB was less than 8 days for 39 of the 46 (85%) continuous-tagged smolts detected at the HCB, so the programmed delay (8 days) was sufficient to assume that a high proportion of delay tags were silent for the entire RM-HCB migration. The last detection at the HCB occurred less than 8 days after tagging for 24 of the 46 (52%) continuous-tagged smolts. Another indicator of no difference in mortality between the delay and continuous tag groups was the similar proportion of stationary tags (mortalities) found via mobile tracking after the migration window ($\chi2$ = 0.000, p = 0.990).

Travel/HCB time

Survivors spent an average of 1.9 (± SE 0.6) days in 2017 and 0.9 (± SE 0.2) days in 2018 within range (~500 m on either side) of the HCB, while only taking an average of 0.2 (± 0.02) and 0.3 (± 0.03) days, respectively, to travel the subsequent 7 km migration segment from HCB-TS (Figure A5). Transmitters categorized as mortalities were detected for an average of 44.2 (± 5.2) days in 2017 and 35.3 days in 2018 within range of the HCB. The entire marine migration from RM-JDF took Big Beef Creek smolts 17.1 days in 2017 and 12.6 days in 2018, while Skokomish smolts took 15.8 days in 2017 and 14.2 days in 2018 (Figure A5).

Stationary transmitters

In 2017, we detected 35 stationary transmitters via mobile tracking, 33 of which were within 3 km of the HCB. The 2 other stationary transmitters were detected in between the HCB and Twin Spits (5.5 and 6 km north of the HCB; Figure A6A). In 2018, we detected 19 stationary transmitters, all of which were located within 3 km of the HCB except for one transmitter found in south Port Gamble Bay (Figure A6B). Several stationary transmitters identified by mobile tracking were also determined to be stationary by the fixed array at the HCB (mixed model analysis). Using both methods, 49 (37%) of the smolts detected at the HCB were found stationary in 2017, and 47 (27%) were found stationary in 2018 (Table A4).

Stationary transmitter locations were concentrated near the HCB and less likely to be found at stations father away from the structure. Locations were distributed along the entire length of the HCB, but a higher density was observed along the western portion, especially in 2018 (Figure A6). Three stationary transmitters were found each year in Port Gamble Bay, where harbor seal haulouts have been documented (Jeffries et al. 2003), in addition to transmitters deposited on the route from HCB to Port Gamble Bay (Figure A6).

Density

Patterns of smolt density near the HCB were similar for survivors in 2017 and 2018, with more frequent occurrence on the south side of the HCB, and high densities observed near the corners formed by the pontoons and center drawspans. Survivors were also more often located on the east side of the HCB compared to the west side, and were located in the open areas under the east and west approach spans that are not covered by submerged pontoons (Figure A7A and A7B).

Density patterns of mortalities were also similar among years, and showed some areas of high density similar to survivors, but differed in other ways. Similar to survivors, mortalities were concentrated along the south side of the HCB and also tended to spend time in corner areas, but were located near the center drawspan less frequently than survivors (Figure A7). Mortalities were more uniformly distributed across the length of the HCB than survivors (Figure A7), but this could be a result of many more VPS locations of mortalities (2017: 18,492 positions; 2018: 28,795 positions (excluding detections of transmitters that became stationary)) than survivors (2017: 3,272 positions, 2018: 3,173 positions).

Crossing Locations

Out of 41 crossing events documented in 2017, thirteen (32%) smolts crossed under the east flank, seven (17%) crossed under the west flank, and 21 (51%) were assumed to have crossed under the pontoons (Figure A8). Twenty-three (56%) of the 2017 crossings occurred during the day, while 18 (44%) occurred at night. In 2018, a higher percentage of smolts crossed under the HCB than in 2017, with 52 (77%) smolts crossing under, and only nine (13%) crossing the east and seven (10%) crossing through the west flank. Fifty-seven (84%) of the 2018 crossings took place during the day, while thirteen (16%) occurred during nighttime hours. Smolts that crossed under the HCB pontoons did not appear to have a preference for certain crossing locations, rather the locations were distributed somewhat evenly along the length of the HCB. Crossing location distribution was similar between years, except that eleven smolts crossed under the center drawspan in 2018, whereas only one smolt crossed at that location in 2017 (Figure A8). Crossing events were much more likely to occur during times of negative (ebbing) current velocity ($t = 17.091$, $df = 108$, $p < 0.001$; Figure A9).

Depth Sensor

Thirty-one smolts implanted with pressure-sensing transmitters were detected at the HCB in 2017. Thirteen of those survived to TS and 18 did not. All 13 survivors exhibited a strong surface orientation. Ninety-one percent of detections indicated migration in the top 1 m of the water column, and 95% in the top 3 m; (Table A5). All 13 survivors migrated past the TS array at average depths less than 1 m. In contrast, only 38% of the depth sensor detections from mortalities (stationary tags excluded) were recorded in the top meter (45% in the top 3 meters; Table A5). Six of the eleven survivors were initially recorded at the surface, then exhibited 1-3 short shallow dives per smolt ($\bar{x}$ = 0.4 per hr), before return to shallow depths < 1 m (for example, Fig A10a; Table 6). The remaining 5 survivors remained exclusively within the top 2 meters while within range of the HCB array. Fifteen of the 18 non-surviving smolts approached the HCB at depths < 1 m, then subsequently exhibited frequent dives ($\bar{x}$ = 4.5 per hr, Fig A10b; Table A6). Six of those 15 mortalities were subsequently detected stationary by the HCB array (for example, Fig A10c). Fifteen of 18 mortalities dove to 38 meters at least once (Table A6). A single mortality exhibited frequent diving behavior (7.5 dives/hr) to intermediate depths (max = 25 m), then was last detected at the surface. Time between first detection at the HCB and the predation event averaged 16.7 hrs, with 5 of the 18 events occurring in less than one hour and all events in less than 2 days.

Depth sensor data for 19 survivors and 13 mortalities detected at the HCB in 2018 revealed behavioral patterns similar to those seen in 2017. Most detections of survivors (82%) occurred at depths in the top meter of the water column (87% in the top 3 meters; Table A5). Nearly all survivors (18 of 19) in 2018 migrated past the TS array in average water depths less than 1 m. At the HCB, mortalities were located in the top meter only 30% of the time (stationary tags excluded) in 2018 (28% in the top 3 meters; Table A5). Four of the 19 survivors remained at depths less than 2 m as they migrated past the HCB, while the remaining 15 surviving smolts exhibited short dives ($\bar{x}$ = 1.1 per hr, max depth = 24.8 m) as they passed the HCB (Fig A10d). Similar to 2017, most mortalities (11 of 13) approached the bridge near the surface (≤ 2 m) and subsequently exhibited frequent ($\bar{x}$ = 4.6 per hr) deep dives, with at least one dive greater than 35 m (Table A6). Six of these 11 frequent deep divers appeared stationary following active behavior. One of the 13 mortalities exhibited a dive profile indicating shallower dives ($\bar{x}$ = 3.8, max = 17 m) occurring markedly more frequently than the other 2018 mortalities (11.5 dives/hr), and did not become stationary. Most predation events (9 of 12) occurred in less than six hours ($\bar{x}$ = 1.6) from the time of initial detection at the HCB, while the remaining three events occurred within 36 to 243 hours. One final 2018 mortality did not display a pattern of predation, but remained nearly exclusively in the top 2 meters (one detection at 3.1 m), indicating that the assumed mortality event took place outside the HCB array.

Temperature tag results

Eleven of the 16 temperature sensors in 2018 non-surviving steelhead exhibited temperature profiles consistent with being consumed by a marine mammal or bird. These 11 transmitters were all initially detected on the HCB array with ambient temperatures (9-14 °C), then recorded for a period of time (1.5-81.5 hrs) at 35 °C before either exiting receiver range or abruptly returning to ambient temperature (Table A7). Six of these mortality sensors with elevated temperature were detected within range of Sisters Rock, a known harbor seal haulout 750 m south of the HCB, and 7 of the 11 warm sensors later became stationary (Table A7). The temperature increase occurred an average of 17.9 hours after arrival at the HCB (4 of 11 events occurred in < 1 hr). The temperature sensors in the remaining 5 mortalities showed no sign of abnormal temperature increase.

We were able to establish the predation location of 15 of 16 (2017) and 7 of 12 (2018) non-surviving depth-tagged smolts, and 10 of the 11 transmitters that exhibited temperature increase (the remaining mortalities did not have a VPS location within 20 minutes of the change in diving behavior/temperature). Predation locations in both study years tended to be closer to the HCB rather than out away from the bridge, and were somewhat spread out, with a slightly western bias, along the bridge length (Figure A11). There were several predation events (13 of 32) over both years that took place in close proximity to the corners formed by the cross-pontoons and drawspan with the main bridge pontoons, and one that appears to have occurred in the west pool (Figure A11A).

Table A1. Tagged smolts

Tag type	Number tagged	Average Length (mm) ± SE	Average Weight (g) ± SE
2017			
BBC V8	61	183 ± 2	57 ± 2
BBC V8 (delay)	49	185 ± 2	61 ± 3
BBC V9P	40	223 ± 4	107 ± 7
Skokomish V8	89	175 ± 1	50 ± 1
Skokomish V9P	9	209 ± 3	86 ± 3
TOTAL	248	188 ± 2	64 ± 2
2018			
BBC V8	92	175 ± 2	51 ± 3
BBC V7P	29	185 ± 5	61 ± 6
BBC V7T	28	185 ± 5	61 ± 5
Skokomish V8	58	166 ± 2	42 ± 1
Skokomish V7P	21	187 ± 6	56 ± 4
Skokomish V7T	22	181 ± 3	55 ± 2
TOTAL	250	177 ± 1	52 ± 1

Table A2. Comparison of 2017 CJS survival (ϕ) and detection probability (*p*) models

Phase 1 model	number of parameters	QAICc	ΔQAICc	weight
ϕ(~segment)*p*(~array + RMarray:pop)	11	745.64	0.00	0.28
ϕ(~segment + REL-RM:pop)*p*(~array + RMarray:pop)	13	746.19	0.56	0.21
ϕ(~segment + RM-HCB:pop)*p*(~array + RMarray:pop)	13	746.31	0.68	0.20
ϕ(~segment)*p*(~array + RMarray:pop + tagtype)	12	747.66	2.02	0.10
ϕ(~segment + REL-RM:pop)*p*(~array + RMarray:pop + tagtype)	14	748.14	2.50	0.08
ϕ(~segment + RM-HCB:pop)*p*(~array + RMarray:pop + tagtype)	14	748.36	2.73	0.07
ϕ(~segment + REL-RM:pop + RM-HCB:pop)*p*(~array + RMarray:pop)	15	749.49	3.86	0.04
ϕ(~segment + REL-RM:pop + RM-HCB:pop)*p*(~array + RMarray:pop + tagtype)	16	751.50	5.86	0.01
ϕ(~segment + REL-RM:pop)*p*(~array)	11	795.83	50.19	0.00
ϕ(~segment + REL-RM:pop + RM-HCB:pop)*p*(~array)	13	799.53	53.90	0.00
ϕ(~segment)*p*(~array)	9	810.45	64.81	0.00
ϕ(~segment + RM-HCB:pop)*p*(~array)	11	814.36	68.73	0.00
Phase 2 model				
ϕ(~segment + HCB-TS:week.numeric)*p*(~array + RMarray:pop)	12	747.97	0.00	0.92
ϕ(~segment + HCB-TS:week.factor)*p*(~array + RMarray:pop)	20	753.22	5.25	0.07
ϕ(~segment)*p*(~array + RMarray:pop)	11	760.10	12.13	0.00
ϕ(~segment + HCB-TS:length)*p*(~array + RMarray:pop)	12	760.42	12.45	0.00
ϕ(~segment + tagtype)*p*(~array + RMarray:pop)	12	760.85	12.89	0.00
ϕ(~segment + HCB-TS:side.middle)*p*(~array + RMarray:pop)	13	761.28	13.31	0.00
ϕ(~segment + HCB-TS:velocity)*p*(~array + RMarray:pop)	12	762.18	14.21	0.00
ϕ(~segment + HCB-TS:day.night)*p*(~array + RMarray:pop)	13	763.18	15.21	0.00
ϕ(~segment + HCB-TS:tide)*p*(~array + RMarray:pop)	13	764.18	16.21	0.00
ϕ(~segment + HCB-TS:pop)*p*(~array + RMarray:pop)	13	764.28	16.31	0.00

ϕ(~segment + HCB-TS:location.250m)*p*(~array + RMarray:pop)	20	773.32	25.35	0.00

Table A3. Comparison of 2018 CJS survival (ϕ) and detection probability (*p*) models

Phase 1 model	number of parameters	AICc	DeltaAICc	weight
ϕ(~segment + REL-RM:pop + RM-HCB:pop)*p*(~array)	11	723.70	0.00	0.23
ϕ(~segment + RM-HCB:pop)*p*(~array + RMARRAY:pop)	11	723.82	0.12	0.21
ϕ(~segment + RM-HCB:pop)*p*(~array)	9	724.17	0.48	0.18
ϕ(~segment + RM-HCB:pop)*p*(~array + RMARRAY:pop + tagtype)	12	725.85	2.15	0.08
ϕ(~segment + REL-RM:pop + RM-HCB:pop)*p*(~array + RMARRAY:pop + tagtype)	14	725.94	2.24	0.07
ϕ(~segment + REL-RM:pop)*p*(~array)	9	753.84	30.15	0.00
ϕ(~segment)*p*(~array)	7	754.69	30.99	0.00
ϕ(~segment + REL-RM:pop)*p*(~array + RMARRAY:pop)	11	756.06	32.36	0.00
ϕ(~segment)*p*(~array + RMARRAY:pop)	9	756.13	32.44	0.00
ϕ(~segment + REL-RM:pop)*p*(~array + RMARRAY:pop + tagtype)	12	756.38	32.68	0.00
ϕ(~segment)*p*(~array + RMARRAY:pop + tagtype)	10	756.83	33.13	0.00
Phase 2 model				
ϕ(~segment + REL-RM:pop + RM-HCB:pop + HCB-TS:week.factor)*p*(~array)	21	712.92	0.00	0.91
ϕ(~segment + REL-RM:pop + RM-HCB:pop + HCB-TS:length)*p*(~array)	12	718.95	6.03	0.04
ϕ(~segment + REL-RM:pop + RM-HCB:pop + HCB-TS:week.numeric)*p*(~array)	12	719.51	6.58	0.03
ϕ(~segment + REL-RM:pop + RM-HCB:pop)*p*(~array)	11	723.70	10.77	0.00
ϕ(~segment + REL-RM:pop + RM-HCB:pop + HCB-TS:velocity)*p*(~array)	12	723.78	10.86	0.00
ϕ(~segment + REL-RM:pop + RM-HCB:pop + HCB-TS:pop)*p*(~array)	13	724.23	11.31	0.00

ϕ(~segment + REL-RM:pop + RM-HCB:pop + tagtype)*p*(~array)	12	725.73	12.81	0.00
ϕ(~segment + REL-RM:pop + RM-HCB:pop + HCB-TS:side.middle)*p*(~array)	13	727.23	14.31	0.00
ϕ(~segment + REL-RM:pop + RM-HCB:pop + HCB-TS:tide)*p*(~array)	13	727.56	14.64	0.00
ϕ(~segment + REL-RM:pop + RM-HCB:pop + HCB-TS:day.night)*p*(~array)	13	727.82	14.90	0.00
ϕ(~segment + REL-RM:pop + RM-HCB:pop + HCB-TS:location.250m)*p*(~array)	20	736.38	23.46	0.00

Table A4. Stationary tags identified by mobile tracking and mixed model analysis

	2017	2018
Number of smolts detected at HCB	134	174
Number of stationary/consumed tags at HCB identified using mixed model	36	40
Additional stationary tags at HCB identified using mobile receiver	13	7
Total stationary (% of tagged smolts)	49 (36.6)	47 (27.0)

Table A5

Depth (m)	2017 Number of survivor detections	2017 Number of mortality detections (proportion of mortalities)	2018 Number of survivor detections	2018 Number of mortality detections (proportion of mortalities)
0 - 1	3806	8007 (0.68)	3198	7944 (0.71)
2	119	644 (0.84)	158	1253 (0.89)
3	47	861 (0.95)	38	842 (0.96)
4 – 10	189	7588 (0.96)	379	11322 (0.97)
11 – 16	37	935 (0.96)	63	2197 (0.97)
16 - 34	0	1556 (1.0)	50	2244 (0.98)
35 - 38	0	1740 (1.0)	0	663 (1.0)

Table A6. Depth sensor summary

Year and fate of tag	N	Hours of behavior sampled	Number of dives per hour (average ± SE)	Dive depth maximum	Number of tags recording >37 m depth
2017 survivors	13	40	0.4 ± 0.1	16.5	0
2017 mortalities	18	104	4.5 ± 0.6	38.0*	15
2018 survivors	19	40	1.1 ± 0.2	24.8	0
2018 mortalities	13	122	4.6 ± 0.2	38.0*	11

*sensor maximum

Table A7. Temperature sensor summary

Fate of tag	N	Temperature maximum (°C)	Number of tags recording > 35°C*	Number of tags detected on Sisters Rock receiver while 35°C	Number of tags that became stationary
Survivor	18	14	0	0	0
Nonsurvivor	16	35*	11	6	7

*sensor maximum

Figure A1

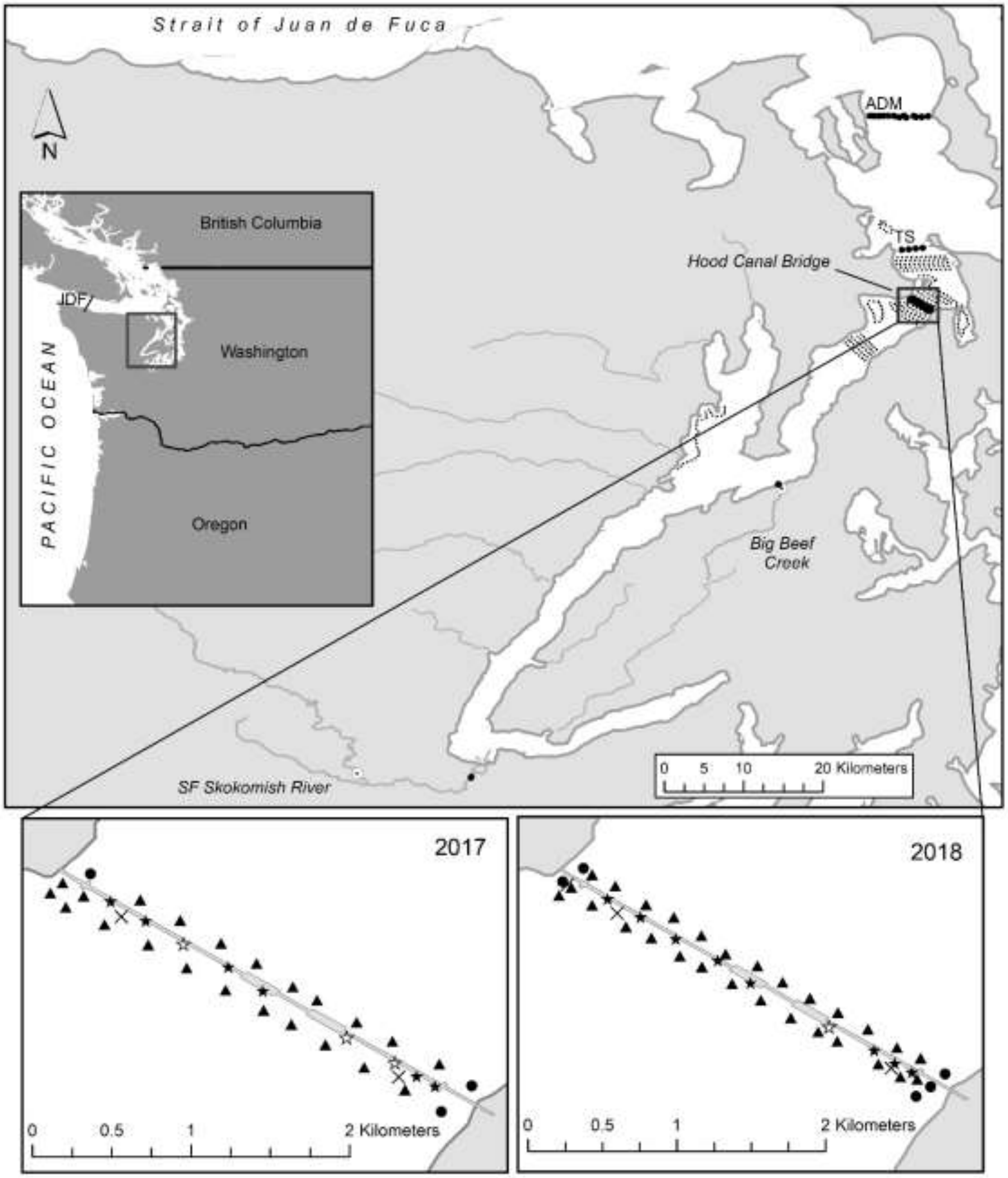
Strait of Juan de Fuca
N
British Columbia
JDF
Washington
PACIFIC OCEAN
Oregon
ADM
TS
Hood Canal Bridge
Big Beef Creek
SF Skokomish River
0 5 10 20 Kilometers
2017
0 0.5 1 2 Kilometers
2018
0 0.5 1 2 Kilometers

Figure A2

A

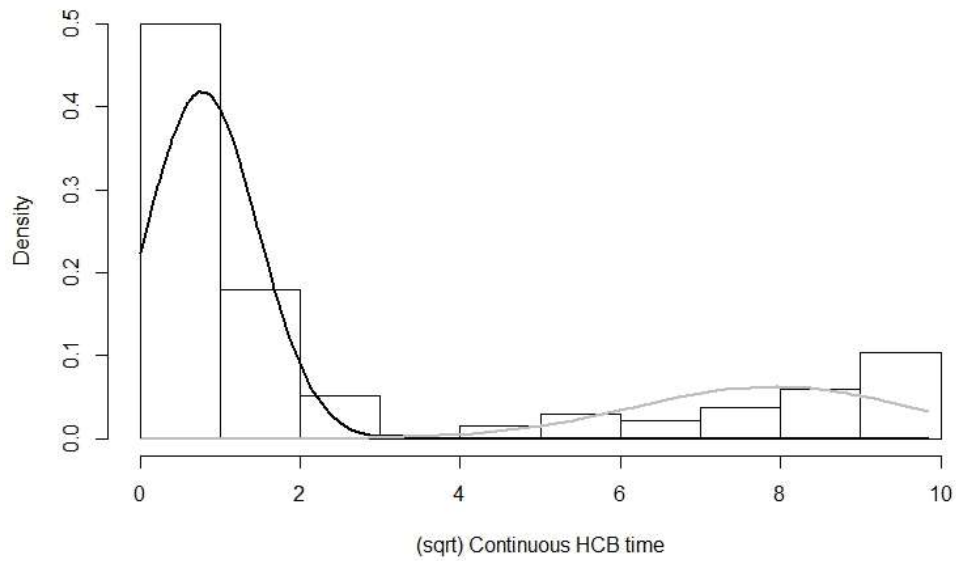
Density
0.0
0.1
0.2
0.3
0.4
0.5
0
2
4
6
8
10
(sqrt) Continuous HCB time

B

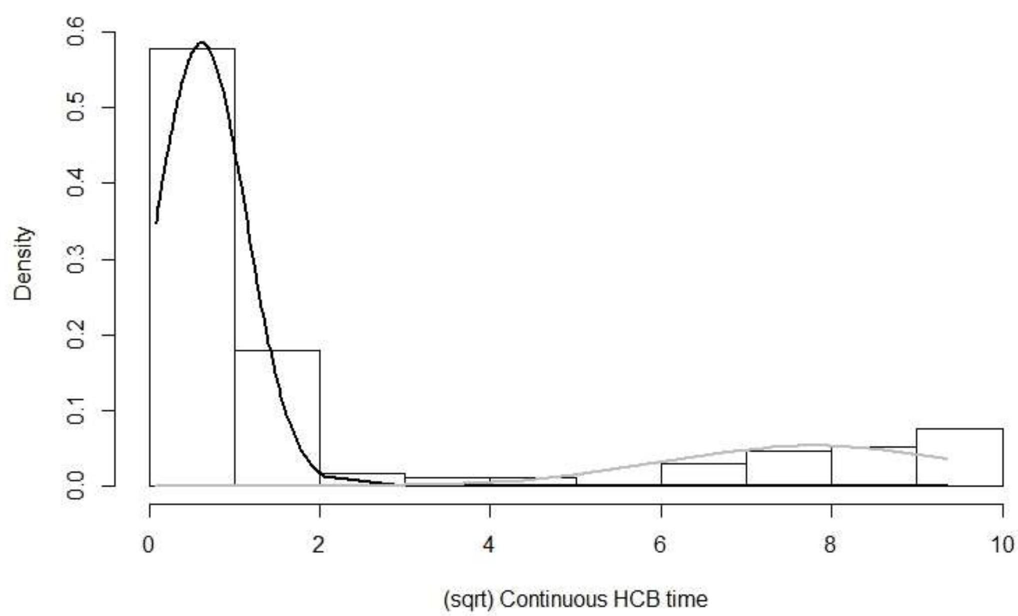
Density
0.0
0.1
0.2
0.3
0.4
0.5
0.6
0
2
4
6
8
10
(sqrt) Continuous HCB time

Figure A3

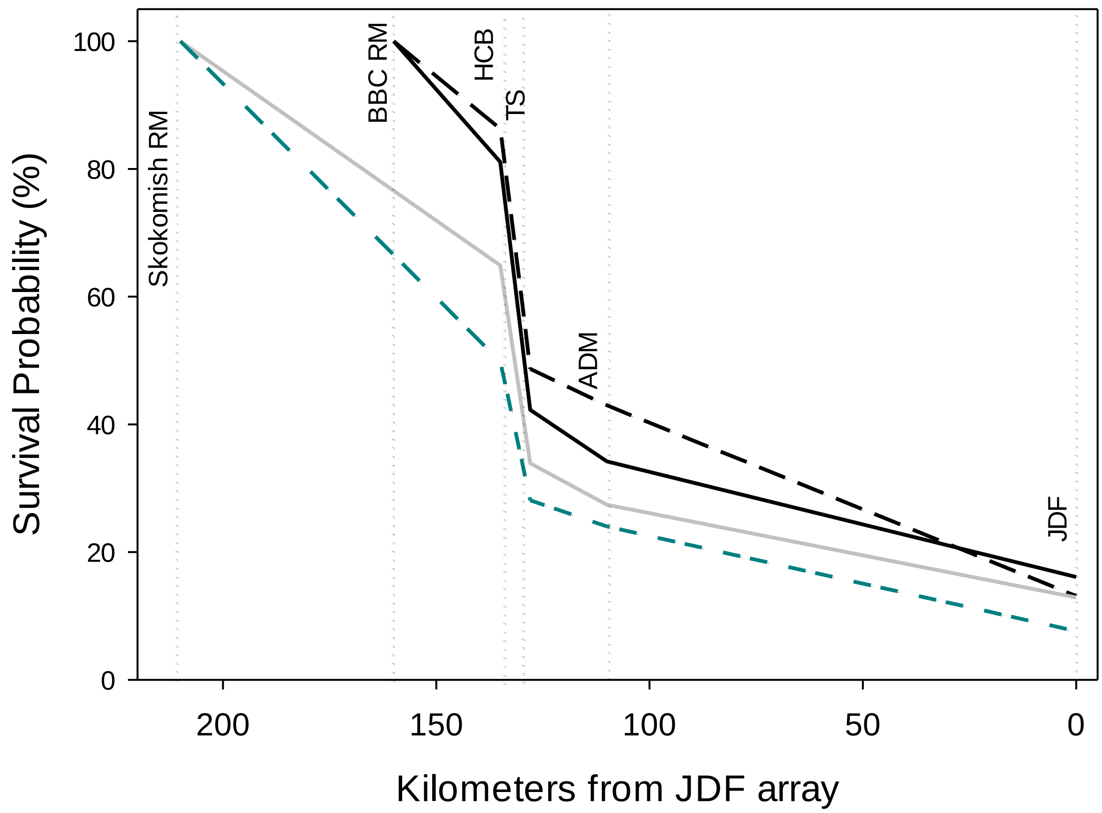
Survival Probability (%)
100
80
60
40
20
0
Skokomish RM
BBC RM
HCB
TS
ADM
JDF
200
150
100
50
0
Kilometers from JDF array

Figure A4

A

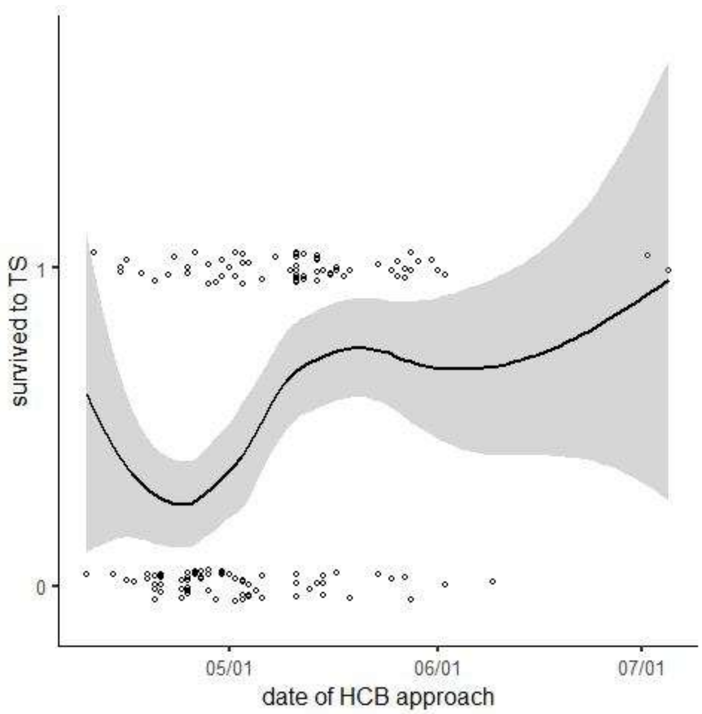
survived to TS
1
0
05/01
06/01
07/01
date of HCB approach

B

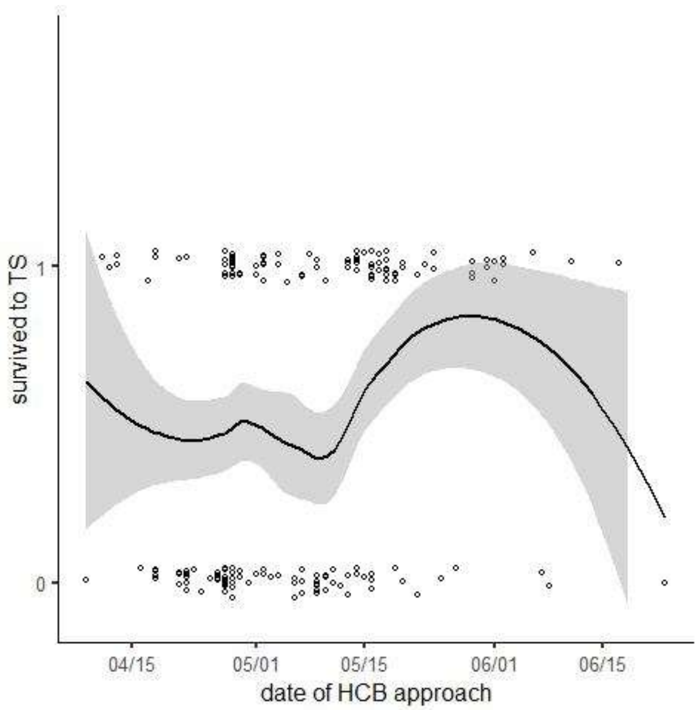
survived to TS
1
0
04/15
05/01
05/15
06/01
06/15
date of HCB approach

Figure A5

A

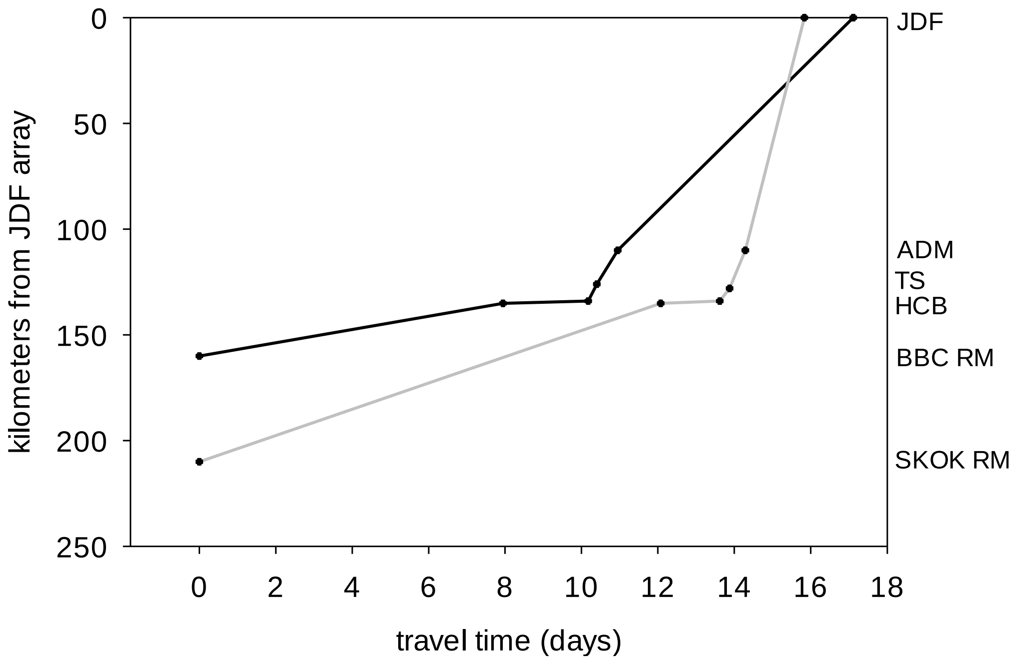

kilometers from JDF array
0
50
100
150
200
250
0
2
4
6
8
10
12
14
16
18
travel time (days)
JDF
ADM
TS
HCB
BBC RM
SKOK RM

B

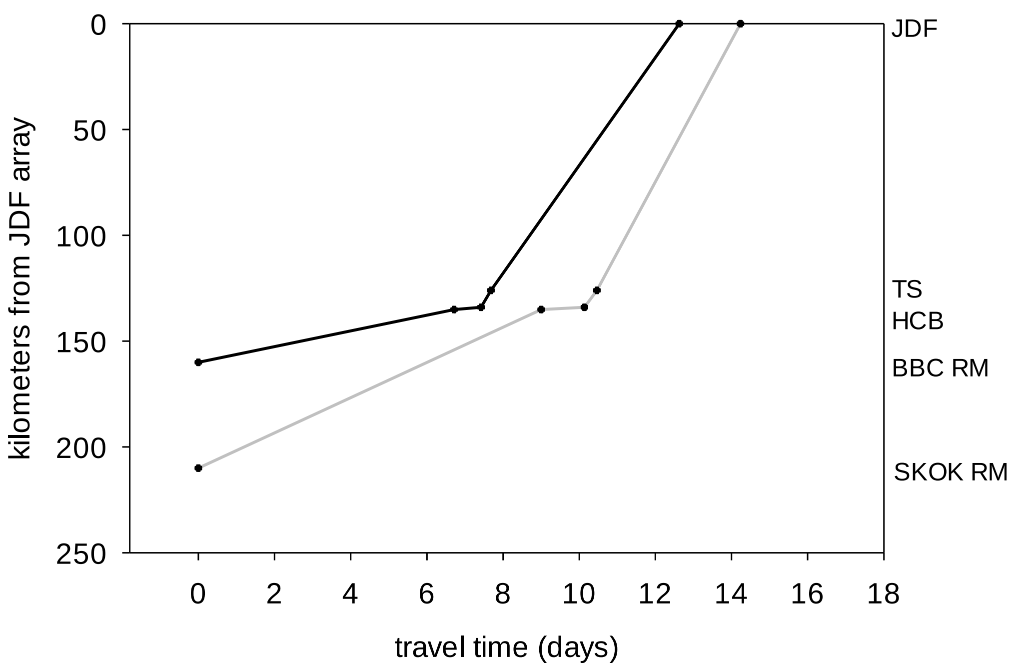

kilometers from JDF array
0
50
100
150
200
250
0
2
4
6
8
10
12
14
16
18
travel time (days)
JDF
TS
HCB
BBC RM
SKOK RM

Figure A6

A

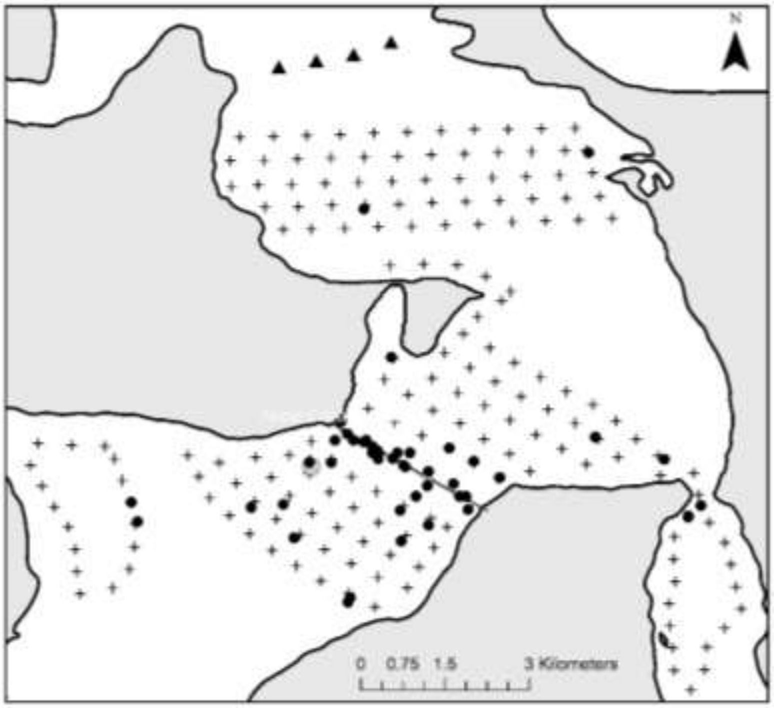

B

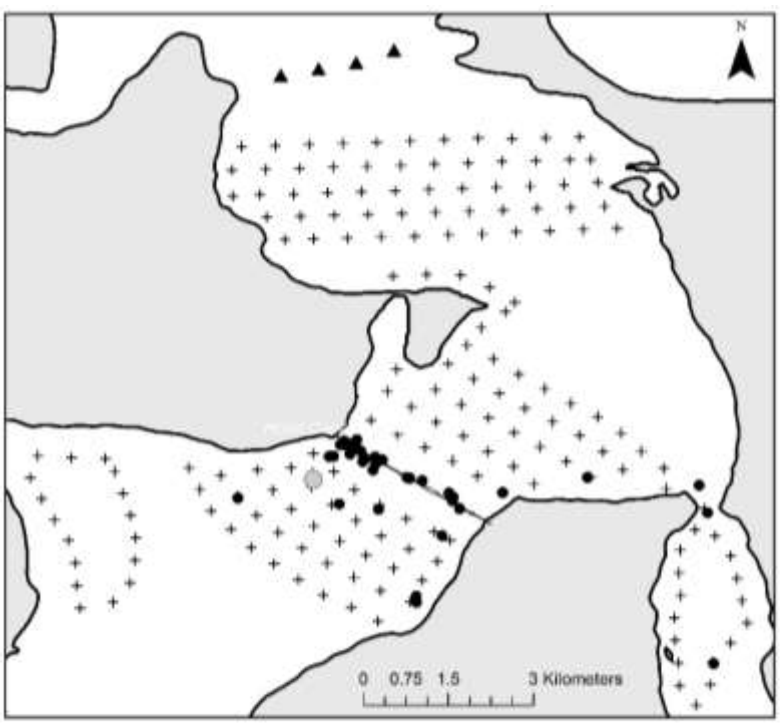

Figure A7

A

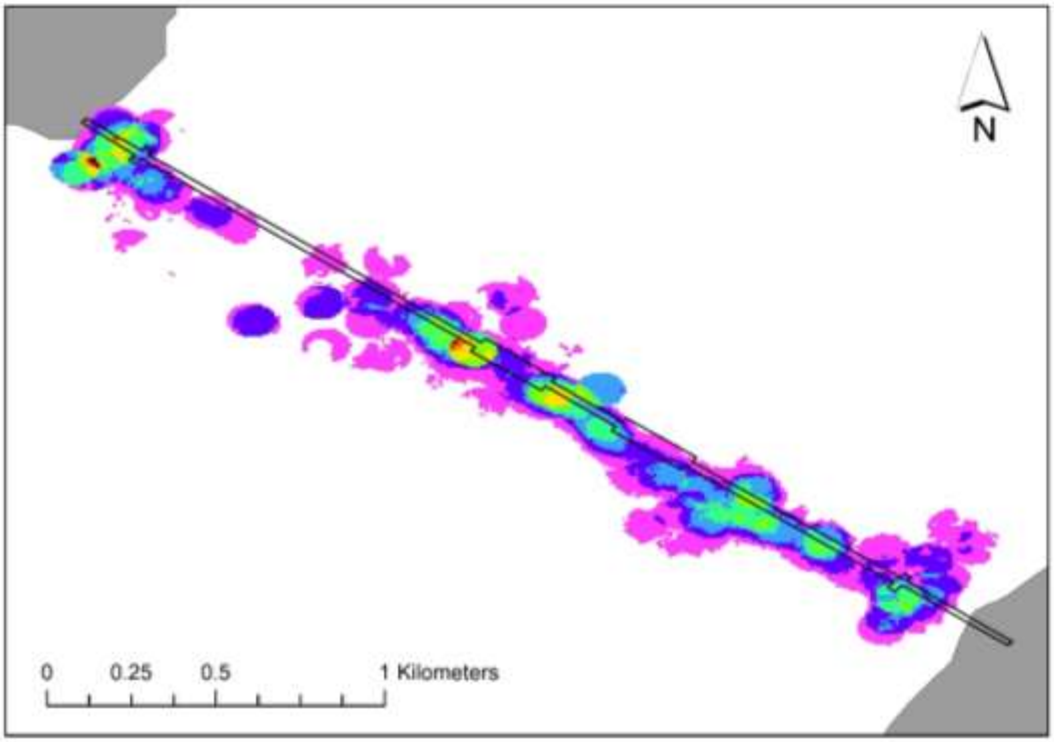

B

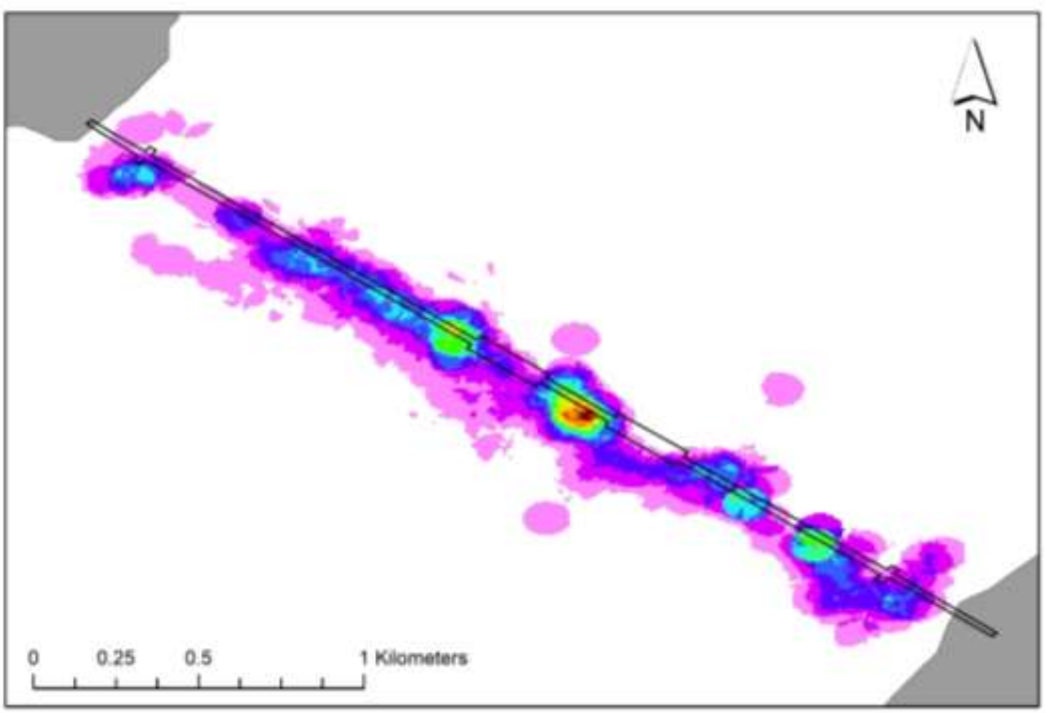

C

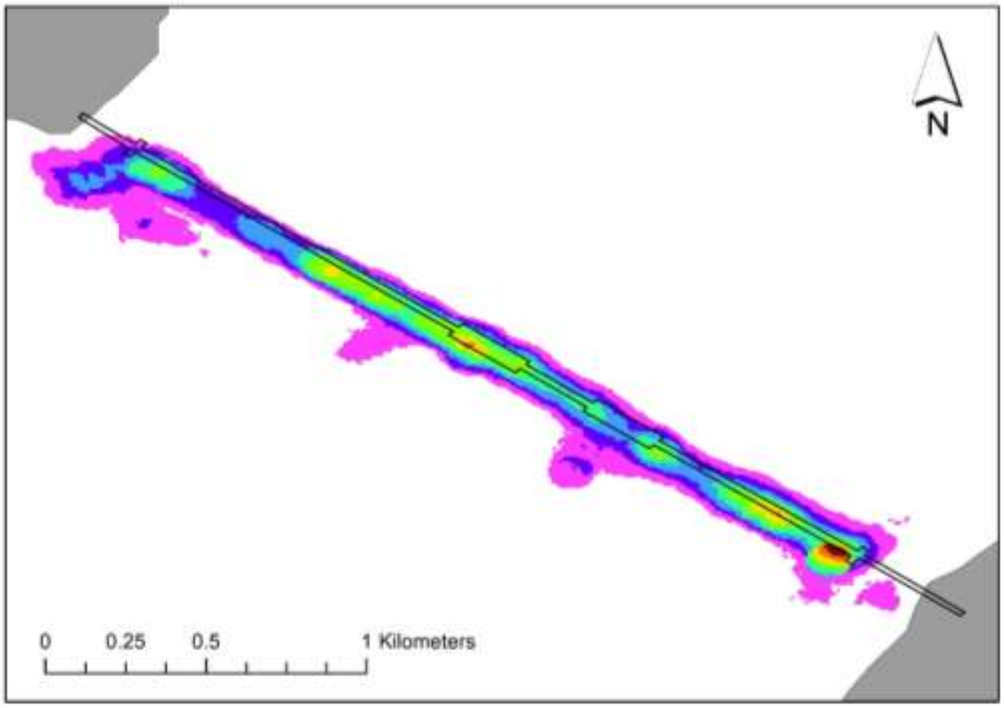

D

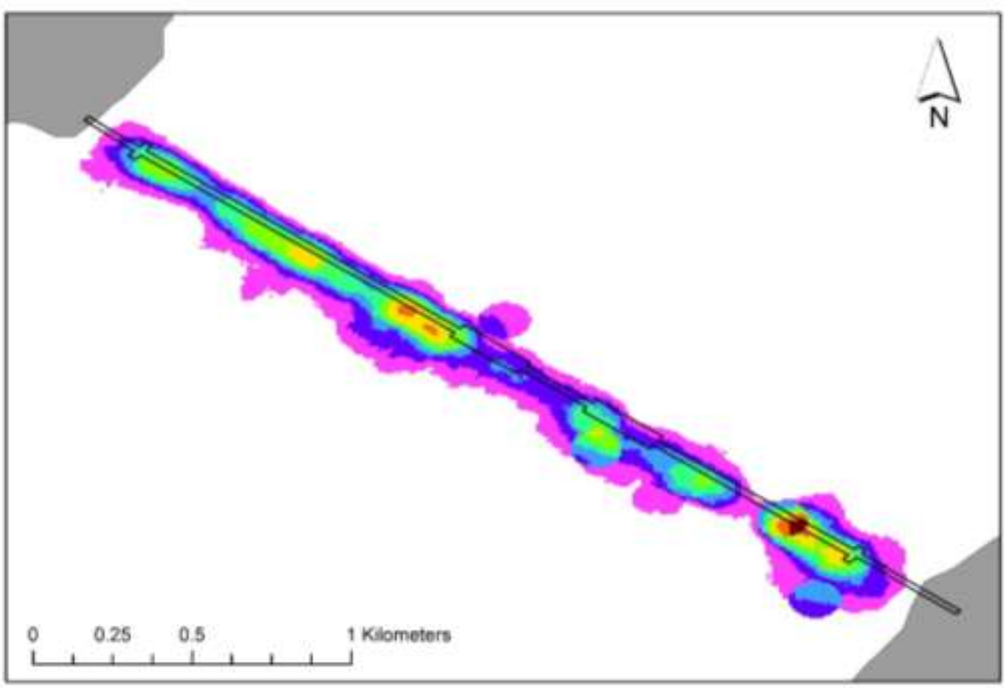

Figure A8

A

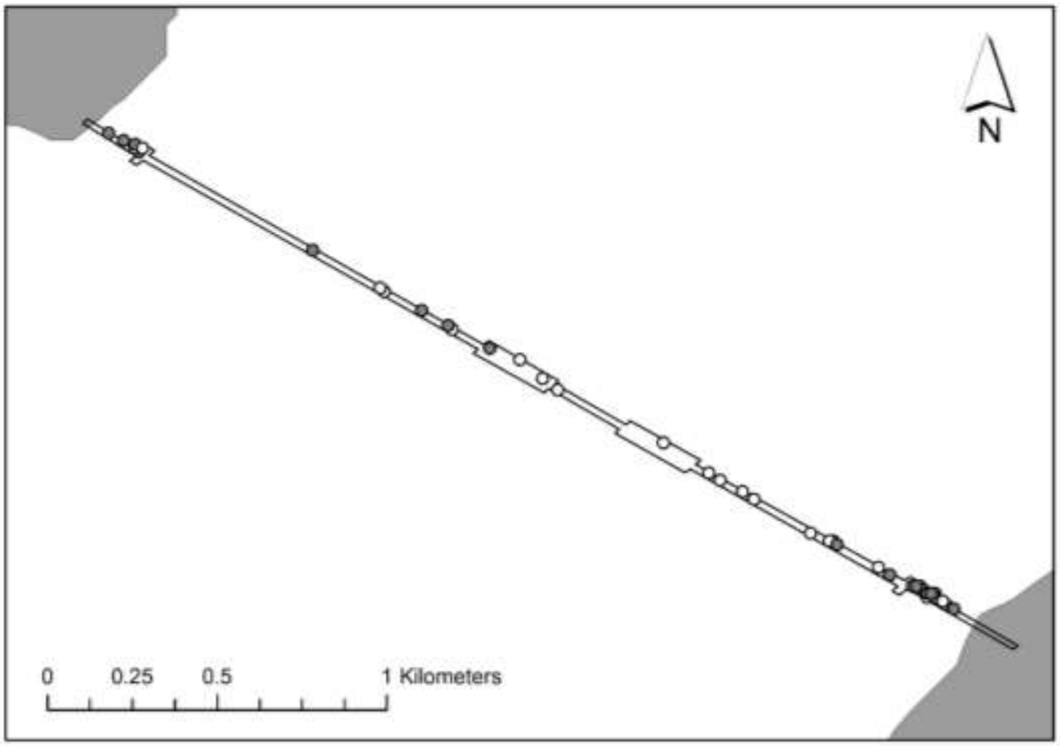

B

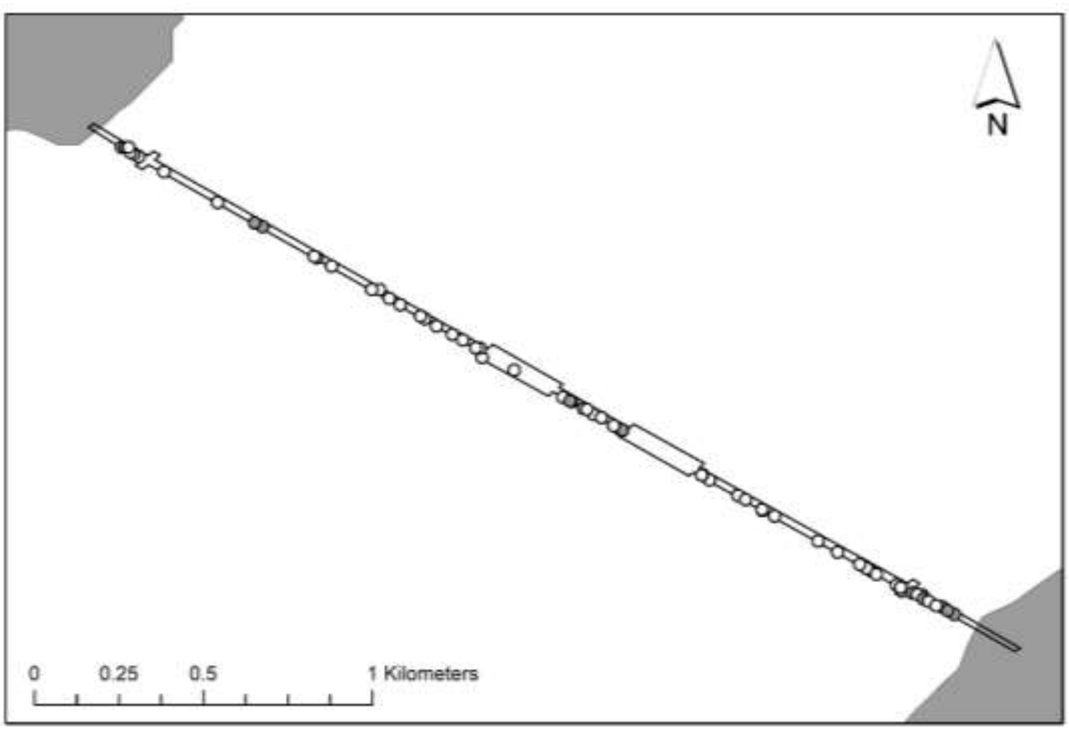

Figure A9

A

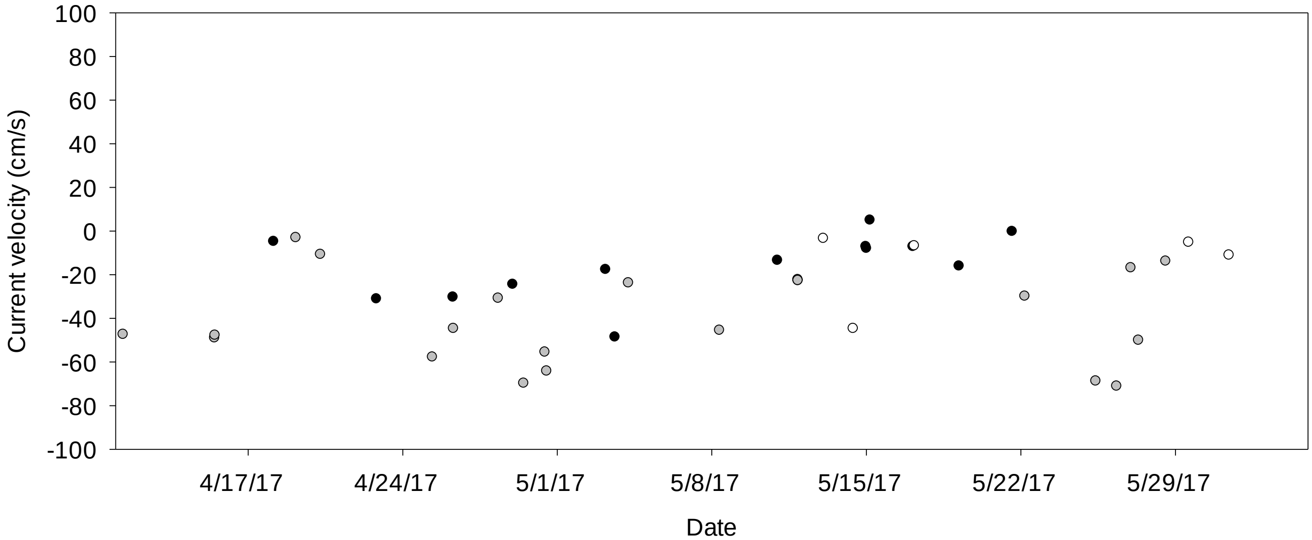
100
80
60
40
20
0
-20
-40
-60
-80
-100
Current velocity (cm/s)
4/17/17
4/24/17
5/1/17
5/8/17
5/15/17
5/22/17
5/29/17
Date

B

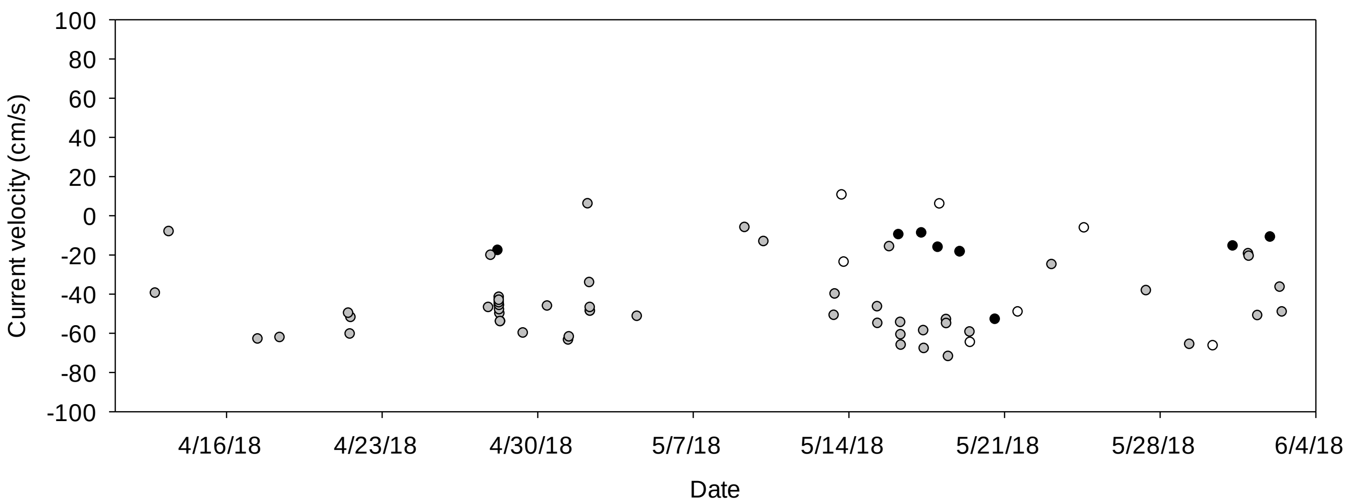
100
80
60
40
20
0
-20
-40
-60
-80
-100
Current velocity (cm/s)
4/16/18
4/23/18
4/30/18
5/7/18
5/14/18
5/21/18
5/28/18
6/4/18
Date

Figure A10

A

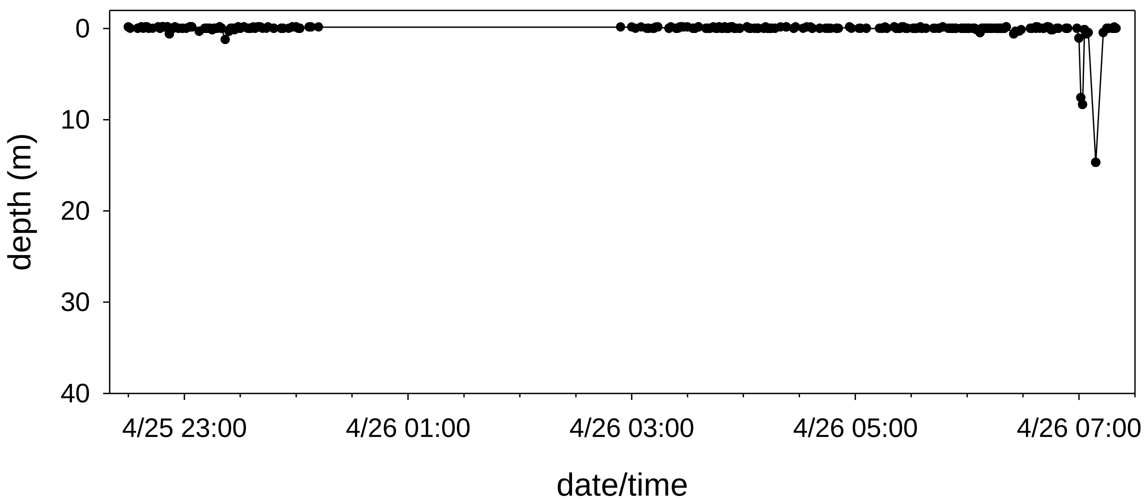

B

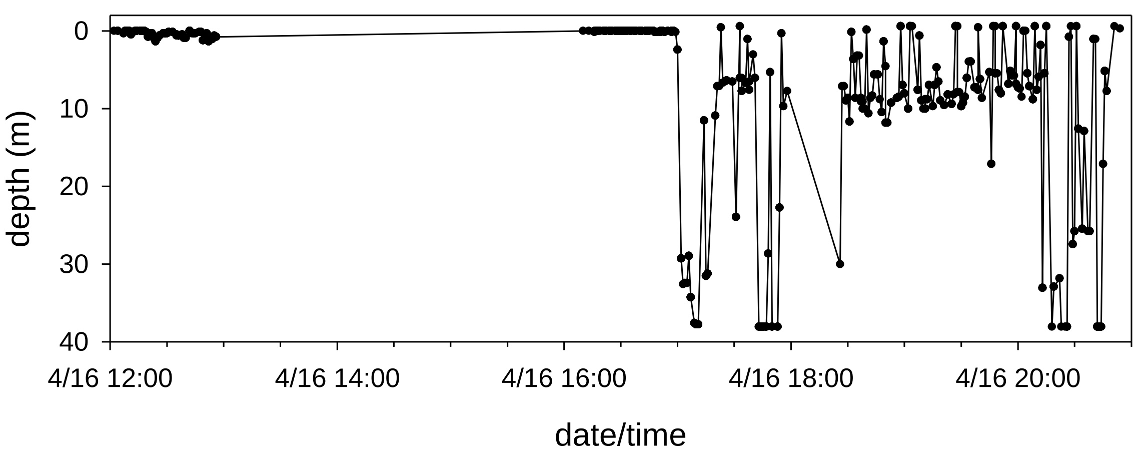

C

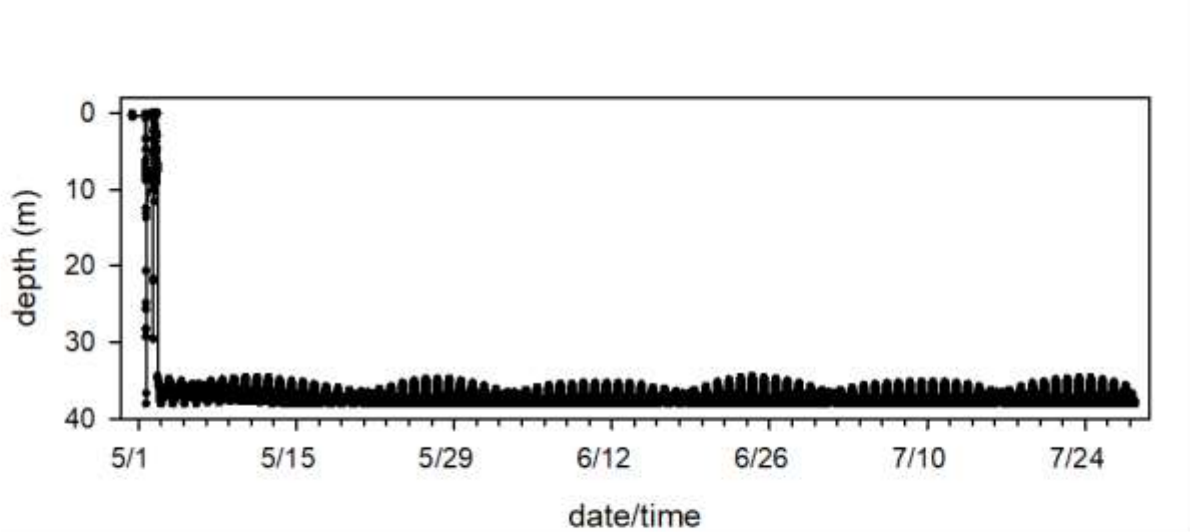

Figure A11

A

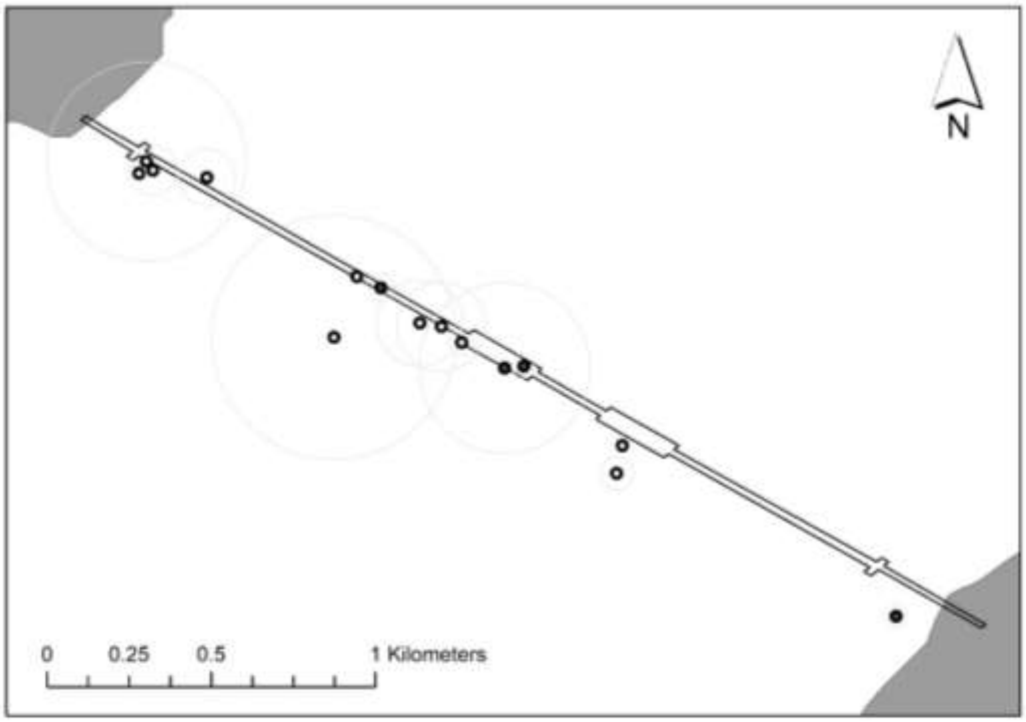

B

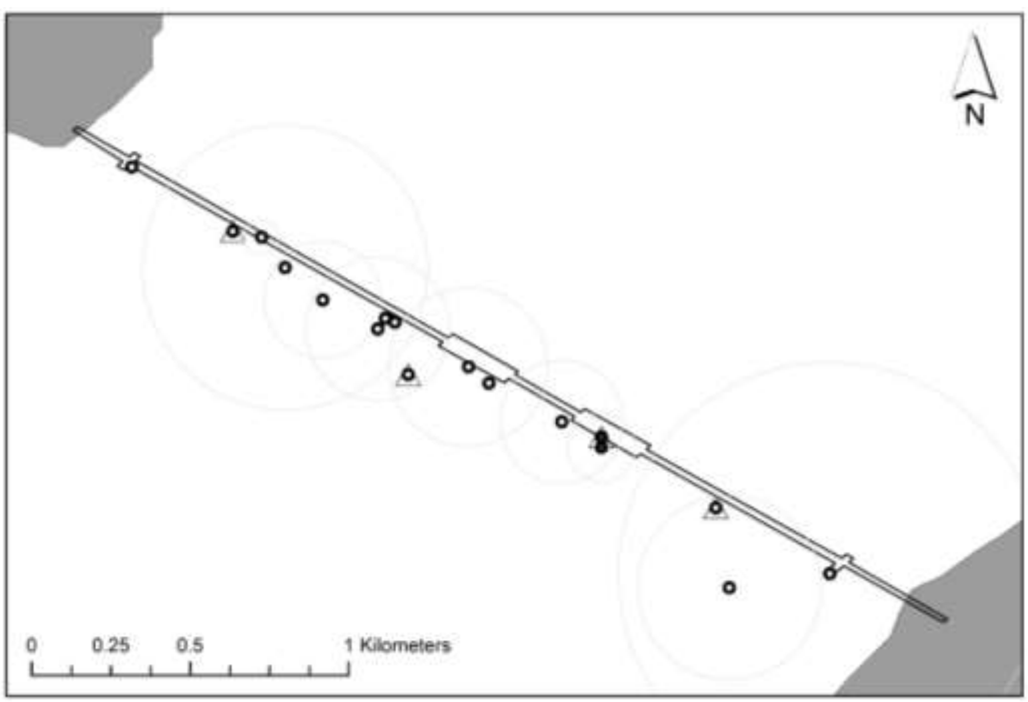

Figure captions

Figure A1. Map of the Hood Canal study area showing receiver locations (black dots) at the mouths of Big Beef Creek and the Skokomish River, the Hood Canal Bridge, at Twin Spits (TS), at Admiralty Inlet (ADM), and the Strait of Juan de Fuca (JDF, black line). Steelhead smolts were collected and released in Big Beef Creek and the South Fork Skokomish River (white circles). Mobile tracking stations are depicted as tiny black dots. Lower insets show locations of VR2AR receivers (black triangles), seabed-moored VR2W receivers (black circles), seabed-moored VR2W receivers with co-located reference transmitter (open stars), VR2W receivers hanging from the bridge railing (black stars), and seabed-moored reference transmitters (black X) that formed the Vemco positioning System (VPS) in 2017 and 2018.

Figure A2. Mixed model fit showing the bimodal distribution of square-root transformed continuous Hood Canal Bridge (HCB) time statistics for tagged steelhead smolts in 2017 (A) and 2018 (B). The black line fits the short HCB time component representing the variation in behavior typical of survivors, while the gray line fits the long HCB time component, indicative of longer variable time periods during which a predator of a tagged smolt continues to forage at the HCB and may deposit the transmitter within range of the HCB.

Figure A3. Survival probability estimated with mark-recapture models using detection data from tagged steelhead smolts from Big Beef Creek (BBC; black solid line = 2017, black dashed line = 2018) or the Skokomish River (gray solid line = 2017, gray dashed line = 2018) from river mouth (RM; km from the Strait of Juan de Fuca (JDF) = 0) to the Hood Canal Bridge (HCB; km from JDF = 135), the Twin Spits array (TS; km from JDF = 128), the Admiralty Inlet array (ADM; km from JDF = 110), to the final JDF array.

Figure A4. Logistic regression plot showing the relationship between survival probability (1 = survived, 0 = did not survive) past the Hood Canal Bridge (HCB) to the Twin Spits array (TS) and the date of HCB approach. The black line depicts the locally estimated scatterplot smoothing (LOESS) function with 95% confidence limits.

Figure A5. Average travel time of steelhead smolts detected at the Skokomish (SKOK; gray line) or Big Beef Creek (BBC; black line) river mouth (RM) to the Hood Canal Bridge (HCB), the Twin Spits array (TS), Admiralty Inlet (ADM; 2017 only) and the Strait of Juan de Fuca (JDF) in 2017 (A) and 2018 (B), plotted in relation to the distance of each population’s distance to the JDF array.

Figure A6. Locations of stationary tags (black circles) identified in 2017 (A) and 2018 (B) by mobile tracking and mixed model analysis. Black crosses represent mobile tracking stations visited to listen for transmitters after the expected smolt migration window.

Figure A7. Density plots, inversely weighted by number of detections per fish, showing the density of VPS positions of tagged smolts encountering the HCB that (A) survived to the TS array or beyond in 2017, (B) survived to the TS array or beyond in 2018, (C) were not detected after the HCB in 2017, and (D) were not detected after the HCB in 2018. Dark red indicates highest densities and pink/purple represent the lowest densities, with green and blue representing intermediate densities (density values differ between figures and scale with sample size).

Figure A8. Locations of where tagged steelhead smolts crossed from the south to the north side of the HCB in 2017 (A) and 2018 (B). Open circles represent crossings that took place between sunrise and sunset (day), while filled circles represent crossings between sunset and sunrise (night).

Figure A9. Crossing location times of smolts that crossed under (light gray circles), around through the east drawspan (black circles), or around through the west drawspan (open circles) in 2017 (A) and 2018 (B) in relation to current velocity (predictions at NOAA current station PUG1603, https://tidesandcurrents.noaa.gov/noaacurrents/Predictions?id=PUG1603_20).

Figure A10. Depth profiles of steelhead smolts exhibiting behavior typical of a surviving smolt (A), a non-surviving smolt that was eaten by a deep and frequently diving predator (B), and a non-surviving smolt that was eaten then deposited by a predator to become stationary until the transmitter battery expired. The maximum value of the depth sensors was 38 m.

Figure A11. Locations of predation events inferred by changes in diving behavior or increases in transmitter temperature in 2017 (A) and 2018 (B). Filled black circles represent predation events that occurred during nighttime hours, while open circles depict events that occurred during the day. Gray circles around most symbols represent the error radius in meters (some are so small they are obscured by the symbol), with triangles surrounding points where data were not available for error calculation.

References

Cormack, R. M. 1964. Estimates of survival from the sighting of marked animals. Biometrika 51:429– 438.

Cunningham, K.A., S.A. Hayes, A.M.W. Rub, C. Reichmuth. 2014. Auditory detection of ultrasonic coded transmitters by seals and sea lions. J Acoust Soc Am 135:1978−1985.

Fletcher, D. 2012. Estimating overdispersion when fitting a generalized linear model to sparse data. Biometrika 99: 230-237.

Jolly, G.M. 1965 Explicit estimates from capture–recapture data with both death and immigration: stochastic model. Biometrika 52:225– 247.

Khangaonkar, T. and T. Wang. 2013. Potential alteration of fjordal circulation due to a large floating structure – Numerical investigation with application to Hood Canal basin in Puget Sound. Applied Ocean Research 39: 146-157.

Laake, J.L. 2013. RMark: An R Interface for Analysis of Capture-Recapture Data with MARK. AFSC Processed Rep 2013-01, 25p. Alaska Fish. Sci. Cent., NOAA, Natl. Mar. Fish. Serv., 7600 Sand Point Way NE, Seattle WA 98115.

Lebreton, J.-D., K. P. Burnham, J. Clobert, and D. R. Anderson. 1992. Modeling survival and testing biological hypotheses using marked animals: a unified approach with case studies. Ecological Monographs 62:67–118.

Moore, M.E.P. and B.A. Berejikian. 2013. A floating bridge disrupts seaward migration and increases mortality of steelhead smolts in Hood canal, Washington State. PLoS ONE 8(9): e73427.

Benaglia, T., D. Chauveau, D.R. Hunter, D. Young. 2009. mixtools: An R Package for Analyzing Finite Mixture Models. Journal of Statistical Software 32:1-29. URL http://www.jstatsoft.org/v32/i06/.

R Core Team. 2019. R: A language and environment for statistical computing. R Foundation for Statistical Computing, Vienna, Austria. URL https://www.R-project.org/.

Romine, J.G., R.W. Perry, S.V. Johnston, C.W. Fitzer, S.W. Pagliughi, and A.R. Blake. 2014. Identifying when tagged fishes have been consumed by piscivorous predators: application of multivariate mixture models to movement of telemetered fishes. Animal Biotelemetry 2:3.

Seber, G.A.F. 1965. A note on the multiple-recapture census. Biometrika 52:249– 259.

Smith, F. 2013. Understanding HPE in the Vemco Positioning System (VPS). Vemco document #: DOC-005457-01.

White, G.C., and K.P. Burnham. 1999. Program MARK: survival estimation from populations of marked animals. Bird Study 46(Suppl.):120–138.

Appendix B. Bishop et al. 2021

The Port Gamble S'Klallam Tribe research component summary is currently in progress, and will be released in early 2021. This summary covers split-beam acoustic surveys, water quality and zooplankton, predator surveys, visual acoustic surveys, light surveys, and gopro and biota surveys.

Factors impacting juvenile salmon migration at the Hood Canal Bridge

Emily Bishop[1], Hans Daubenberger[2], Heather Gordon[3], Chris Jones[2], and Julianna Sullivan[2]

[1] Westward Ecology, PO Box 701, Port Townsend, WA 98368

[2] Port Gamble S'Klallam Tribe, 31912 Little Boston Road NE, Kingston, WA 98386

[3] Immrama Ecology, PO Box 433, Chimacum, WA 98325

Appendix C. Stocking & Pearson 2019

EVALUATING THE POTENTIAL INFLUENCE OF THE HOOD CANAL BRIDGE

ON PISCIVOROUS BIRD AND MAMMAL DENSITY

November 2019

Jessica J. Stocking[1] and Scott F. Pearson[1]

With contributions from

K. Beach, C. Cowles, M. Lance, C. Norris, D. Schwitters, W. Simper and E. Weiss

[1] Washington Department of Fish and Wildlife, Wildlife Science Division, 1111 Washington St. SE, Olympia, WA 98501

This research was completed as a deliverable under contract # 17-07799 with Long Live the Kings and was part of the Hood Canal Bridge Ecosystem Impact Assessment Project that is supported State, Federal and Tribal partners

Washington Department of FISH and WILDLIFE

INTRODUCTION

Human-built structures can dramatically change predator-prey dynamics. For example, dams can act as a barrier to migrating species like salmon. Dams can either dramatically slow or halt migration, and the fish ladders that allow fish to bypass a dam concentrate fish through a single, narrow passageway where they are vulnerable to predation. The end result is a numerical and functional response by pinnipeds, unusually high hunting success, and ultimately, unusually high predation rates (Keefer et al. 2012, Schakner et al. 2017). Another example of human-built structures influencing pinniped predation rates on salmon are the bridges across the Puntledge River, British Columbia, Canada, where harbor seals (*Phoca vitulina*) regularly position themselves side-by-side, ventral side up, in the upstream shadow of two bridges near the light-shadow boundary (Yurk and Trites 2000). The seals swim against the river current and hold their position in the water using minimal movements of their hind flippers. This feeding strategy results in an almost continuous barrier for surface-migrating salmon and results in high interception of downstream drifting salmon smolts that is aided by the bridge lights that illuminate the water surface (Yurk and Trite 2000). In these examples, the seals and sea lions are the proximate cause of high predation rates but the human-built structures are ultimately responsible.

The Hood Canal Bridge is a 1.5-mile long floating bridge that carries vehicle traffic across the northern outlet of Hood Canal. Its pontoons span much of the width of Hood Canal and extend 12 feet underwater. Because of its location, all salmon and steelhead originating from Hood Canal rivers and streams must pass the Hood Canal Bridge on their migration to and from the Pacific Ocean. Recent studies indicate the bridge is a barrier to fish passage (Moore et al. 2013). Slower migration times and higher mortality rates associated with the bridge suggest it is impeding migration and reducing survival. The proximate (e.g., predation) and ultimate (e.g., the bridge structure) mechanisms responsible for reduced salmon survival have not been identified.

Recent research indicates that the bridge may disrupt water circulation (Khangaonkar and Wang 2013). Fjords, like Hood Canal, depend upon strong surface flows associated with tidal exchanges to be replenished with well oxygenated water. The surface water layer is responsible for the outflow of water from the fjord and is important for the flushing of the basin and water quality maintenance. Modeling indicates that the Hood Canal Bridge may have increased water residence times in the basin by 8-13%, which could be an important factor affecting water quality and ultimately fish passage rates.

In 2015, federal, state, tribal, and nonprofit partners convened to develop the Hood Canal Bridge Ecosystem Impact Assessment Plan (Plan). The Plan was designed to determine how the bridge is negatively affecting Endangered Species Act-listed juvenile steelhead and salmon survival and the health of the Hood Canal ecosystem, and guide actions that simultaneously address ecosystem impacts and maintain the bridge. Specifically, the Plan focuses on how the bridge acts as a barrier to juvenile steelhead and salmon migration and how the bridge impacts the entire ecosystem including water circulation, water quality, and predator assemblages and densities.

The specific objectives of this aspect of the Hood Canal Research Project were:

1) Estimate the density of potential steelhead smolt predators within 4 km of the Hood Canal Bridge during the outmigration period (1 April - 30 May).

2) Determine if potential bird and mammal steelhead smolt predators are more abundant near the Hood Canal Bridge during the outmigration period.

3) Provide spatial locations for all potential steelhead smolt predators within 4 km of the bridge during the outmigration period.

This work was conducted concurrent with work to quantify fish densities in the same study area, relative to the bridge. Ultimately, if predation is responsible for high juvenile salmon and steelhead mortality, we would predict that the bridge would concentrate both predators and their prey near the bridge.

METHODS

Survey area

We established transects running perpendicular to the bridge and extending 4 km northeast (bounded by shoreline) and 6 km southwest of the bridge (Fig. C1). Transect lines were spaced regularly throughout the survey area, 500 m apart and extending to 250 m off each shore. We selected these distances between transects and the shore based on previous experience and results using this same methodology in the same region. For density estimation, we discard the most distant 5% of each species detections to improve modeling of detection functions and reduce the potential undue influence of very distant detections (see below). In our experience, the resulting effective detection distances for nearly all species is less than 250 m. This assumption was well supported by our data in this study (see effective survey distances in Table C1). No observations were discarded because of distance from the boat in our distribution analysis.

Boat-based survey methods

Surveys were conducted from a 26-foot Lee Shore boat (R/V *Fog Lark*) with twin-outboard engines traveling at between eight and 12 knots. The starting transect and direction of travel were rotated systematically. The survey team consisted of one boat operator, two observers, and one data recorder; crew members regularly switched duties to avoid survey fatigue. The two observers scanned from 0° off the bow to 90° abeam of the vessel on their respective sides. Observers scanned continuously, with a complete scan of the survey area taking approximately 4-8 seconds. Slightly more effort was spent watching for predators forward of the boat, close to the transect line (within 45° of line). Observers scanned far ahead of the boat for predators that flushed or dove in response to the boat and communicated between observers to minimize missed detections or double counting. Crew members communicated via wireless headsets; data were recorded using DLOG2 software (R.G. Ford, Inc., Portland, OR) that collects real time location data at regular intervals and for each observation. For each predator detected, we collected the following data: group size, species, distance from the vessel, distance and direction from the transect line, and behavior. Additional data such as transect, sea condition, glare and observer initials were recorded manually into the DLOG2 program. Binoculars were used for species verification, but not for detecting animals. Survey effort was ended if glare obstructed the view of observers, or if Beaufort wind scale was 3 or greater for more than 200 m.

We collected the data for analysis in a distance sampling framework, to account for detection error as a function of distance from the transect line (Buckland et al. 2001). Accurate distance estimates are critical to the success of this approach. Technological methods, such as laser range finders, do not reliably read objects that are low profile (e.g. harbor seal heads) or that are only visible or stationary for a fraction of a second (e.g. diving or flushing birds). As a result, substantial time was spent practicing and visually calibrating distance estimates before surveys began, followed by weekly testing throughout the survey period. We estimated the distance from the vessel to the animal and from the transect line to the animal, then calculated the location (i.e., geographic coordinates) of each animal using the vessel's position and the time of the observation and the estimated distances and direction data (Fig. C2).

Our species selection was driven largely by a previous examination into potential juvenile steelhead and salmonid predators (Pearson et al. 2015). We erred on the side of being too conservative, including some species that do not appear to have much dietary overlap but were abundant enough in the study area to potentially have an impact (e.g. pigeon guillemot and grebes). We omitted non-piscivorous waterfowl species (Anatidae) because they do not normally eat fish. Unless we observed flying birds landing or foraging within the survey area, we assumed they were passing through and did not count them. The exception to this rule was for aerial hunters including bald eagles, osprey, and terns. Due to small numbers of observations for some species, they were grouped for analysis with species that were closely related and have similar diets. For example, double-crested cormorant (*Phalacrocorax auritus*), pelagic cormorant (*P. pelagicus*), and Brandt's cormorant (*P. penicillatus*) were combined into the group "Cormorants." A similar approach was taken for loons, grebes, and mergansers. This approach has the added benefit of allowing inclusion of birds that were identified to genus but were not identified to species (e.g. unidentified loon).

Because we were focusing on animals that could potentially be foraging on juvenile salmon and steelhead, we removed all harbor seals and cormorants within 100 m of the Sisters "haulout site" (henceforth, haulout; see Figure C1). Most of the animals detected within 100 m of the haulout were either resting on the rocks (the size of the haulout above the water level depends on the tide height), transiting to or from the haulout, or bottom resting (in the case of harbor seals), and therefore not actively foraging.

Bridge pool surveys

Underneath the bridge are covered pools of water, approximately 90 x 20 m, which receive the retracted bridge deck during bridge openings. Biologists working for the Port Gamble S'Klallam Tribe estimated the density of predators in these pools using a survey method intended to produce comparable density estimates to our boat-based surveys. Specifically, surveyors observed the pools for 40 seconds and recorded the number of each predator species present during that survey. The 40-second survey duration was based on the estimated time it would take to observe the same area traveling in our boat at a speed of 8-12 knots as described in the methods above.

Distribution analysis.

In order to present distribution of potential steelhead predators in the study area, we generated a continuous distribution surface of estimated density for each species or species group using the Kernel Density tool in ArcMap 10.4.1 (Spatial Analyst; ESRI 2011. Redlands, CA). All transects (n = 23) were included in this analysis. Transects were surveyed more times in 2017 than 2018 (Appendix C2). To standardize effort across the two years, we selected the fourteen surveys in 2017 that most closely aligned with the fourteen dates surveyed in 2018. Maps thus reflect the *pooled* relative density of all animals observed over the course of the season (April 4 – June 1). Color value is broken into seven quantiles that vary for each species group; darker areas indicated greater estimated density.

Near-far comparative analysis.

We used a subset of the data for evaluating the effect of the bridge on bird and mammal distribution. We isolated the four interior transects on either side of the bridge in order to minimize the effect of the shoreline on the density of species (i.e. transects 7-10, 17-20; Fig. C1). We then divided transects into three strata: 0-300 m from the bridge (Stratum A); 301-1200 m (Stratum B); and 1201-3000 m (Stratum C). Transects extended to 50 m from the bridge, allowing the crew to observe animals at the bridge.

We used the program DISTANCE 7.3 (Thomas et al. 2010) to estimate f(0), the probability density function of perpendicular detection distances evaluated from the transect line (henceforth, detection function) and the mean number of animals per group [or cluster size, E(s)] for each species. We compared four binning approaches for the detection function: continuous (no binning), and three, five and seven bins of equal intervals. The detection function was calculated using the entire dataset for each species and could take one of two forms: uniform or half-normal, each with the possibility of a cosine adjustment. The models were compared using AIC (Burnham and Anderson 1998), and model fit was evaluated using a Chi-squared goodness of fit (GOF) test. Due to size and behavioral differences, the effective sampling distance differs across species. For this reason, we truncated the data to contain 95% of observations for each species based on distance (Buckland et al. 2001). Discarding detections far from the transect line can also improve modeling of detection functions (Buckland et al. 2001).

We estimated density (animals per km^2) for each stratum by using the estimates and encounter rate (number of animals observed per km, ER) from DISTANCE with the following formula:

$$\hat{d} = 1000 * f(0) * \hat{E}(s) * ER/2$$

The "hats" over the letters designate estimates. DISTANCE used the mean observed cluster size as $\hat{E}(s)$ unless an internal test found evidence that detection was a function of cluster size, in which case DISTANCE applied a correction (Buckland et al. 2001). We used density estimates and 95% confidence intervals to compare densities of potential predators in the three strata for each year.

For marine mammals, detection on the line can be imperfect (i.e. $g(0) \neq 1$) due to long dive times. To address this, we applied correction factors based on published measures: g(0) = 0.204 for harbor seals (Laake et al. 1997) and g(0) = 0.292 for harbor porpoise (Wilson et al. 2014, Jefferson et al. 2016). These correction factors were also applied to the US Fish and Widlife Service survey data for comparison.

To provide context to the densities reported in this study, we compared our densities to those derived using nearly identical survey methods and analytical approach in other areas of the Salish Sea ("US Fish and Wildlife Service (USFWS)" data points in Figs. 13-21). For details on the survey methodology please see Raphael et al. (2007) and for details on this specific survey year please see McIver et al. (2019) and Pearson and Lance (2019). Note that although the survey effort is focused on marbled murrelets, we record all other birds and mammals detected during these surveys. These surveys were conducted by the same survey crew and survey platform as used in this study and were conducted between 15 May and 30 July 2018, and therefore overlap our Hood Canal effort for about two weeks. Because of the differences in the timing of these two survey efforts, we only included comparative densities for year-round resident species and not migratory species that are likely moving through the area during the April-May period.

RESULTS

We surveyed the 23 transects over 29 days between 3 April - 2 June, 2017 and over 15 days between 4 April - 31 May, 2018. We recorded observations of 13,133 individual animals. We observed 22 piscivorous avian species and three marine mammal species (Appendix C1). Mean effective survey distance was 226 m and ranged from 174 m (marbled murrelet; *Brachyramphus marmoratus*) to 290 m (loons; Table C1), but all species were truncated to 250 m to reduce the potential of double-counting of animals. Numbers of observations for some species (e.g. loons, cormorants) were quite low, and estimates could not be derived for every stratum-year (see mergansers, Fig. C21).

For in-pool surveys, fourteen surveys were completed of the east pool and ten were completed of the west pool between the two survey years. Only two species were observed in the bridge pools (pigeon guillemots and harbor seals); results can be found in their respective sections with data points labeled "in-pool" (Figs. C13 and C17).

For four species (rhinoceros auklet, grebes, harbor seal and harbor porpoise), even the distance function with the lowest AIC value provided a poor fit to the data (Table C1), due to fewer observations on the transect line than observations in the next bin farther from the line. This could be a violation of the assumption that individuals on the line are detected perfectly. In our study, we suspect this to be evidence of evasive behavior of animals in the boat's path before detection occurs. However, we have no reason to expect that bias differs over time or space within our study (i.e. should not vary within our data) and maintain that the relative densities are useful for the purposes of the study. It should be noted, however, that particular caution should be exercised in comparing those densities to other studies/methodologies.

Because each species exhibited fairly unique density patterns among strata and between years, we focus on species-specific results rather than generalizable patterns among species. Pigeon guillemots (*Cepphus columba*) were the most numerous species observed throughout the study (Appendix C1). Distribution was fairly consistent during the two years, with higher densities along shores and at the bridge (Fig. C3). In the near-far analysis, the three strata were significantly different from one another, with guillemot density decreasing with distance from bridge (Fig. C13). Guillemots in the bridge pools and elsewhere in the region (USFWS) were more consistent with the stratum farthest from the bridge.

Rhinoceros auklets (*Cerorhinca monocerata*) were more abundant in the second year of the study but did not show a strong preference between strata (Fig. C14). Interestingly, they were observed almost exclusively on the northeast side of the bridge in both years (Fig. C4). Overall, rhinoceros auklets were less dense compared to other areas in the region (Fig. C14), particularly in 2017.

Horned grebes (*Podiceps auritus*) were the second most numerous species observed during the study, and all grebe species were relatively abundant (Appendix C1). Grebe species were most numerous along the shorelines and in bays (Fig. C5) and showed no preference for the bridge in either year (Fig. C15).

Marbled murrelets comprised the fourth most numerous species observed during the study (Appendix C1). Murrelets had higher relative densities in 2017 and on the southwest side of the bridge (Fig. C6). In the near-far analysis, densities were higher in 2018, and birds showed no preference for the near-bridge stratum (Stratum A) relative to the other two more distant strata. Murrelet densities in the study area were generally consistent with data from elsewhere in the region (Fig. C16).

Harbor seals (*Phoca vitulina*) and harbor porpoises (*Phocoena phocoena*) showed similar patterns. Both species had generally low densities throughout the study area (Figs. C7, C8) and were typically observed as single animals (Table C1). Seals and porpoise had higher density in Stratum A near the bridge in 2017, although there was some overlap in confidence intervals with the other strata (Figs. C17, C18). This pattern did not hold in 2018, when all strata had approximately equal density estimates. Seals appeared to have slightly lower densities in this study than elsewhere in the region (Fig. C17), while porpoise had more similar densities (Fig. C18).

Loons were composed of three species: common (*Gavia immer*), Pacific (*G. pacifica*) and red-throated (*G. stellate*; Appendix C1). Common loons were relatively abundant in the study area, and red-throated loons were infrequently observed (Appendix C1). Loons were distributed along the shorelines and in bays, with the pattern particularly evident in 2018 (Fig. C9). Loon density was lowest in Stratum C, farthest from the bridge, with non-overlapping confidence intervals in 2017 (Fig. C19).

Comorants were similarly distributed in 2017 and 2018 and appeared to be avoiding the center of the channel (Fig. C10). Density was higher near the bridge in 2017 and generally low in strata B and C, but there were no observations in Strata A in 2018 (Fig. C20). Densities were generally low (Table C1).

Three species of mergansers were observed during the study, dominated by red-breasted merganser (*Mergus serrator*; Appendix C1). In general, mergansers occurred along the shorelines (Fig. C11) and in groups of 2-3 individuals (Table C1). In 2017, merganser density was significantly higher near the bridge in 2017 when stratum C density could not be estimated, and only a single observation occurred in near-far transects in 2018 (Fig. C21).

Caspian terns (*Hydroprogne caspia*) were observed more to the northeast of the bridge (Fig. C12). There were too few observations in the near-far subset of the data to compare densities between strata.

DISCUSSION

The only species demonstrating consistently higher densities near the bridge than far from the bridge was the pigeon guillemot, and we suspect this pattern is occurring because they are nesting in suitable crevices provided by the bridge structure. Generally, pigeon guillemot diet during the nesting season is focused on nearshore species like gunnels and sculpin (Ewins 1993, Bishop et al. 2016). However, because the water is deep along the bridge, it is possible that birds nesting on cavities in the structure of the bridge are not foraging in the nearshore and, as a result, they might eat more juvenile salmon than they would normally. There is little overlap in the length of prey generally consumed by guillemots and the length of outmigrating juvenile steelhead (Ewins 1993, Pearson et al. 2015). However, juvenile Chinook, coho and chum would be within the preferred prey length of this species.

Harbor porpoise and seal both spent more time near the bridge in 2017 than in 2018. These inter-annual differences likely reflect variation in prey distribution. There is no strong numerical response by either of these species to the bridge. It is possible, however, that individuals of these two species are eating more listed salmon near than far from the bridge (a functional response), but this possibility cannot be evaluated without diet composition information.

Several species of birds and mammals show some evidence for greater density near the bridge in at least one year. However, it is difficult to evaluate the cumulative impacts of multiple predators on listed salmon and steelhead near the bridge without specific diet information for these species both near and far from the bridge. Because no species other than the guillemot is exhibiting a strong potential numeric response to the bridge, and if predators are exhibiting a top-down influence on listed salmon and steelhead at the bridge, it might be the cumulative influence of multiple predator species that is causing this effect. We only present this idea as a potential hypothesis to investigate. The distribution of some bird species (loons, mergansers and to some degree, cormorants) suggest that the bridge essentially acts as an extended shoreline out into the deep water in the middle of Hood Canal – a pattern that we don't see in other areas of Puget Sound.

A very surprising outcome of this study was pattern of two bird species being largely restricted to one side of the bridge or the other. The rhinoceros auklet was found almost exclusively north of the bridge and the marbled murrelet was more abundant to the south. These patterns raise questions about the influence of the bridge on the movement of birds into or out of Hood Canal and ultimately have large-scale influences on predator-prey dynamics and the health of both fish and predator populations. We don't know if the bridge has anything to do with this pattern. The bridge is placed near the confluence of Hood Canal and Admiralty Inlet, an area with considerable tidal exchange, strong currents, and the mixing of fresh and salt water. As a result, these patterns of bird distribution may have occurred prior to bridge construction.

ACKNOWLEDGEMENTS

A special thanks to Michael Schmidt and Iris Kemp from Long Live the Kings for supporting and coordinating this project. Megan Moore provided very helpful comments on an earlier version of this report. Hans Daubenberger and Emily Bishop with the Port Gamble S'Klallam Tribe provided the "in-pool" used density comparisons. The Northwest Forest Plan Effectiveness Monitoring Program provided the "USFWS" densities. Thank you all very much!

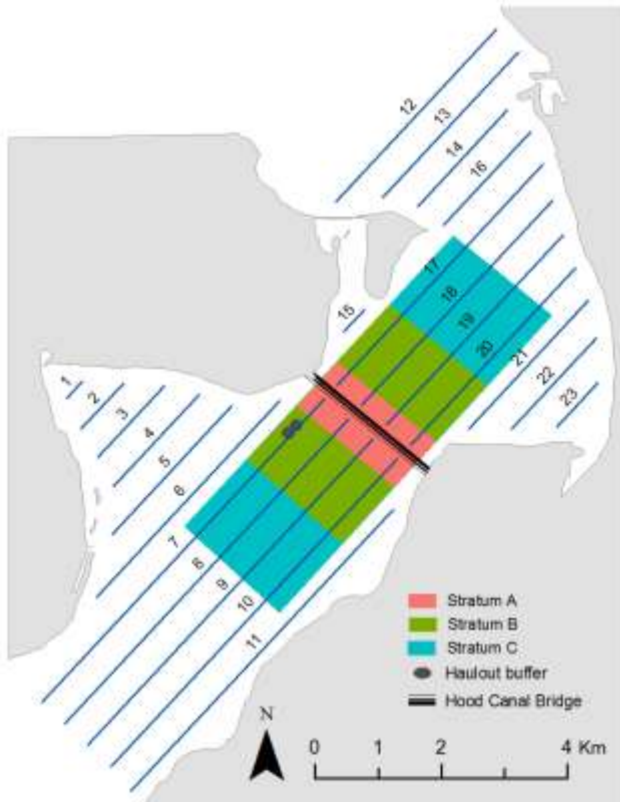

Figure C1. Study area and perpendicular transect lines for surveys of potential steelhead predators in area of Hood Canal Bridge. Bold blue lines indicate the section of transects used for the near-far analysis; color blocks indicate the three distance strata from the bridge (A=0-300 m; B=301-1500 m; C=1501-3000 m).

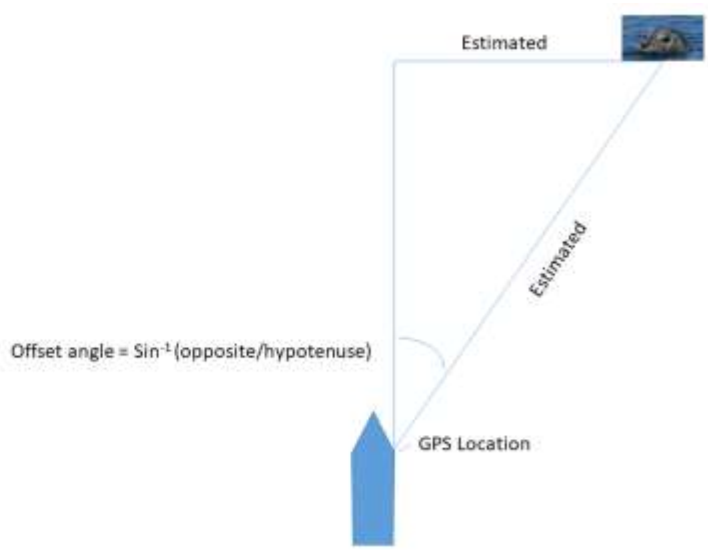

Figure C2. Illustration of technique for calculating an animal's position using estimated distances from vessel and transect line.

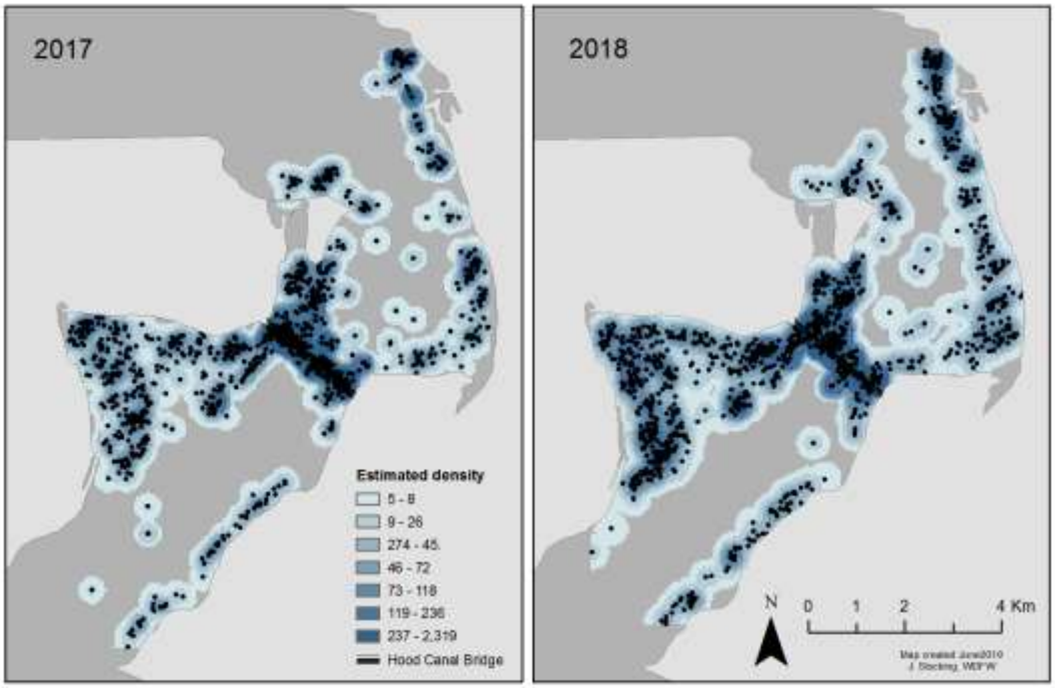

Figure C3. Relative density of pigeon guillemot (*Cepphus columba*) in line transect surveys of Hood Canal bridge, WA during steelhead outmigration 2017-2018 (n=14visits/year). Points represent observations.

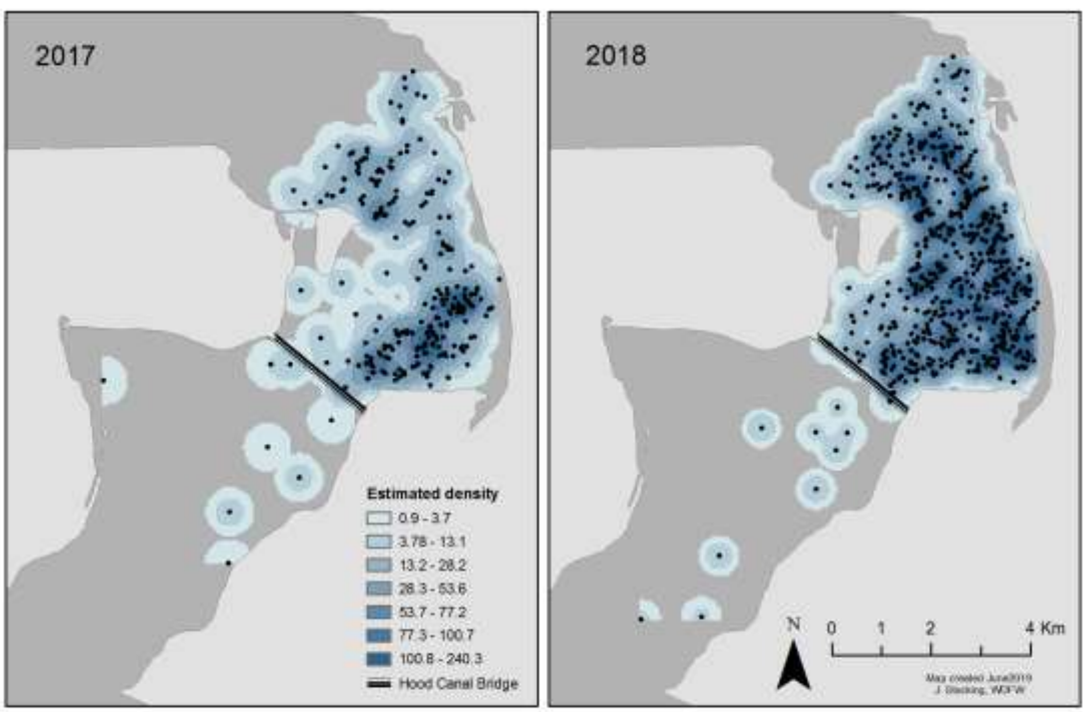

Figure C4. Relative density of rhinoceros auklet (*Cerorhinca monocerata*) in line transect surveys of Hood Canal bridge, WA during steelhead outmigration 2017-2018 (n=14visits/year). Points represent observations.

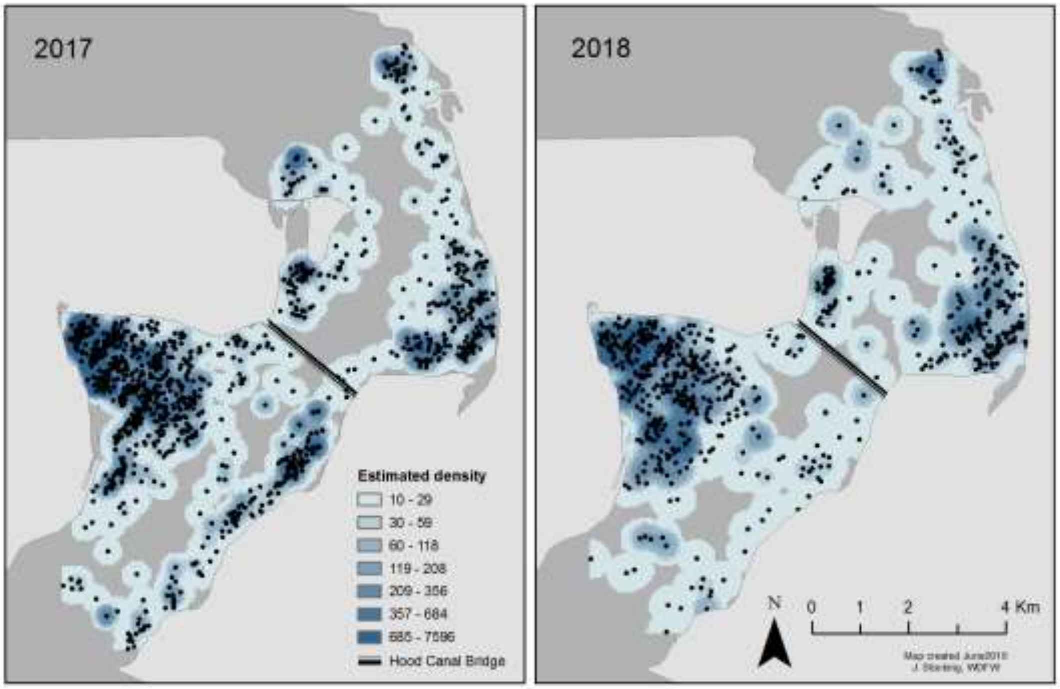

Figure C5. Relative density of grebes (Family Podicipedidae) in line transect surveys of Hood Canal bridge, WA during steelhead outmigration 2017-2018 (n=14visits/year). Points represent observations.

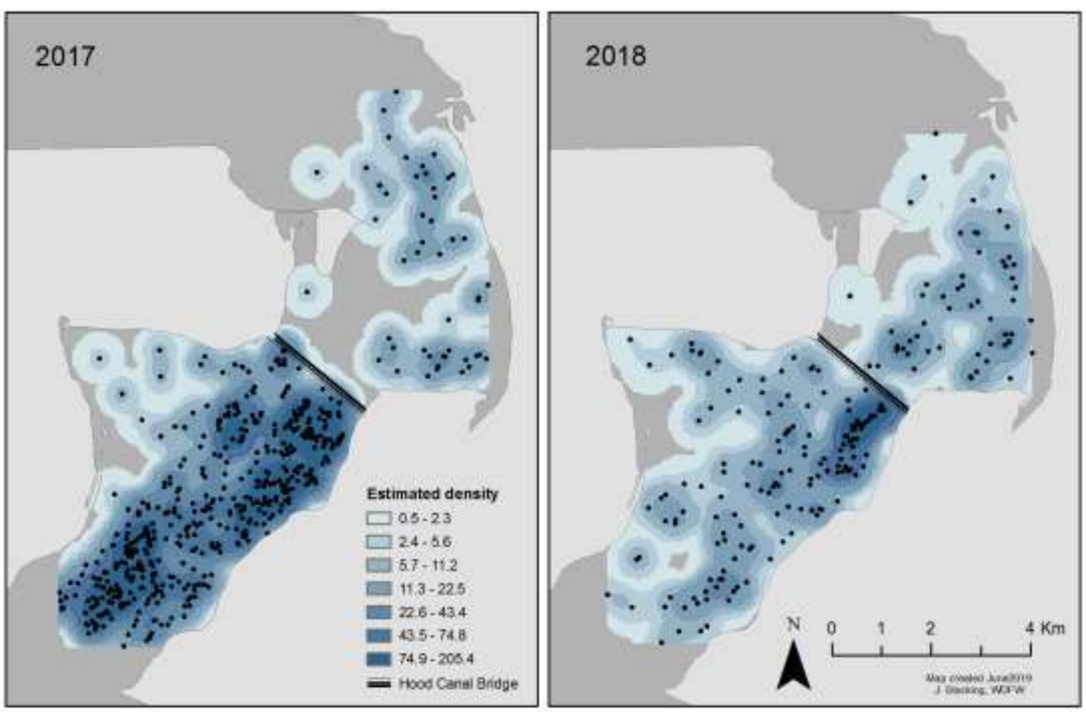

Figure C6. Relative density of marbled murrelet (*Brachyramphus marmoratus*) in line transect surveys of Hood Canal bridge, WA during steelhead outmigration 2017-2018 (n=14visits/year). Points represent observations.

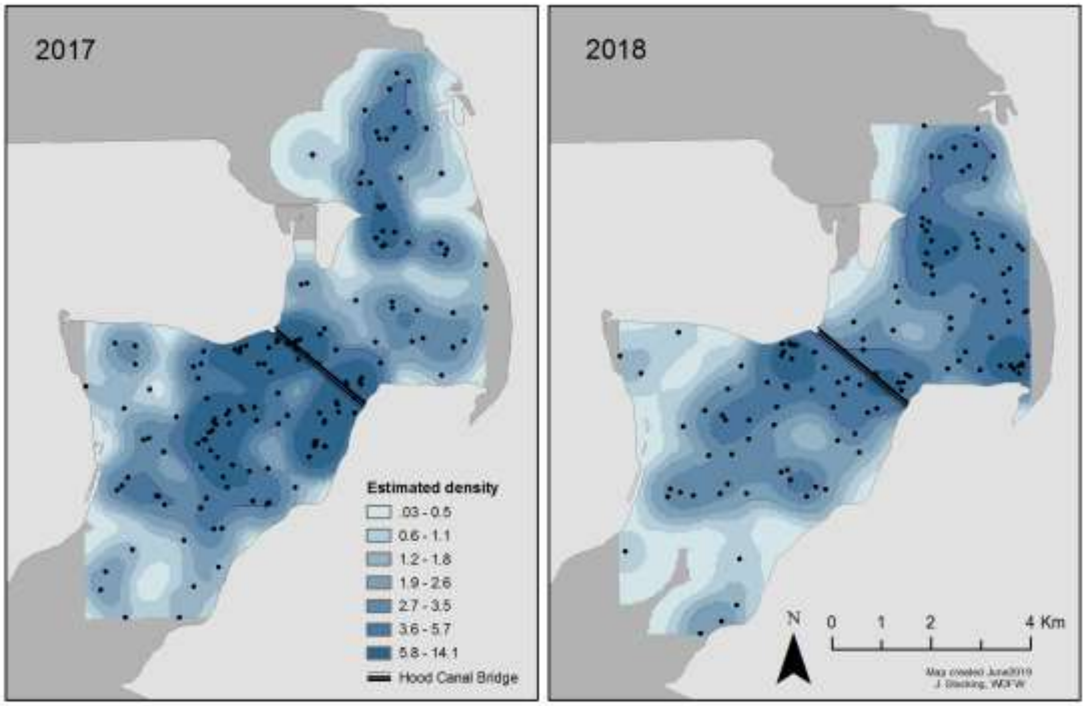

Figure C7. Relative density of harbor seal (*Phoca vitulina*) in line transect surveys of Hood Canal bridge during steelhead outmigration 2017-2018 (n=14 visits/year). Points represent observations.

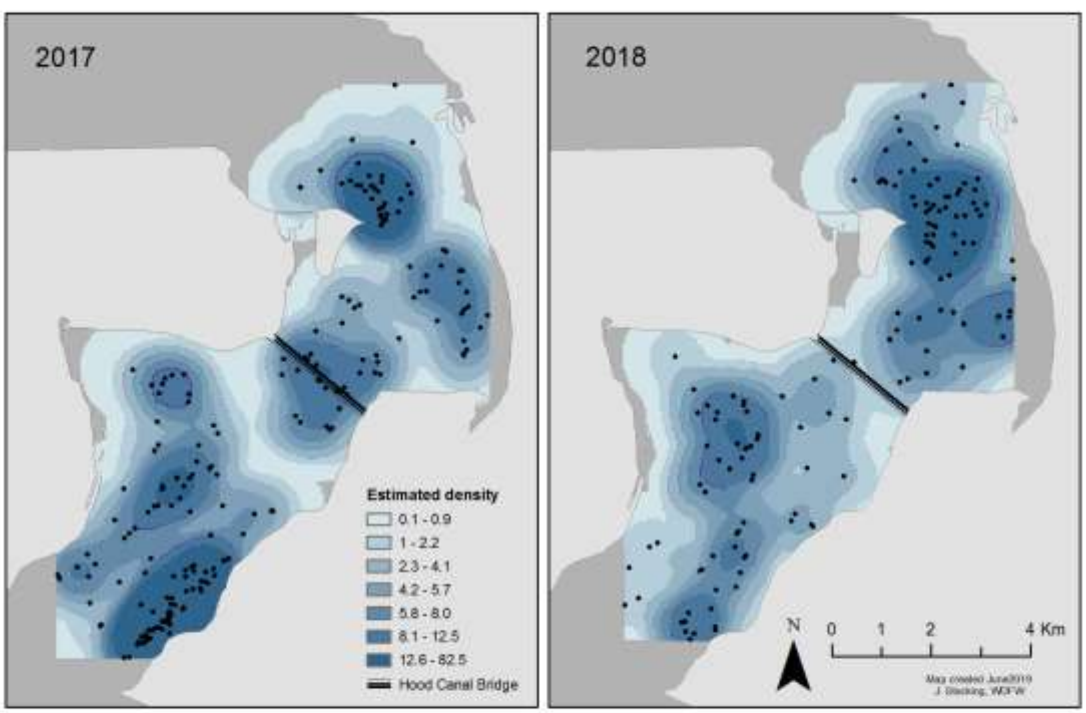

Figure C8. Relative density of harbor porpoise (*Phocoena phocoena*) in line transect surveys of Hood Canal bridge during steelhead outmigration 2017-2018 (n=14 visits/year). Points represent observations.

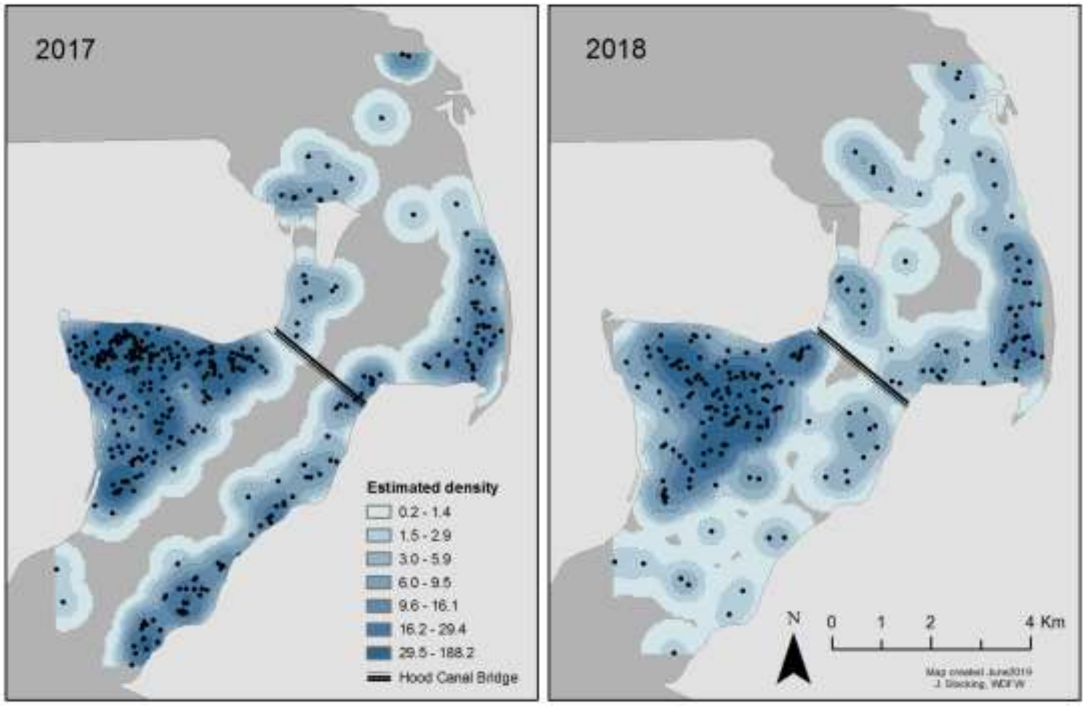

Figure C9. Relative density of loons (*Gavia spp.*) in line transect surveys of Hood Canal bridge during steelhead outmigration 2017-2018 (n=14visits/year). Points represent observations.

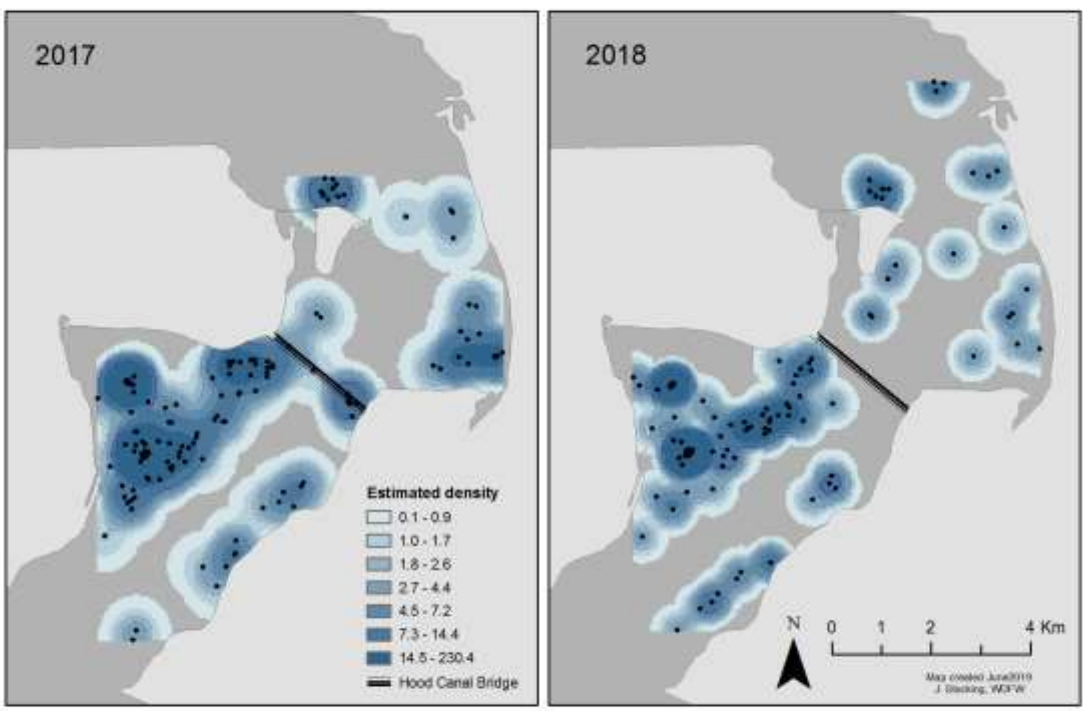

Figure C10. Relative density of cormorants (*Phalacrocorax spp.*) in line transect surveys of Hood Canal bridge during steelhead outmigration 2017-2018 (n=14visits/year). Points represent observations.

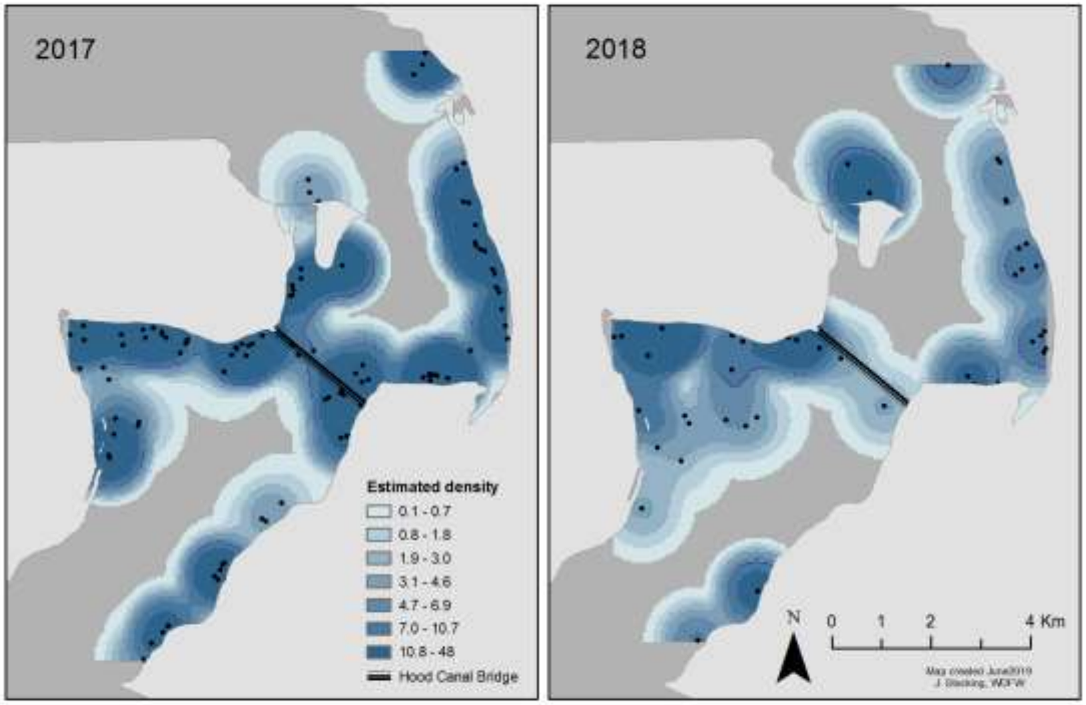

Figure C11. Relative density of mergansers (*Mergus spp*) in line transect surveys of Hood Canal bridge during steelhead outmigration 2017-2018 (n=14visits/year). Points represent observations.

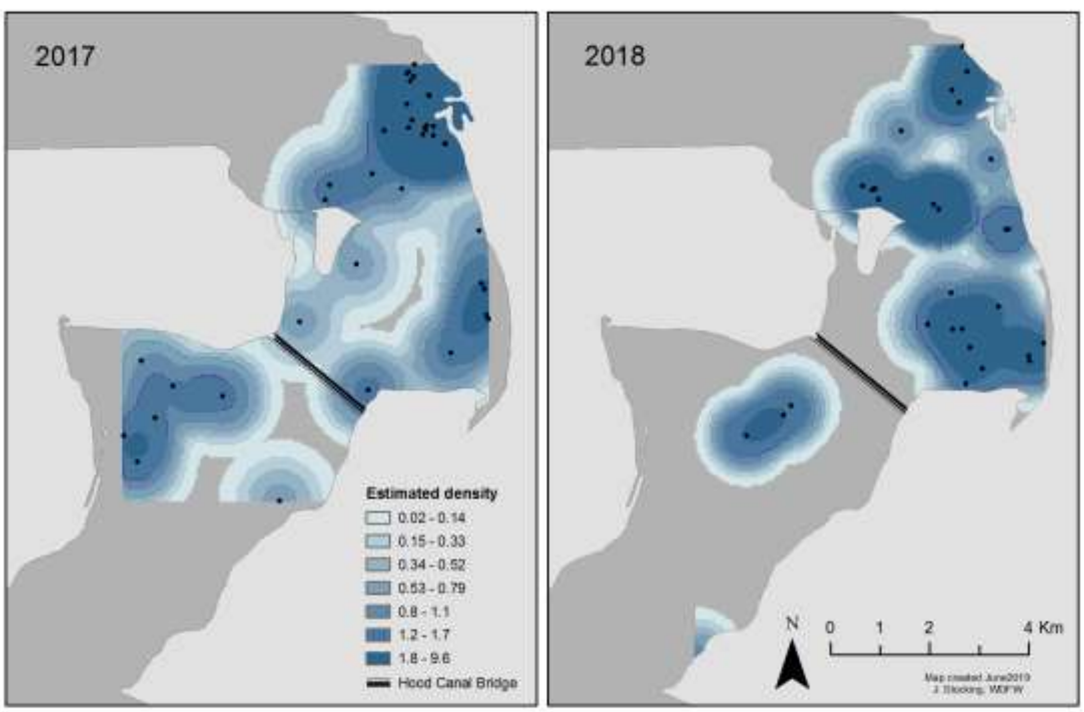

Figure C12. Relative density of Caspian tern (*Sterna caspia*) in line transect surveys of Hood Canal bridge during steelhead outmigration 2017-2018 (n=14visits/year). Points represent observations.

Table C1. Data and distance analysis summary for potential steelhead predator species near Hood Canal Bridge, WA.

Species	#obs	Effective survey distance (m)[a]	Estimated density animals (km^2)	Density Lower 95% CI	Density Upper 95% CI	Estimated abundance	Abundance Lower CI	Abundance Upper CI	Detection model	Distance bins [b]	p-value GOF	Mean cluster size
Pigeon guillemot	730	232	8.496	6.85	10.53	103	82	126	Uniform+	5	0.821	4.2
Rhinoceros auklet	290	207	2.367	1.79	3.12	28	22	37	HN	3	0.070	1.9
Grebes[†]	135	221	1.749	1.06	2.89	21	13	35	HN	5	0.087	3.6
Marbled murrelet	128	174	1.590	0.98	2.59	19	12	31	Uniform+	5	0.997	2.4
Harbor seal	89	226	1.466	1.06	2.03	18	13	24	HN	3	0.349	1.0
Harbor porpoise	82	224	1.118	0.81	1.55	2	1	5	Uniform	3	0.127	1.7
Loons[†‡]	32	250	0.103	0.06	0.18	1	1	2	HN	5	0.813	1.1
Cormorants[†]	29	235	0.077	0.05	0.12	1	1	1	Uniform	5	0.883	1.3
Mergansers[†]	26	226	0.144	0.09	0.24	2	1	3	Uniform	5	0.860	2.7

[a] Represents distance in which 95% of observations were documented and beyond which data are truncated.
[b] Number of distance bins (intervals) in detection function with lowest AIC value.
[†] Multiple species were lumped into this group.
[‡] Forced truncation at 250 m due to distance between transects.

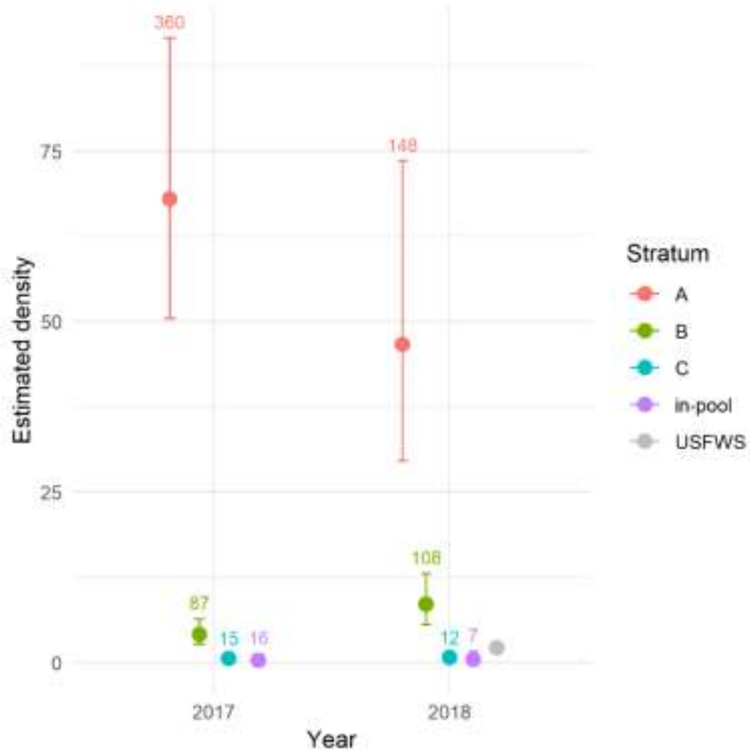

Figure C13. Density estimates (birds/km^2) derived by distance sampling of pigeon guillemot (*Cepphus columba*) near Hood Canal Bridge, WA during steelhead outmigration in 2017-2018. Stratum A is 0 - 300 m from the bridge; Stratum B is 301 – 1200 m; Stratum C is 1201 – 3000 m. In-pool refers to animals observed in the two pools within the structure of the bridge; USFWS is estimated density from summer 2018 surveys in the Salish Sea for comparison (see Methods). Error bars represent 95% confidence interval; numbers above bars represent sample size.

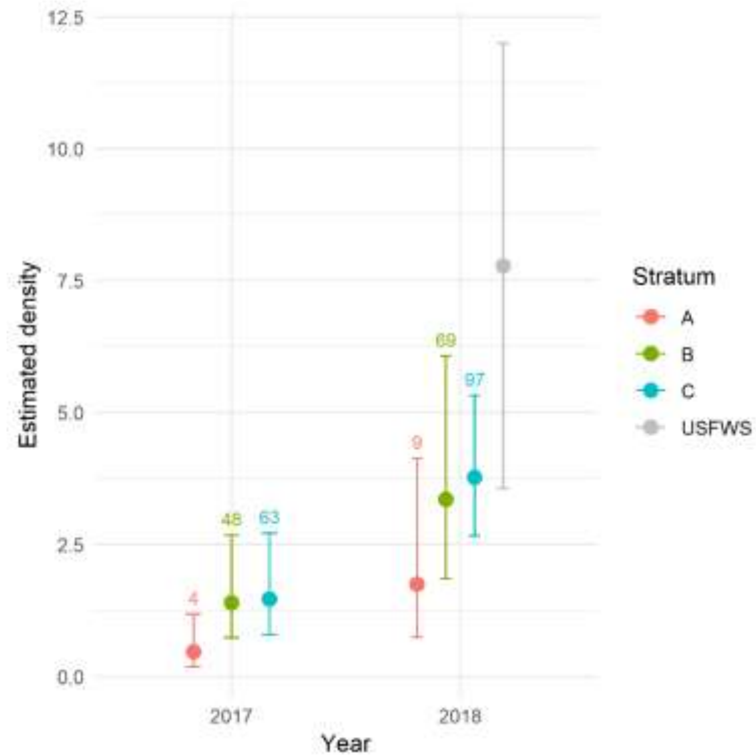

Figure C14. Density estimates (birds/km^2) derived by distance sampling of rhinoceros auklet (*Cerorhinca monocerata*) near Hood Canal Bridge, WA during steelhead outmigration in 2017-2018. Stratum A is 0 - 300 m from the bridge; Stratum B is 301 – 1200 m; Stratum C is 1201 – 3000 m. USFWS is estimated density from summer 2018 surveys in the Salish Sea for comparison (see Methods). Error bars represent 95% confidence interval; numbers above bars represent sample size.

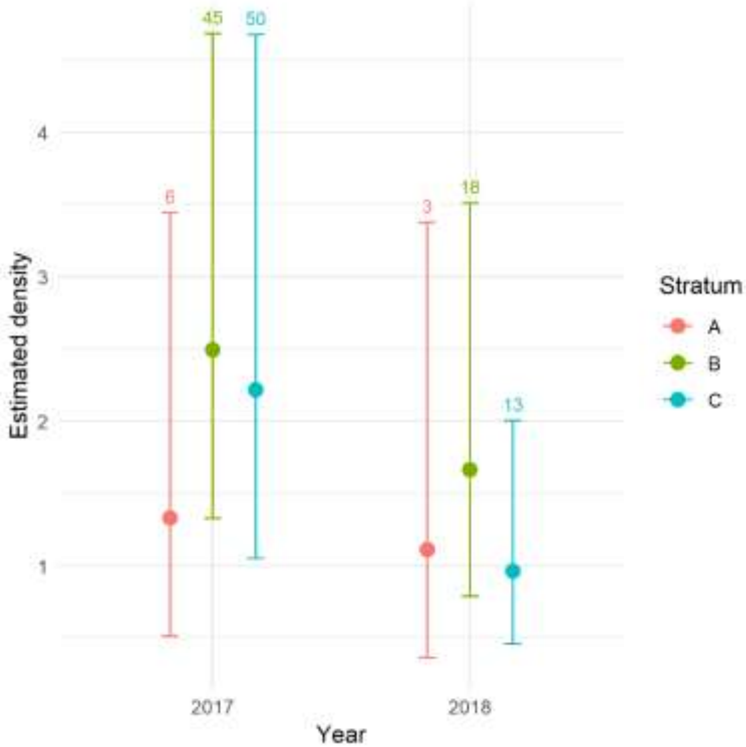

Figure C15. Density estimates (birds/km^2) derived by distance sampling of grebes (Family Podicipedidae) near Hood Canal Bridge, WA during steelhead outmigration in 2017-2018. Stratum A is 0 - 300 m from the bridge; Stratum B is 301 – 1200 m; Stratum C is 1201 – 3000 m. Error bars represent 95% confidence interval; numbers above bars represent sample size.

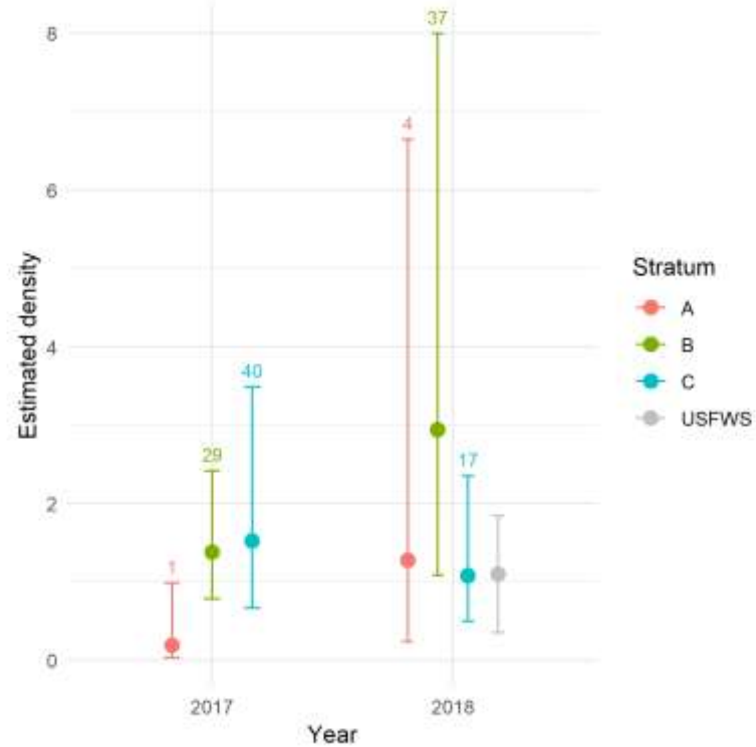

Figure C16. Density estimates (birds/km^2) derived by distance sampling of marbled murrelet (*Brachyramphus marmoratus*) near Hood Canal Bridge, WA during steelhead outmigration in 2017-2018. Stratum A is 0 - 300 m from the bridge; Stratum B is 301 – 1200 m; Stratum C is 1201 – 3000 m. USFWS is estimated density from summer 2018 surveys in the Salish Sea for comparison (see Methods). Error bars represent 95% confidence interval; numbers above bars represent sample size.

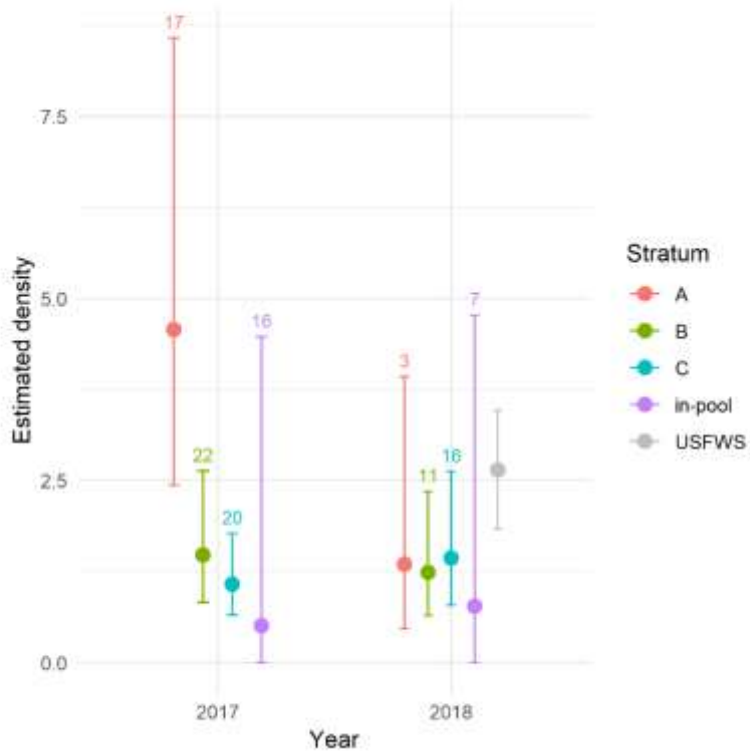

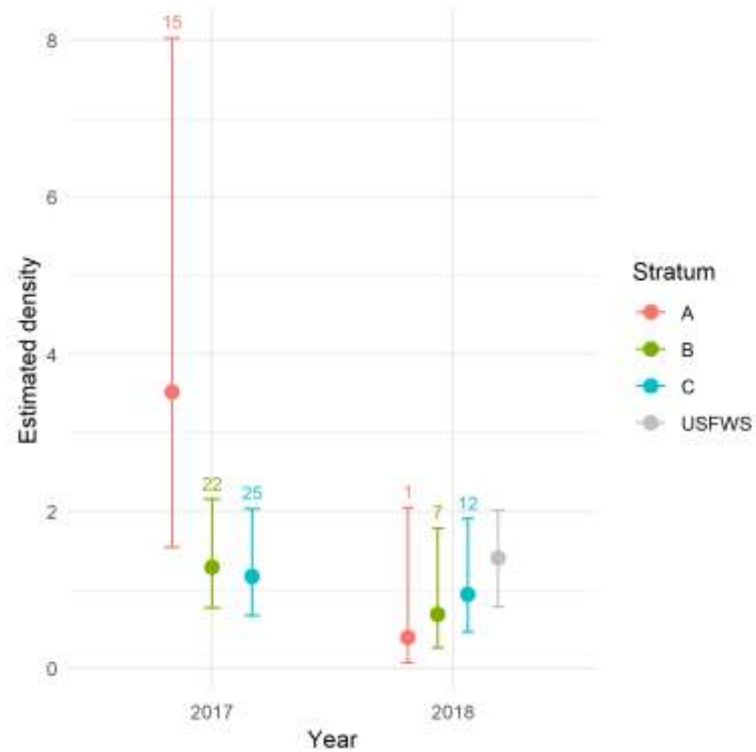

Figure C17. Density estimates (animals/km^2) derived by distance sampling of harbor seal (*Phoca vitulina*) near Hood Canal Bridge, WA during steelhead outmigration in 2017-2018. Stratum A is 0 - 300 m from the bridge; Stratum B is 301 – 1200 m; Stratum C is 1201 – 3000 m. In-pool refers to animals observed in the two pools within the structure of the bridge; USFWS is estimated density from summer 2018 surveys in the Salish Sea for comparison (see Methods). Error bars represent 95% confidence interval; numbers above bars represent sample size.

Figure C18. Density estimates (animals/km^2) derived by distance sampling of harbor porpoise (*Phocoena phocoena*) near Hood Canal Bridge, WA during steelhead outmigration in 2017-2018. Stratum A is 0 - 300 m from the bridge; Stratum B is 301 – 1200 m; Stratum C is 1201 – 3000 m. USFWS is estimated density from summer 2018 surveys in the Salish Sea for comparison (see Methods). Error bars represent 95% confidence interval; numbers above bars represent sample size.

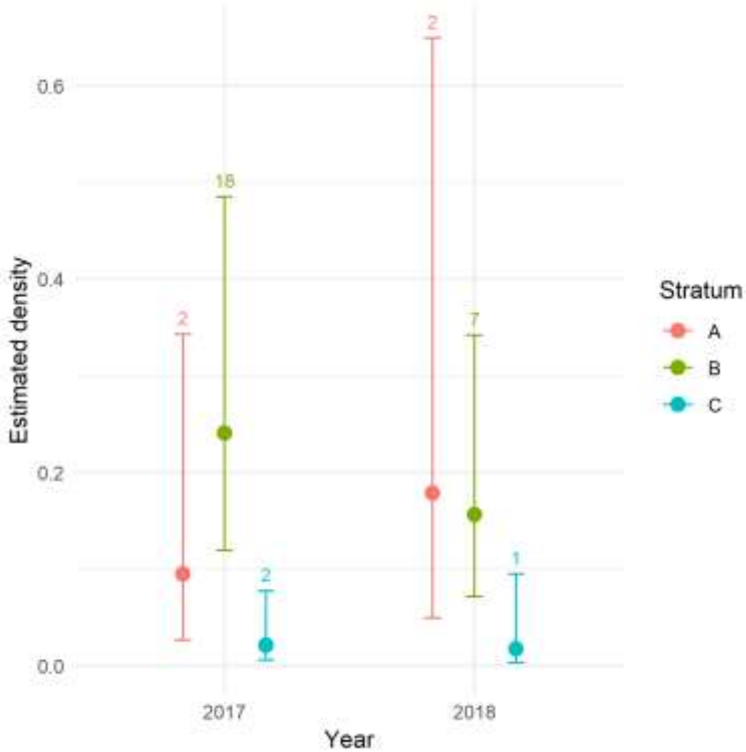

Figure C19. Density estimates (birds/km^2) derived by distance sampling of loons (*Gavia spp*.) near Hood Canal Bridge, WA during steelhead outmigration in 2017-2018. Stratum A is 0 - 300 m from the bridge; Stratum B is 301 – 1200 m; Stratum C is 1201 – 3000 m. Error bars represent 95% confidence interval; numbers above bars represent sample size.

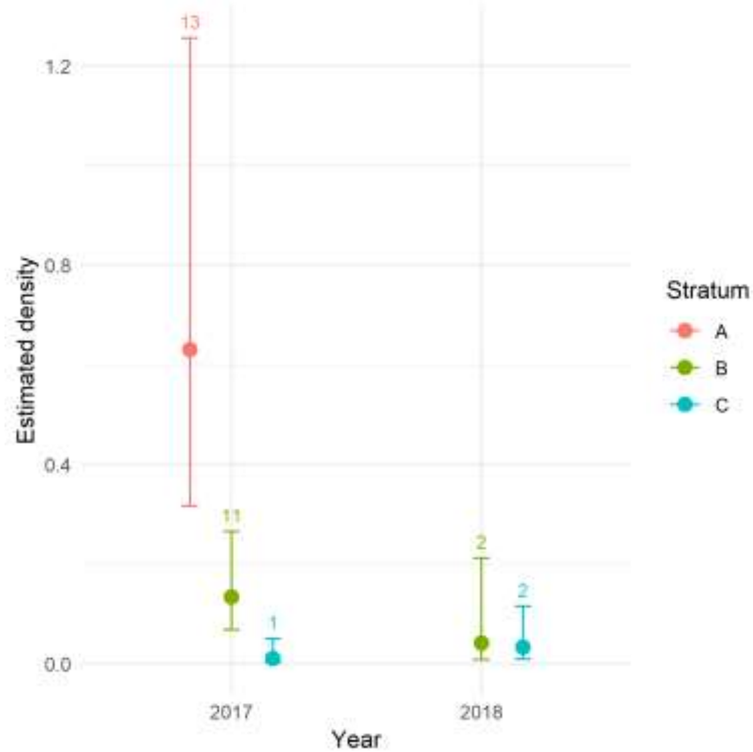

Figure C20. Density estimates (birds/km^2) derived by distance sampling of cormorants (*Phalacrocorax spp*.) near Hood Canal Bridge, WA during steelhead outmigration in 2017-2018. Stratum A is 0 - 300 m from the bridge; Stratum B is 301 – 1200 m; Stratum C is 1201 – 3000 m. Error bars represent 95% confidence interval; numbers above bars represent sample size. Missing points indicate insufficient data to generate an estimate for that stratum-year.

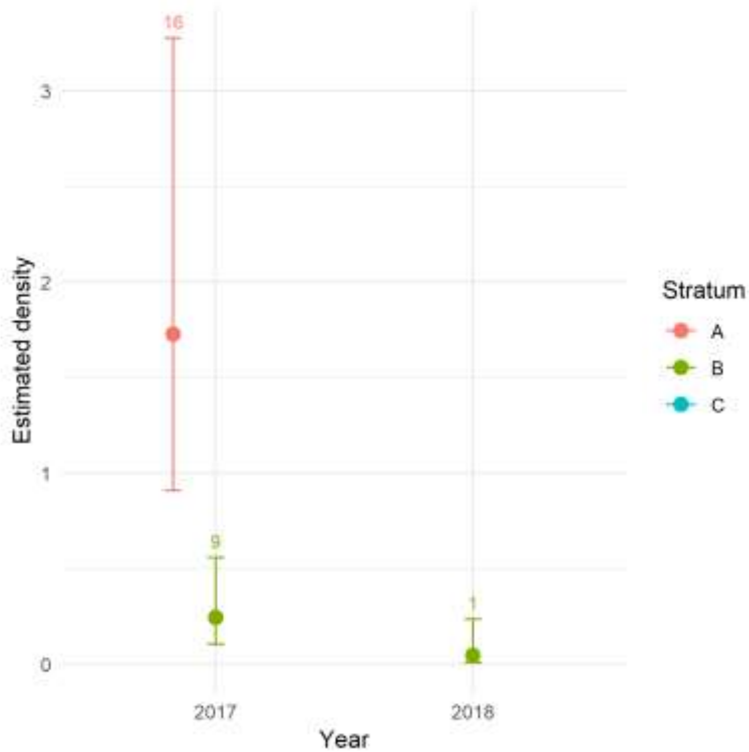

Figure C21. Density estimates (birds/km^2) derived by distance sampling of mergansers (*Mergus spp.*) near Hood Canal Bridge, WA during steelhead outmigration in 2017-2018. Stratum A is 0 - 300 m from the bridge; Stratum B is 301 – 1200 m; Stratum C is 1201 – 3000 m. Error bars represent 95% confidence interval; numbers above bars represent sample size. Missing points indicate insufficient data to generate an estimate for that stratum-year.

References

Bishop, E., G. Rosling, P. Kind, F. Wood. 2016. Pigeon guillemots on Whidbey Island, Washington: A six-year monitoring study. Northwestern Naturalist 97(3):237-245.

Buckland, S. T., D. R. Anderson, K. P. Burnham, J. L. Laake, D. L. Borchers, and L. Thomas. 2001. Introduction to distance sampling: estimating abundance of biological populations. Oxford University Press, New York.

Burnham, K.P. and D.R. Anderson. 1998. Model selection and inference: a practical information-theoretical approach. Springel-Verlag, New York.

Ewins, P.J. 1993. Pigeon guillemot (Cepphus columba). In The Birds of North America, No. 49 (A. Poole and F. Gill, eds.). The Acadamey of Natural Sciences, Philadelphia, PA, and The American Ornithologists' Union, Washington, D.C.

Keefer, M.L., R.J. Stansell, S.C. Tackley, W.T. Nagy, K.M. Gibbons, C.A. Peery, and C.C. Caudill. 2012. Use of Radiotelemetry and Direct Observations to Evaluate Sea Lion Predation on Adult Pacific Salmonids at Bonneville Dam, Transactions of the American Fisheries Society, 141:5, 1236-1251.

Khangaonkar, T., and T. Wang. 2013. Potential alteration of fjordal circulation due to a large floating structure – Numerical investigation with application to Hood Canal basin in Puget Sound. Applied Ocean Research 39:146-157. http://dx.doi.org/10.1016/j.apor.2012.11.003

McIver, W., J. Baldwin, M.M. Lance, S.F. Pearson, C. Strong, N. Johnson, D. Lynch, M.G. Raphael, R. Young, T. Lorenz and K. Nelson. 2019. Marbled murrelet effectiveness monitoring, Northwest Forest Plan: 2018 summary report. 22 p.

Moore, M., Berejikian, B. A., & Tezak, E. P. (2013). A floating bridge disrupts seaward migration and increases mortality of steelhead smolts in Hood Canal, Washington State. PloS one, 8(9), e73427.

Pearson, S.F., S.J. Jeffries, M.M. Lance and A.C. Thomas. 2015. Identifying potential juvenile steelhead predators in the marine waters of the Salish Sea. Washington Department of Fish and Wildlife, Wildlife Science Division, Olympia.

Pearson, S.F., and M.M. Lance. 2019. Washington 2018 at-sea marbled murrelet population monitoring: Research Progress Report. Washington Department of Fish and Wildlife, Wildlife Science Division.

Raphael, M.G.; J. Baldwin; G.A. Falxa; M.H. Huff; M. Lance; S.L. Miller; S.F. Pearson; C.J. Ralph; C. Strong; and C. Thompson. 2007. Regional population monitoring of the marbled murrelet: field and analytical methods. Gen. Tech. Rep. PNW-GTR-716. Portland, OR: U.S. Department of Agriculture, Forest Service, Pacific Northwest Research Station. 70 p. Available at: http://www.fs.fed.us/pnw/pubs/pnw_gtr716.pdf

Schakner Z.A., Petelle M.B., Tennis M.J., Van der Leeuw B.K., Stansell R.T., Blumstein D.T.. 2017 Social associations between California sea lions influence the use of a novel foraging ground. R.Soc.opensci.4: 160820.http://dx.doi.org/10.1098/rsos.160820

Thomas, L., S. T. Buckland, E. A. Rexstad, J. L. Laake, S. Strindberg, S. L. Hedley, J. R. B. Bishop, T. A. Marques, and K. P. Burnham. 2010. Distance software: design and analysis of distance sampling surveys for estimating population size. Journal of Applied Ecology 47: 5-14. DOI: 10.1111/j.1365-2664.2009.01737.x. Distance 6.0. < http://www.ruwpa.st-and.ac.uk/distance/> (2 June 2011).

Yurk, H., and A.W. Trites. 2000. Experimental attempts to reduce predation by harbor seals on out-migrating juvenile Salmonids. Transactions of the American Fisheries Society 129:1360–1366.

Appendix C1. Total observations and total observations by kilometer surveyed of birds and mammals detected during line transect surveys of Hood Canal survey area during steelhead outmigration in 2017 and 2018. Survey effort in 2017 was greater than in 2018, observations/km columns are to facilitate comparison between years (see Appendix C2).

		Observations		Observations/km	
Common name	**Scientific name**	**2017**	**2018**	**2017**	**2018**
Bald eagle	*Haliaeetus leucocephalus*	48	12	0.05	0.02
Belted kingfisher	*Megaceryle alcyon*	0	1	0.00	0.00
Brandt's cormorant	*Phalacrocorax penicillatus*	56	23	0.06	0.04
Caspian tern	*Hydroprogne caspia*	55	29	0.05	0.05
Common loon	*Gavia immer*	321	115	0.32	0.19
Common merganser	*Mergus merganser*	3	4	0.00	0.01
Common murre	*Uria aalge*	35	3	0.03	0.00
Double-crested cormorant	*Phalacrocorax auritus*	43	19	0.04	0.03
Great blue heron	*Ardea Herodias*	7	22	0.01	0.04
Horned grebe	*Podiceps auritus*	1211	397	1.21	0.65
Marbled murrelet	*Brachyramphus marmoratus*	665	211	0.66	0.35
Osprey	*Pandion haliaetus*	22	9	0.02	0.01
Pacific loon	*Gavia pacifica*	78	42	0.08	0.07
Pelagic cormorant	*Phalacrocorax pelagicus*	138	29	0.14	0.05
Peregrine falcon	*Falco peregrinus*	1	0	0.00	0.00
Harbor porpoise	*Phocoena phocoena*	329	141	0.33	0.23
Harbor seal	*Phoca vitulina*	277	144	0.28	0.24
Pigeon guillemot	*Cepphus columba*	1649	1265	1.64	2.07
Red-breasted merganser	*Mergus serrator*	118	16	0.12	0.03
Red-necked grebe	*Podiceps grisegena*	394	121	0.39	0.20
Red-throated loon	*Gavia stellate*	17	5	0.02	0.01
Rhinoceros auklet	*Cerorhinca monocerata*	545	606	0.54	0.99
Unidentified alcid	Alcidae	17	10	0.02	0.02
Unidentified cormorant	Phalacrocoracidae	110	63	0.11	0.10
Unidentified grebe	Podicipedidae	131	64	0.13	0.10
Unidentified loon	Gaviidae	166	46	0.17	0.08
Unidentified merganser	Anatidae	49	23	0.05	0.04
Unidentified sea lion	Otariidae	0	1	0.00	0.00
Western grebe	*Aechmophorus occidentalis*	475	169	0.47	0.28
California sea lion	*Zalophus californianus*	13	3	0.01	0.00

Appendix C2. Number of replicates for each steelhead predator survey transect included in distance sampling analysis in 2017 and 2018.

Transect	2017	2018
07	21	14
08	22	14
09	22	14
10	22	14
17	25	14
18	25	14
19	25	14
20	25	14

Appendix C3. Literature review of dive profiles of predator species observed at the Hood Canal Bridge.

Table 1. Summary table of literature sources described in Table 2.

	mean depth (m)	max depth (m)	mean duration (s)	max duration (s)	notes
cormorants	2.2 - 38.2	>100 (BRAC)	22 - 51	120	
loons	no data	no data	33 - 94	124‡	‡the Birds of North America account suggests that 10-min (!) dives are very rare, but I
mergansers	<4*	6	~20	120	
common murre	13.4 - 50	180	41 - 71	212	
grebes	<6	no data	25 - 30	73	
marbled murrelet	no data	50*	20 - 44	115	
harbor porpoise	14 - 41	226	44 - 103	321	
harbor seal	50 - 60†	481†		135	†multiple papers suggest seals dive to bottom
pigeon guillemot	10 - 20	50′	30 - 87	204	′black guillemot; none found for PIGU
rhinoceros auklet	<10 - 14	57	15-53	148	
* based on single study					

Table 2. Literature sources describing dive profile characteristics of predator species.

date	author	species	location	depth mean	depth sd	max depth (m)	duration mean	duration sd	max duration (s)	notes
1911	Clay	BRAC								caught in nets at 55-70m
1990	Ainley, et al.	BRAC				>100 m				
1973	Scott, J.M.	BRAC					30.45 sec	13.2	90-100	duration closely related to water depth

1990	Ainley, et al.	BRAC					51 sec		95	
2008	Coleman, JTH	DCCO	NY			25.8	22	10		V-shaped dives
1974	Ross, R.K.	DCCO	Nova Scotia	4.7 m		7.9				
1936	Mendall, H.L.	DCCO					19.3-22 s in 3 m; 22.5-27.7 s in 4.5 m		41 s	
2009	Coleman, JTH	DCCO	NY	10-15 m?		25.8	22 s		17-34 s range	
1995	King et al.	DCCO	MS				11.9 s		45 s	shallow catfish ponds (1.4m)
1929	Lewis, H.F.	DCCO	Ontario						70 s	
2011	Kotzerka et al.	PECO	Gulf of Alaska	2.2-38.2 (median)		32.1-42.2	28-76 (median)		90-120sec (range)	corms most often either made shallow (1-6m) or deep (28-33m) dives
2011	Kotzerka et al.	PECO				42.2 m	4-120 sec range			same paper as referenced above (but different stats pulled)
1985	Hobson & Sealy	PECO					34.9 s	4.1		**FOR depth 2-5m (and adults only)**
1964	Dow, D.D.	PECO					45.3 s	1.35		**FOR depth 1.5-6.1m**
1990	Ainley, et al.	PECO					45 s		70 s	
1959	van Tets, G.F.	PECO					31.3 s			
1973	Scott, J.M.	PECO					28.8 s	7.7		
unpubl.	Vlietstra, L.S.	COLO	CA				94 s			
1988	Parker, K.E.	COLO	NY				42.6 s			
1999	Paruk, J.D.	COLO	MI, WI				33.3 s			n=8
2002	Nocera & Burgess	COLO	Canadian Maritimes				30 - 50 s, depending on chick status		124	
1999	Paruk, J.D.	COLO							>120 s (uncommon); >10min! very rare	
unpubl.	Vlietstra, L.S.	PALO	CA				77 s	25		
unpubl.	Vlietstra, L.S.	RTLO	CA				49 s			

1980	Reimchen & Douglas	RTLO	Queen Charlotte	70% of foraging in ≤1 m deep						
1996	Alvo, R.	COME		"prefers" <4 m depth						
1977	Cramp & Simmons	COME					<30 s		up to 2 min	
1972	Nilsson, L.	COME	Sweden			6 m			20-28 s range	longer in deeper (appears to be contradicted elsewhere in BNA account)
1980	Bowles, W.F. Jr.	RBME					16 s			FOR <2 m depth
1963	Hending et al.	RBME					17 s			
1985	Piatt & Nettleship	COMU	Newfoundland	20-50 m "normal depth"		often to 70 m; occasionally 180 m				
1924	Dewar, J.M.	COMU					15 s			FOR <2 m depth
1924	Dewar, J.M.	COMU					61 s			FOR >8 m depth
1973	Cody, M.L.	COMU	WA				41 s		70	
1990	Ainley, et al.	COMU	CA				55 s		71	
1973	Scott, J.M.	COMU	OR				71 s		140	
2003	Tremblay et al.	COMU	Norway			37 m			119 s	
2009	Hedd et al.	COMU		30 m	0.8	152 m	64 s	1.3	212 s	
2010	Regular et al.	COMU				177 m				
2010	Thaxter, et al.	COMU	UK	13.4 (shallow), 50.4 (deep)	8.9, 7.4		46.4 (shallow), 118.4 (deep)	27.4, 17.2	175ish	
table 2 in	Boyd&Croxall	COMU					66		204	
1924	Dewar, J.M.	HOGR		<6 m (generally)						
VARIED	VARIED	HOGR	VARIED				7-25 s (norm)		73 s	tends to feed at bottom of

										shallow waters (0-4 m
1970	Simmons	RNGR					24.8 s	0.7		FOR ~2 m depth; "capable of much longer foraging dive times"
1950	Lawrence	WEGR					30.4 s		63 s	
1989	Thoresen, A.C.	MAMU	WA			"within 50m of surface"	20-44 s		2-115 s range	vary with water depth
2003	Henkel, et al.	MAMU	CA				24.8 s	15.7		single radio-tagged bird
1999	Jodice&Collopy	MAMU	OR				26.84			
2009	Peery et al.	MAMU					23.5 s	9	~58 s	
1985	Westgate, et al.	PHPH	Bay of Fundy	14	16	226	44	37	321sec	fewer, deeper dives at night
1985	Westgate, et al.	PHPH	Bay of Fundy	41	32		103	67		individual range (with above)
2013	Linnenschmidt et al.	PHPH	Denmark			14,25, 34 (n=3 indiv)			94,138,213sec	water typically <50m deep
2007	TEILMANN, et al.	PHPH	Danish Belt seas			132m				
1999	Bowen, et al.	PHVI	Nova Scotia			59m			90 - 135sec	
1998	Lesage et al.	PHVI	St. Lawrence Estuary	5.8m			40s			V-shaped dives
1999	Lesage et al.	PHVI	St. Lawrence Estuary	to bottom (20m)						U-shaped dives
2005	Eguchi and Harvey	PHVI	Monterey Bay	5-100 (median)		481		35.25m		
1998	Tollit, et al.	PHVI	Scotland	80% of dives 20-40m; 75% of dives						multiple individuals

				50-60m						
table 2 in	Boyd&Croxall	PHVI					96		138	
multiple papers suggest that seals (PHVI) dive to the bottom										
1994	Clowater & Burger	PIGU	Vancouver Island	15-20m (mode)			87sec (37-144)		144	
1987	Duffy et al.	PIGU	SeaWorld				28.4	9.1		
1973	Scott, J.M.	PIGU		10-20 m "optimal efficiency"					10-144 s range	
1985	Piatt & Nettleship	BLGuillemot	Newfoundland			50m				
table 2 in	Boyd&Croxall	PIGU					84		204	
1993	Burger, et al.	RHAU	B.C.			30m mean deepest dive,	45sec		69sec	90% of time was spent in the top 10m, but most birds had dives to 20-60m

						n=16 (12-60 range)				
1987	Duffy et al.	RHAU	SeaWorld				15.3	6.4		
2016	[Shoji et al.] - see Kuroki paper	RHAU	table 1	14		57	53		148	
2000	Davoren, G.K.	RHAU					37	1.3		
2003	Kato, et al.	RHAU	Japan	12.1	5.5	51.6	42.7 s	17.7	131	
2003	Kuroki, et al.	RHAU	Japan	14	1.8	57	53	8	148	

Appendix D. Deng et al. 2018

Hood Canal Bridge noise impact assessment: phase 1 findings

Daniel Deng[1], Xiaoqin Zang[1], Jayson Martinez[1], Jun Lu[1], Scott Titzler[1]

[1] Pacific Northwest National Laboratory, 1100 Dexter Ave N, Seattle, WA 98109

Appendix E. Khangaonkar et al. 2018

Hydrodynamic zone of influence due to a floating structure in a fjordal estuary – Hood Canal Bridge impact assessment

Tarang Khangaonkar[1], Adi Nugraha[1], and Taiping Wang[1]

[1] Pacific Northwest National Laboratory, 1100 Dexter Ave N, Seattle, WA 98109

Appendix F. Khangaonkar & Nugraha 2019

Hood Canal Bridge impact on basin-wide water quality – initial analysis

Tarang Khangaonkar[1] and Adi Nugraha[1]

[1] Pacific Northwest National Laboratory, 1100 Dexter Ave N, Seattle, WA 98109

Appendix G. Hood Canal Bridge Impact Assessment Matrix

The Assessment Team's September 2019 revisit and update to the Assessment Matrix included in the Hood Canal Bridge Ecosystem Impact Assessment Plan: Framework and Phase 1 Details (2016) Appendix B. The 2019 update does not reflect further analysis and synthesis completed in 2020.

Appendix H. Assessment Team and Management Committee Ranking Exercise: Phase 2 Solutions

This represents the Assessment Team's September 2019 initial brainstorming and discussion regarding options for Phase 2 actions. It does not reflect further analysis or synthesis completed in 2020, nor does it reflect the later engineering consultations, initial solutions development, or prioritization described in Appendix I.

Appendix I. R2 Resource Consultants: Phase 2 Scoping and Recommendations